DOKUZ EYLÜL UNIVERSITY
GRADUATE SCHOOL OF NATURAL APPLIED SCIENCES

RELEASING OF PROMETHAZINE HYDROCHLORIDE FROM VARIOUS MATERIALS

by
Yoldaş SEKİ

January, 2007
İZMİR

RELEASING OF PROMETHAZINE HYDROCHLORIDE FROM VARIOUS MATERIALS

A Thesis Submitted to the
Graduate School of Natural and Applied Sciences of Dokuz Eylül University
In Partial Fulfillment of the Requirements for the Degree of Doctor of Philosophy in Chemistry Program

by
Yoldaş SEKİ

January, 2007
İZMİR

Ph.D. THESIS EXAMINATION RESULT FORM

We have read the thesis entitled "**RELEASING OF PROMETHAZINE HYDROCHLORIDE FROM VARIOUS MATERIALS**" completed by **Yoldaş Seki** under supervision of **Prof. Dr. Kadir YURDAKOÇ** and we certify that in our opinion it is fully adequate, in scope and in quality, as a thesis for the degree of Doctor of Philosophy.

……..

Prof. Dr. Kadir YURDAKOÇ

Supervisor

Prof. Dr. Melek MERDİVAN

……

Jury Member

Doç. Dr. Mehmet BALCAN

……..

Jury Member

Prof. Dr. Zeki TEZ

……

Jury Member

Prof. Dr. Çetin GÜLER

. …….

Jury Member

_____

Prof. Dr. Cahit HELVACI

Director

Graduate School of Natural and Applied Sciences

ACKNOWLEDGMENTS

The author is grateful to the supervisor of this thesis, Prof. Dr. Kadir YURDAKOÇ, for his valuable guide, help and advice, at all stages of this thesis study.

I am also gratefull to Research Foundation of Dokuz Eylul University (Project No: 03.KB.021 and 2005.KB.FEN.023 for finincial support. I would like to thank to TUBİTAK for the financial aid

In addition, I wish to express my gratefulness to all friends for their continuous helpful encouragement and valuable supports.

Finally, I would like to thank my family for bringing me in this situation with their unique patience and supports.

Yoldaş Seki

RELEASING OF PROMETHAZINE HYDROCHLORIDE FROM VARIOUS MATERIALS

ABSTRACT

The releasing of Promethazine hydrochloride (PHCl) from two clays (KSF and iron rich smectite, IRS) and three hydrogels (ChitEPI400, ChitEPI600 and ChitEPI800) was investigated in pH=1.2 and pH=7.4 phosphate buffer solutions (PBS). Adsorption capacities for PHCl sorption on KSF and IRS, were obtained by using Langmuir, Freundlich and Dubinin Raduschkevich (DR) adsorption isotherm equations. When the adsorption capacity values (C_m and K_f) obtained from Langmuir and Freundlich equation were compared, IRS had much greater capacity than that of KSF. It was obtained that sorption kinetics follow pseudo-second-order kinetic model for PHCl sorption onto both KSF and IRS. Thermodynamic parameters were also determined. From the release study, the maximum amount of PHCl released from KSF was almost 56.8 % of the total in the range studied (0-540 min) at PBS. Release of PHCl from KSF in acidic solution was less than 1%. Releasing of PHCl from IRS was 14.5 % at 715 min at pH=7.4. Besides, there was very little release from IRS (lower than 1.2%) in acidic medium (pH=1.2). The hydrogels were synthesized by using Chitosan crosslinked by epichlorohydrin (EPI) at various amounts (400, 600, 800 μL). SEM, FTIR and DSC analysis were conducted. The DSC measurements indicated that ChitEPI hydrogels did not exhibit better thermal stability when compared to Chitosan. Moreover, equilibrium swelling studies showed that equilibrium swelling was reached in a very short time. Swelling behavior of Chitosan-EPI hydrogel film was pH dependent. Furhermore, when the pH values were changed repeatedly, ChitEPI hydrogel showed a reversible swelling behaviour with a fast response. The release of PHCl from synthesized hydrogels at pH 7.4 was quite low. Only about 10 % of the loaded drug was released during 600 min for all hydrogels. Considering PHCl release at pH 1.2 the highest value was observed as 49 % for ChitEPI600. ChitEPI hydrogels may be used for the delivery of drug in stomach and gastrointestinal tract whose pH rised from 1.5 to 3.

Keywords: releasing, promethazine hydrochloride, chitosan, cross-linking, pH sensitivity.

PROMETHAZIN HİDROKLORÜRÜN ÇEŞİTLİ METARYELLER ÜZERİNDEN SALINIMI

Promethhazine hidroklorürün (PHCl) iki kil örneği (KSF ve demirce zengin smektit) ve üç hidrojel (ChitEPI400, ChitEPI600 and ChitEPI800) üzerinden pH=1.2 ve pH=7.4 fosfat tamponu ortamındaki salınımı incelenmiştir. PHCl' ün KSF ve IRS üzerine sorpsiyonu için sorpsiyon kapasite değerleri Langmuir, Freundlich ve Dubinin-Raduskevich (DR) denklemleri kullanılarak belirlenmiştir. Langmuir ve Freundlich denkleminden bulunan C_m ve K_f sorpsiyon kapasiteleri değerleri karşılaştırıldığında IRS'nin KSF'den daha büyük bir adsorpsiyon kapasitesi değerine sahip olduğu gözlenmiştir. PHCl'ün hem IRS hem de KSF üzerine adsorpsiyonun yalancı ikinci mertebe kinetiğe uyduğu bulunmuştur. Termodinamik parametreler de aynı zamanda belirlenmiştir. Salınım çalışmaları, maksimum PHCl salınımının KSF üzerinden fosfat tamponu ortamında (pH=7.4) 540 dakikada %56.8 olduğunu göstermiştir. Asidik ortamdaki salınımın ise % 1 den azdır. IRS den PHCl salınımı ise pH=7.4' de 715 dakikada %14.5 civarında gerçekleşmiştir. Bunun yanında asidik ortamdaki salınım ise %1.2 den daha az olarak gözlenmiştir. Hidrojeller, chitosan'ın farklı miktarlardaki (400, 600, 800 μL) epiklorohidrin ile çapraz bağlanması sonucu sentezlenerek SEM, DSC ve FTIR analizleri yapılarak karakterize edilmişlerdir. DSC analizlerinden ChitEPI hidrojellerin Chitosan ile karşılaştırıldığında daha kötü bir termal kararlılığa sahip olduğu gözlenmiştir. Ayrıca denge şişme çalışmaları, denge şişmesinin çok kısa bir sürede sağlandığını göstermiştir. ChitEPI hidrojel filmin şişme davranışı pH duyarlıdır. Ayrıca pH değerlerinin değiştirilmesi sonucu, hidrojellerin hızlı cevap veren tersinir şişme davranışına sahip olduğu görülmüştür. PHCl'in sentezlenen hidrojellerden pH 7.4 deki salınımı oldukça düşüktür. Yaklaşık bütün hidrojeller için 600 dakikada % 10 civarında bir salınım gözlenmiştir. PHCl'nin asidik ortamdaki salınımı dikkate alındığında en yüksek değer %49 olarak ChitEPI600 için gözlenmiştir. ChitEPI hidrojeller, pH 1,5 ile 3 arasında değişen mide ve gastrointestinal bölgede salınması gereken ilaçların salınımında kullanılabilir.

Anahtar sözcükler: salınım, promethazin hidroklorür, chitosan, çapraz bağlanma, pH duyarlılık

CONTENTS

Page

CHAPTER ONE

INTRODUCTION

1 Hydrogels

1.1 General Definitions

A hydrogel can be seen as a container of water made of three-dimensional mesh. Gel is a solid material in dried state. The dried hydrogel is called a **xerogel** or **dry gel**. However, a hydrogel swells when water is added, until it reaches the swelling equilibrium. The term hydrogel implies that the materials are already swollen in water. Hydrogels combine glassy behavior (when in the dry state) with elastic (when sufficient water is absorbed. During the drying process water evaporates from the gel and surface tension causes collapse of the gel body. Thus the gel shrinks to only a small fraction of its swollen size. If water is removed without disturbing the polymer network either by lyophilization (a method of drying food or blood plasma or pharmaceuticals or tissue without destroying their physical structure; material is frozen and then warmed in a vacuum so that the ice sublimes i.e., freeze-drying) or by extraction with organic solvents. The remaining material is extremely light with porosity as high as 98 percent. Such a dehydrated hydrogel is called an **aerogel** or **sponge**. The feature of swelling is a function of the network characteristic (such as degrees of swelling, diffusion coeffcient, crosslink density, mesh size, etc.)

Hydrogels are hydrophilic polymer networks which may absorb from 10–20 % (an arbitrary lower limit) up to thousands of times their dry weight in water. Hydrogels may be chemically stable or they may degrade and eventually disintegrate and dissolve. They are called ‘reversible’, or ‘physical’ gels when the networks are held together by molecular entanglements, and/or secondary forces including ionic, H-bonding or hydrophobic forces (Campoccia et al., 1998; Prestwich et al., 1993). Hydrogels are called ‘permanent’ or ‘chemical’ gels when they are covalently-cross-linked networks. Chemical hydrogels may also be generated by crosslinking of water-soluble polymers, or by conversion of hydrophobic polymers to hydrophilic

polymers plus cross-linking to form a network (Figure 1.1). In the crosslinked state, crosslinked hydrogels reach an equilibrium swelling level in aqueous solutions which depends mainly on the crosslink density (estimated by the MW between crosslinks, *M*). Like physical hydrogels, chemical hydrogels are not homogeneous. They usually contain regions of low water swelling and high crosslink density, called 'clusters', that are dispersed within regions of high swelling, and low crosslink density. This may be due to hydrophobic aggregation of crosslinking agents, leading to high crosslink density clusters (Campoccia et al., 1998; Prestwich et al., 1993).

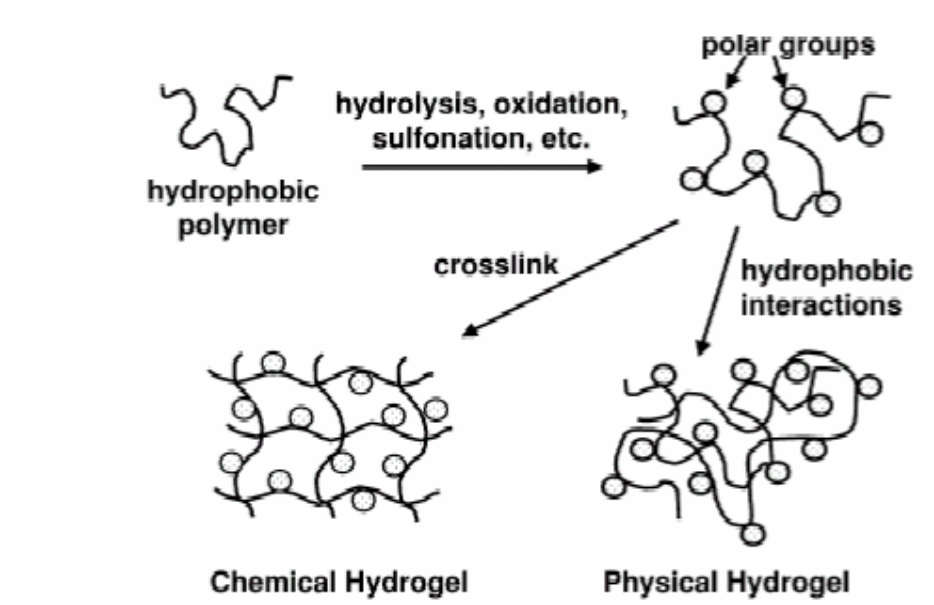

Figure 1.1 The schematic representation of production of hydrogel

Hydrogels are usually made of hydrophilic polymer molecules, which are crosslinked either by chemical bonds or other cohesion forces such as ionic interaction, hydrogen bonding, van der Waals forces or hydrophobic interactions. As water enters into the polymer, the chains extend and exert a resistive force. The equilibrium degree of reached when this resistive force balances the osmotic force driving water into the polymer (Park & Shalaby, 1993).

Hydrogen bonding, which is predominantly an interaction, exists between electronegative atoms (e.g., O, N, F,) and H atoms which are covalently bound to similar electronegative atoms. Hydrogen bonding results in a lowering of the total entropy. The strength of hydrogen bonding (<10 kcal/mol) is far weaker than covalent bond energy (>100 kcal/mol) but still much stronger than van der Waals interaction energies (~1 kcal/mol) (Figure 1.2). Hydrogen bonding occurs primarily at low temperature and is disrupted by heating.

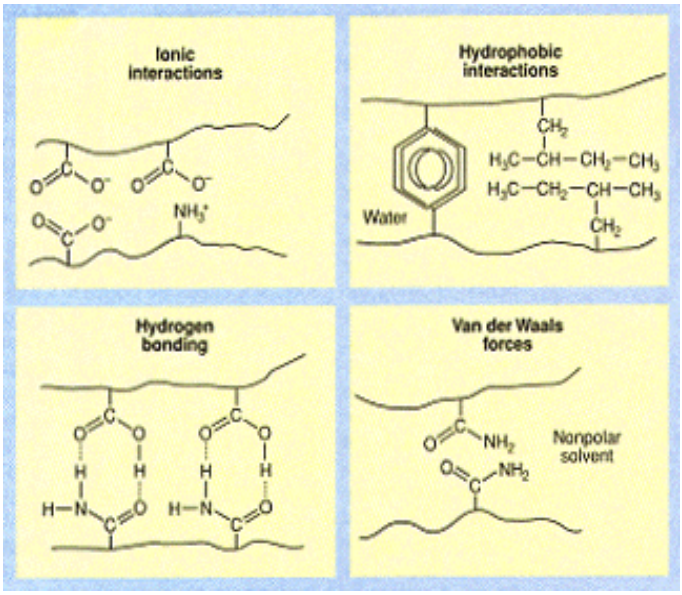

Figure 1.2 The interaction between the atoms

Diffusion involves migration of water into pre-existing or dynamically formed spaces between hydrogel chains. Swelling of the hydrogel involves larger scale segmental motion resulting, ultimately, in an increased distance of separation between hydrogel chains (Yıldız, 2001). Swelling equilibria of polyelectrolyte networks are determined by a balance of three primary forces: (i) the free energy of mixing of the network chains with solvent, (ii) the net osmotic pressure within the network resulting from the mobile counterions surrounding the fixed charged groups (ion osmotic pressure), and (iii) the elastic retractive response of the network (network swelling pressure) (Yıldız, 2001; Siegel & Firestone, 1988).

1.2 Responsive Hydrogels.

One of the important properties of hydrogels is their ability to swell in the presence of water and to shrink in the absence of water. This property is common to all hydrogels. In addition to this, the most important properties of is the ability to swell or shrink in response to a signal. It can be said that these hydrogels can be defined as "intelligent hydrogels" or "responsive hydrogels" or "stimuli-reponsive hydrogel" (Figure 1.3). These changes are swelling, shrinking, bending and degradation. They can change their swelling ratio rater abruptly upon small changes in environmental factors. These environmental factors that cause volume change in hydrogels are pH, temperature, electric field; salt, light, external stres, solvent pressure, and ionic strength (Gupta et al., 2002). This case can be shown schematically as below;

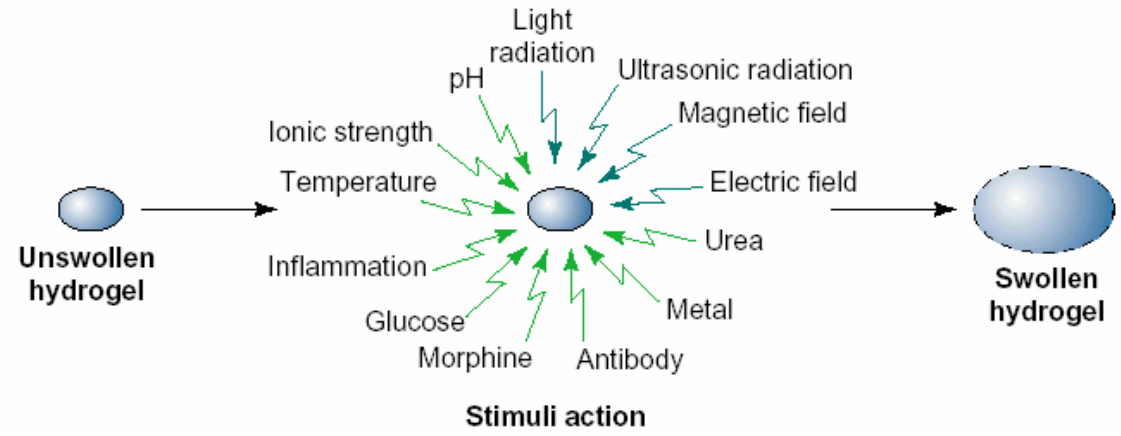

Figure 1.3. The swelling behaviors of hydrogel

1.2.1 pH-Responsive Hydrogels

Variations in pH are known to occur at several body sites, such as the gastrointestinal tract (Guyton & Hall, 1998), vagina (Deshpande, 1992) and blood vessels, and these can provide a suitable base for pH-responsive drug release Figure 1.4). In addition, local pH changes in response to specific substrates can be generated and used for modulating drug release. The pH-responsive drug delivery systems have been targeted for peroral controlled drug delivery (Bilia, 1992; Ito, 1994), taste-

masking of bitter drugs (Ito, 1994) and intravascular drug release during elevated blood pH in certain cardiovascular defects (Brazel & Peppas, 1996; Gupta et al., 2002).

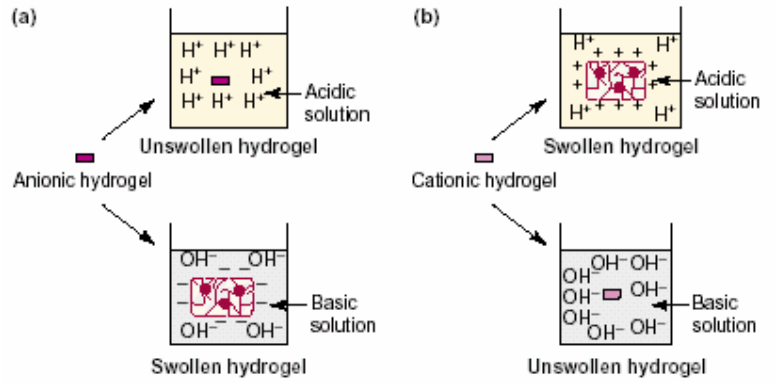

Figure 1.4 The pH-responsive swelling of **(a)** anionic and **(b)** cationic hydrogels

1.2.2 Temperature-Responsive Hydrogel

The thermosensitive hydrogel could be described as either a positive or a negative temperature sensitive system. In a positive temperature sensitive system, hydrogels with upper critical solution temperature (UCTS) shrink by cooling below the UCTS, while the hydrogels with lower critical solution temperature (LCTS) contract by heating above the LCTS in a negative temperature sensitive system (Lee et al., 1996).

Poly(N-isopropylacrylamide) (PNIPAM) non-biodegradable polymer with a LCST 32- 8 °C in water (Heskins & Guillet, 1968), and cross-linked gels of this material collapse around this temperature (Hoffman et al., 1986; Hirotsu et al., 1987). The PNIPAM LCST can be controlled by copolymerization with other monomers. The addition of hydrophilic monomers typically increases the LCST whereas the incorporation of more hydrophobic units has the opposite effect (Feil et al., 1993).

1.2.3 Application of Temperature-Responsive Hydrogel

P(NIPAM-co-AA) solutions were investigated as cell matrices in refillable bioartificial pancreas (Vernon et al., 1996; Bae et al., 1998; Vernon et al., 1999;

Gappa, et al., 2001; Chae, et al., 2002; Chae, et. al., 2001). The idea originated from the observation that islets of Langerhans tend to malfunction at some point after considered transplantation and have to be replaced. Also, aggregation of the islets can lead to necrosis. The thermosensitive solutions were proposed as an extracellular matrix for islets placed in an immunoprotecting pouch installed in diabetic patients. An islet/polymer solution can be injected into the pouch where the polymer forms a gel, immobilizing the islets. To replace the islets, the polymer matrix is cooled below the critical temperature, causing the gel to redissolve. The solution is then withdrawn, and a fresh islet/polymer suspension is injected. It was shown that the copolymer efficiently immobilized rat islets without impairing insulin secretion (Vernon et al., 1996; Bae et al., 1998; Vernon et al., 1999). Compared to free islets, entrapment in the gel resulted in prolonged insulin secretion (Vernon et al., 1999). Moreover, P(NIPAM-co-AA)-entrapped rat islets responded faster and with greater magnitudes to changes in glucose concentration than islets in an alginate gel. The addition of glucagon-like peptide-1, a potent islet stimulant, was also investigated (Gappa et al., 2001). Its presence in the preparation significantly enhanced insulin secretion without affecting islet viability. Similarly, a hemoglobin–PEO conjugate was used, as it is believed that the low functionality and viability of immunoprotected islets are closely associated with low oxygen tension (Chae et al., 2002). Insulin secretion functions, as well as islet viability, were significantly enhanced by the addition of hemoglobin. The same approach was later taken to develop a biohybrid artificial liver (Park & Bae, 2002). Hepatocytes cultured as spheroids in the thermoreversible matrix exhibited greater viability and enhanced liver-specific functions vs. control cells. These studies demonstrated the potential of the system as a temporary cell-supporting matrix, but the non-biodegradability of the polymer may limit its biomedical applications.

1.3 Applications of Hydrogels in Biotechnology

Hydrogels, crosslinked hydrophilic polymers, represent an important class of biomaterials in biotechnology and medicine because many hydrogels exhibit excellent biocompatibility, causing minimal inflammatory responses, thrombosis,

and tissue damage (Graham, 1998). Hydrogels can also swell large quantities of water without the dissolution of the polymer due to their hydrophilic but crosslinked structure, thus giving them physical characteristics similar to soft tissues. In addition, hydrogels have high permeability for oxygen, nutrients, and other water-soluble metabolites. Over the past three decades, a number of hydrogels differing in structure, composition, and properties have been developed. Hydrogel materials have been used extensively in medicine for applications such as contact lenses, biosensors, linings for artificial implants (Peppas, 1987; Peppas & Bures, 2000).

1.4 The Properties of Chitosan

Chitosan (2-amino-2deoxy-(1→4)-β-D-glucopyranan), a polyaminosaccharide, normally obtained by alkaline deacetylation of chitin is the principal component of living organisms such as fungi and crustacea. When its DA (degree of N-acetylation) is lower than 50%, the chitin becomes soluble in aqueous acidic solution and is named chitosan. Up to the present time only a few cationic polymers exist and chitosan may be used as a flocculation and chelating polymer (Dung et al.,1994)

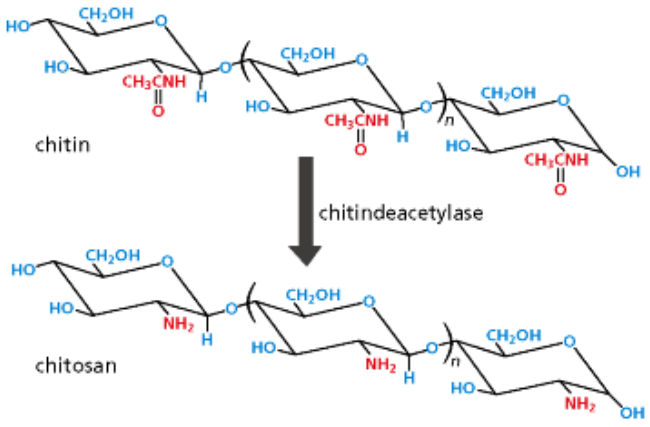

Chitosan a linear polymer of mainly anhydroglucosamine which behaves as a linear polyelectrolyte at acidic pH is nontoxic and bioabsorbable. At pH below 6.5, chitosan in solution carries a high positive charge density, one charge per glucosamine unit. Since chitosan is one of the few cationic polyelectrolytes, it is an exception to the current industrial high molecular weight polysaccharides, which are

mostly neutral or polyanionic. It was documented that oral administration of chitosan with drugs enhanced their absorption from intestines into blood in animals. Chitosan is being evaluated in a number of biomedical applications including wound healing and dressing, dialysis membranes, contact lenses, fibers for digestible sutures, liposome stabilization agents, antitumor uses and drug delivery uses and controlled-release systems. In these uses chitosan's key properties are 1) biocompatibility 2) nonantigenicity 3) nontoxicity (its degradation products are known natural metabolites) 4) the ability to improve wound healing/or clot blood 5) the ability to absorb liquids and to form protective films and coatings, and 6) selective binding of acidic liquids, thereby lowering serum cholesterol levels. But chitosan has some drawbacks, it is only soluble in aqueous medium in the presence of a small amount of acid such as AcOH and its mechanical properties are not good for some biomedical application. Therefore many researchers tried to modify its properties.

Polyethylene glycol (PEG) is a faculty of water soluble polymers with many different moleculer weights that exhibits usefull properties such as protein resistance, low toxicity and immunogenicity. PEGs have frequently been chosen as drug carriers due to biocompatibility and minimal toxicity and good solubility in water or other commen solvents. PEGs have frequently been co-polymerized with linear aliphatic polyesters like poly(lactic acid) for use in drug delivery systems and tissue engineering and also for improving the biocompatibility. Because of the good biological activities of chitosan and PEG, a combination of chitosan and PEG may have benefical effects on the biological characteristics of complex membranes. The major advantages of this approach are its simplicity, low cost and improved mechanical properties and biocompatibility. In the last few decades many different types of peroral controlled release (CR) formulations have been developed to improve clinical efficacy of the drug and patient compliance. These formulations are designed to deliver the drugs at a controlled and predetermined rate, thus maintaining their therapeuticaly effective concentrations in systems in systemic circulation for prolonged periods of time. In-vivo performance of these dosage forms depends greatly on their physical and structural properites, and consequently on their drug release mechanisms and its kinetics (Sood & Panchagnula, 1998).

CHAPTER TWO

DRUG: PROMETHAZINE HYDOCHLORIDE

2.1 The properties of Promethazine hydrochloride

Moleculer Formula of Promethazine hydrochloride is $C_{17}H_{20}N_2S$,HCl. The structural formula was shown in Figure 2.1

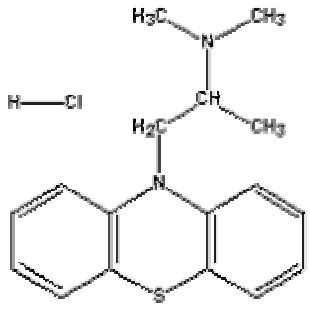

Figure 2.1 The structural formula of Promethazine hydrochloride

Promethazine is used for the treatment of allergic symptoms, often given at night because of its marked sedative effects. Drug hypersensitivity reactions have also been treated with promethazine (Weil, 1968). Promethazine is usually given orally for the treatment of allergic conditions but can be given by deep intramuscular injection or slow intravenous injection in emergencies.

Promethazine is sometimes used for its sedative effects and in some countries is marketed for this purpose, including the sedation of young children. Promethazine is used as an anesthetic premedication to produce sedation, reduce anxiety and also to reduce post operative nausea and vomiting. The drug is often given in conjunction with an opiate analgesic such as pethidine, particularly in obstetrics. Taken before traveling, promethazine is effective in preventing motion sickness. Vomiting from other causes can be treated with higher or more frequent doses.

Other less common uses: Promethazine has been used to control extrapyramidal disorders in children caused by metoclopramide (http://www.inchem.org/-documents/pims/pharm/prometha.htm) and levodopa induced dyskinesias in patients

with Parkinson's disease (Tarsy, 1975). In young children undergoing dental procedures it has been suggested (Houpt, 1985) that promethazine be used in conjunction with chloral hydrate to produce sedation as there was a lower incidence of nausea than when chloral hydrate was administered alone. In some countries, promethazine is available as a 2 % cream for the treatment of allergic skin conditions, however topical use is not recommended due to skin sensitization reactions (Martindale (1989).

2.2 Toxicodynamics of Promethazine hydrochloride

The pharmacology of promethazine is complex and for this reason toxicological mechanisms are not completely understood. Most reference texts suggest that the toxicity of promethazine is mainly due to its anticholinergic actions at muscarinic receptors. Many of the signs and symptoms of poisoning are similar to those observed with atropine. In the presence of anticholinergic effects, serious manifestations such as seizures, hallucinations, hypertension and arrhythmias have been reversed (in some cases) by the administration of physostigmine. As well as anticholinergic effects, promethazine can also exhibit toxic effects typical of antipsychotic phenothiazines. Hypotension and extrapyramidal signs may be attributable to antidopaminergic actions of promethazine (http://www.inchem.org/documents/pims/pharm/prometha.htm)

2.3 Interactions

Concomitant administration of promethazine and other CNS depressants (ethanol, narcotics, other phenothiazines and antihistamines, barbiturates and benzodiazepines) may lead to excessive CNS depression and possible respiratory depression. The combination of promethazine and tricyclic antidepressant drugs (e.g. amitriptyline, doxepin) or other drugs with anticholinergic actions, may result in additive anticholinergic effects (Hansten & Horn, 1989). Many preparations containing promethazine also contain other drugs, such as codeine, dextromethorphan,

phenylephrine and ephedrine. The toxic effects of these drugs must be considered if compound preparations have been ingested.

2.4 Drug Release

Drug release generally involves simultaneous absorption of water and desorption of drug via a swelling-controlled mechanism (Rao & Devi, 1988). The rate-controlling factor mediating drug delivery is the resistance of the polymer to an increase in volume and change in shape (Bouwstra & Junginger, 1993).

A glassy hydrogel, on coming into contact with water or any other thermodynamically compatible medium allows solvent penetration into free spaces on the surface between the macromolecular chains. When enough water has entered the matrix, the glass transition temperature of the polymer drops to the experimental temperature. The presence of solvent in a glassy polymer causes the development of stresses that are accommodated by an increase in the radius of gyration and end-to-end distance of polymer molecules, which is seen macroscopically as swelling (Gupta et al., 2002).

Controlled drug delivery applications include both sustained (over days /weeks/months/years) delivery and targeted (e.g. to a tumor, diseased blood vessel, etc.) delivery on a one-time or sustained basis. Although the field of controlled drug delivery encompasses a wide range of drugs, two key factors which stimulated the emergence of the field are the rise of proteins as potential pharmaceuticals and the demonstration that sustained release of active proteins macro-molecules rather than small polymer-permeable drugs from polymer matrices was possible.

There are two general methods for loading of hydrogels as drug carriers. In one method, the hydrogel monomer is mixed with drug, an initiator, with or without a cross-linker, and allowed to polymerize, trapping the drug within the matrix (Song, 1981). In the second approach, a preformed hydrogel is allowed to swell to equilibrium in a suitable drug solution. The drug loaded hydrogel is dried and device

is obtained. The latter method has some advantages over the first method because polymerization conditions may have deleterious effects on drug properties and the difficulties in device purification after loading and polymerization often remain (Kim et al., 1992).

CHAPTER THREE

CLAYS

3.1 General Definitions

Clay has two definitions. According to the clay mineralogist, a clay mineral is a layer silicate mineral (also called a phyllosilicate) or other mineral which imparts plasticity and which hardens upon drying or firing. The word "clay" is also used to refer to a particle size in a soil or sediment. The term is used in the U.S. and by the International Society of Soil Science for a rock or mineral particle in the soil having a diameter less than 0.002 mm (2 microns), whereas sedimentologists classify particles smaller than 0.004 mm as clay (Seki, 2003).

Clay minerals are hydrous aluminum phyllosilicates, sometimes with variable amounts of iron, magnesium, alkali metals, alkaline earths and other cations. Clays have structures similar to the micas and therefore form flat hexagonal sheets. Clay minerals are common weathering products and low temperature hydrothermal alteration products. Clay minerals are very common in fine grained sedimentary rocks such as shale, mudstone and siltstone and in fine grained metamorphic slate and phyllite.

Clay minerals include the following groups

- Kaolinite group which includes the minerals kaolinite, dickite, halloysite and nacrite.
    - Some sources include the serpentine group due to structural similarities (Bailey, 1980).
- Smectite group which includes pyrophyllite, talc, vermiculite, sauconite, saponite, nontronite and montmorillonite.

- Illite group which includes the clay-micas. Illite is the only common mineral.

- Chlorite group includes a wide variety of similar minerals with considerable chemical variation(http://en.wikipedia.org/wiki/Clay_minerals)

Montmorillonite are dioctahedral smectites in which isomorphous substitution occurs. Aluminum, iron or both ions substitutes for silicon in the tetrahedral layer. At the same time, iron or magnesium ions for aluminum in the tetrahedral layer (Newman, 1987). As a result of the isomorphous substitutions, crystalline order is reduced and structural imperfections arise (Seki, 2003).

Schematical presentation of montmorillonite was shown as below. MONTMORILLONITE(Grim, 1968).

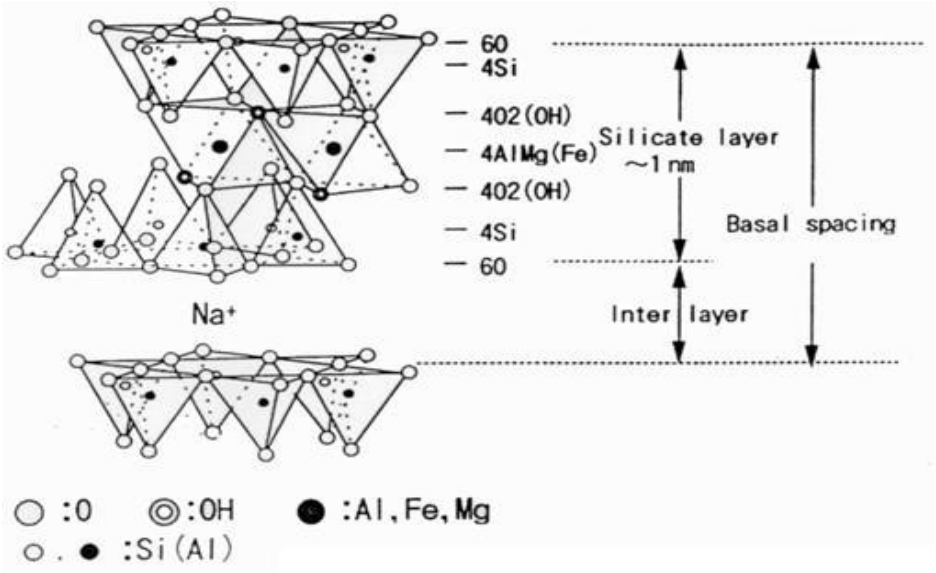

3.2 Uses of clay minerals in health care and therapeutic products

Clay minerals are included in several health care formulations. In particular, they are presented in many semisolid preparations with different functions, including stabilization of suspensions and emulsions, viscosizing and other special rheological

tasks, protection against environmental agents, adhesion to the skin, adsorption of greases, control of heat release, etc. These functions are possible because of the special disposition of clay mineral particles when dispersed in polar solvents, due to their high surface areas and colloidal dimensions. When necessary, clays are processed or even modified to exalt or change some properties and new claylike materials with special features are also synthesized. Finally, clays are frequently used concomitantly with other rheological modifiers to obtain synergic effects, influencing the stability and/or other technical properties of the health care products.(Viseras et al., 2006)

3.3 Use of clays as drug delivery systems

The need for safe, therapeutically effective and patient-compliant drug delivery systems continuously leads researchers to design novel tools and strategies. Clay minerals are widely used materials in drug products both as excipients and active agents. When administered simultaneously, drug–clay interactions have been observed and studied, but until recently were not considered as a possible mechanism to modify drug release. In recent years, and based on their high retention capacities as well as swelling and colloidal properties, clays have been proposed as very useful materials for modulating drug delivery. In particular, clays are used to delay and/or target drug release or even improve drug dissolution (Aguzzi et al., 2006)

In the 1960's it was observed that oral absorption of several drugs was reduced by co-administration of clay-based intestinal adsorbents or by the presence of clay stabilizers (e.g., suspending or emulsifying agents) in liquid formulations. Specifically, it was found that the absorption of promazine, an antidepressant agent, decreased when the drug was administered in association with antidiarrhea mixtures containing attapulgite (Sorby,1965; Sorby & Liu, 1966). Many studies have reported a decrease in bioavailability of several drugs by coadministration with antacid (Mg trisilicate), antidiarrheal (attapulgite, kaolin) and suspending agents (talc, bentonite) (Thoma et al., 1966; El-Nakeeb &Yousef, 1968; Iwuagwu & Aloko, 1992; Jain & Kakkar, 1992; Arayne & Sultana; 1993; Vatier et al., 1994). It was soon realised that

the effects of such interactions in the concomitant administration of clay minerals with active substances might not be purely negative, but could also be used to achieve technological and biopharmaceutical benefits. This was the starting point in the use of clays in modified drug delivery systems (Aguzzi et al., 2006).

3.4 Clay-Drug Interactions

Among the several approaches proposed to achieve controlled release formulations, the ion exchange process has received considerable attention from researchers in recent years (Vikas et al., 2001). It may take place by mixing solid substrates (namely ion exchangers) with ionic drugs in solution. In biological fluids, "counterions" can displace the drug from the substrate and deliver it into the body. The exchanger may be then eliminated or biodegraded (Figure 3.1).

Clay minerals are naturally occurring inorganic cationic exchangers and so they may undergo ion exchange with basic drugs in solution. Smectites, especially montmorillonite and saponite, have been the more commonly studied because of their higher cation exchange capacity compared to other pharmaceutical silicates (such as talc, kaolin and fibrous clay minerals). Nevertheless, there are several mechanisms that may be involved in the interaction between clay minerals and organic molecules, Hydrophobic interactions are observed between the clay with neutral sites and organic functional groups involved uncharged non polar (e.g., aromatic, alkyl C). Hydrogen bonding may occur between any clay with oxygen surfaces (e.g kaolinite) and between organic molecules containing amines, carbonyl carboxyl, phenylhydroxyl, heterocycle N. Protonation may generate between Aluminosilicate edge sites, Fe and Al oxides, allophane, imogolite and organic functional groups involved amines, heterocycle N, carbonyl, and carboxylate. Cation exchange are exhibited by smectite, vermiculite, illite and organic moleclues carrying amines, ring NH, heterocyclic N. For the mechanism of pH-dependent charge sites (anion Exchange usually, cation exchange rarely), mineral examples are Aluminosilicate edge sites, Fe and Al oxides, allophane, imogolite and functional groups are Carboxylate for anion exchange, amines, ring NH, heterocyclic N for cation exchange

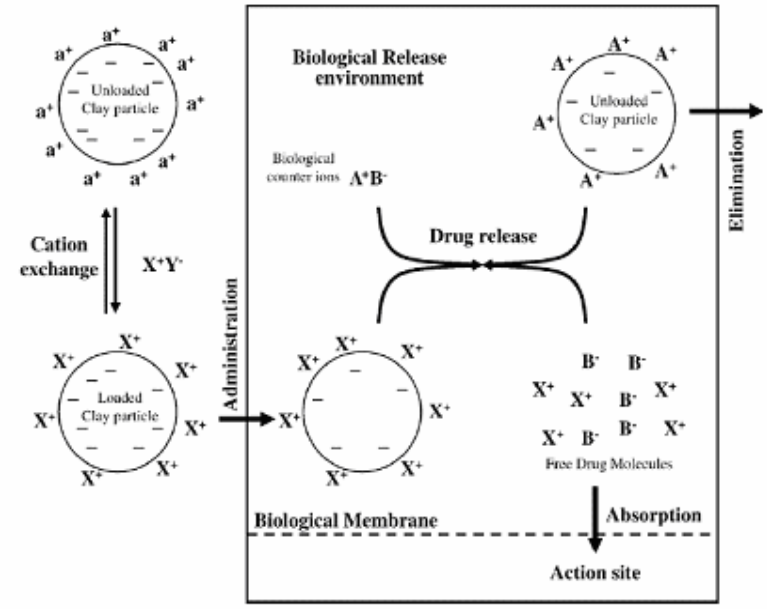

Figure 3.1 Idealization of clay–drug complexation and in vivo drug release mechanisms (clay mineral surface charge (−);compensating cations (a^+); cationic drug (X^+); drug associated anions (Y^-); in vivo counter ions (A^+); anions associated with the counter ions (B^-)).

The relevance of a specific mechanism depends on the clay mineral involved (Browne et al., 1980) as well as on the functional groups (Lagaly, 2001) and the physical–chemical properties (Tolls, 2001) of the organic compounds. Wai & Banker (1966) investigated the interaction between montmorillonite and four alkaloids, finding some differences in bonding mechanisms depending on molecule size and basicity. In some cases (methapyrilene and triethylamine) drug molecules were quantitatively bound to the clay mineral via cation exchange; besides ion exchange other mechanisms contributed to drug adsorption of larger molecules (brucine); and niacinamide was not bounded to the clay, because it mainly occurred in the neutral form. McGinity & Lach (1976) confirmed that basic molecules bonded strongly to montmorillonite; on the other hand, complexes with anionic and non-ionic drugs exhibited much weaker interaction bonds and more rapid desorption kinetics. Bonding via adsorption (Carstensen & Kenneth, 1971) and ion–dipole interactions (Kenneth & Carstensen, 1972) of acidic and non-ionised molecules with

montmorillonite were previously reported. The crucial effect of the ionisation degree of drug molecules on their interaction with smectites was then corroborated by Castela-Papin et al. (1999), using dioctahedral smectite as the adsorbent substrate. Besides smectites, other silicates were investigated to vehicle bioactive compounds. Fibrous clay minerals (attapulgite (USP 29, 2006a) (palygorskite) and magnesium trisilicate (USP 29, 2006b) (sepiolite)) and kaolinite in particular were considered because of their large surface area and/or widespread pharmaceutical application. Adsorption studies of benzoic acid and crystal violet on kaolin suggested that anionic species (benzoic acid) were adsorbed on the edge faces of the mineral, and cationic (crystal violet) on the basal plane surfaces (Armstrong & Clarke, 1971; Clarke & Armstrong, 1972). The adsorption isotherms of some β-blockers (including propranolol, acebutolol, metoprolol, nadolol, oxprenolol) (Al-Gohary et al., 1988) and mebeverine (Al-Gohary, 1991) with fibrous clay minerals and kaolinite were investigated, at different pH and temperature.

Viseras et al. (2003) used a factorial design to concomitantly investigate the influence of some critical parameters (drug concentration, temperature and adsorption time) on the interaction between timolol and sepiolite. The adsorption isotherms of 5-aminosalicilyc acid with halloysite and sepiolite samples were investigated by Viseras et al. (2005).

3.5 Applications of Clays for Release Systems

For extended release systems clays and clay minerals are used. Pharmaceutical grade clay minerals (including smectites, kaolinite and fibrous clay minerals) have been extensively applied for prolonged release, especially of basic drugs. Smectites in particular have been the most commonly used substrates, as they can retain large amounts of drug due to their high cation exchange capacity. Forni et al. (1987) developed a system based on the surface deposition of papaverine on papaverine–montmorillonite complex. This system was able to deliver the complexed papaverine according to zero order kinetics, after the release of an initial priming dose of surface deposed drug. The ability of montmorillonite to modify drug release from polymeric matrices containing cationic drugs was also reported (Forni et al., 1989).

Formulations of salbutamol (Sayed et al., 1991) and chlordiazepoxide (El-Sayed et al., 1993) with montmorillonite were described. Aguzzi et al. (2003) examined drug release in different media magnesium aluminium silicate (blend of montmorillonite and saponite (USP 29, 2006b) loaded with natural or semisynthetic tetracyclines and found a significant decrease in dissolution rate for all the complexes compared to their physical mixtures. In vivo experiments of smectite based formulations have also been reported. The effectiveness of montmorillonite–amphetamine complexes in reducing drug bioavailability in human volunteers was reported by McGinity & Lach (1977). Kahela & Hurmerinta (1979) found that the absorption of spironolactone in dogs was successfully reduced by administration of its complex with bentonite. Formulations based on phenformin-loaded bentonite were effective for 10–11 h in reducing blood sugar levels in rabbits (Maheshwari et al., 1988). Microencapsulation of terbutaline–saponite complexes with cellulose acetate butyrate provided sustained responses in human patients suffering reversible chronic air flow obstruction (El-Gindy et al., 2000; Abdel-Mohsen et al. 2001) observed an extended duration of the anaestethetic activity of lidocaine in rabbits from topical buffered poloxamer gels containing lidocaine–montmorillonite complexes. Kaolin (Delgado et al., 1994) and fibrous clay minerals (Cerezo, 2003) were successfully used to prolong the dissolution rates of amylobarbitone and timolol. Levis & Deasy (2003) studied drug release from halloysite loaded with two basic antihypertensives differing in aqueous solubility (diltiazem and propranol). Propranolol (less soluble) showed a more prolonged release effect, while for diltiazem drug-loaded halloysite tubes were coated with different polymers (including chitosan and cross-linked chitosan) to further reduce the dissolution rate.

Modified clays are also used for the extended release systems. In the development of clay based extended release formulations, modulation of the properties of the clay mineral (specific surface area, porosity, hydrophilic character, kind of exchangeable cations) may be needed to improve its affinity with the bioactive molecules. Both thermal and chemical (mineral acid dissolutions, intercalation with inorganic or organic compounds) treatments have been reported to be useful for this purpose. Heat-treated sepiolite showed controlled-release of antifungal and antibacterial isothiocyanates for sanitary protection in kitchens and food preservation (Corma

Canos et al., 2000). Bojemueller et al. (2001) found that adsorption of metolachlor onto bentonite was enhanced by calcinating the clay mineral, because of the enrichment of Al^{3+} ions at the edges of the silicate. In acid-treated clay minerals, depopulation of octahedral sheets and formation of amorphous silica was observed, providing materials with increased surface area, high porosity and acid character (Vicente-Rodríguez et al., 1996; Dékány et al., 1999). Some authors reported that acid-treated bentonites were more effective than the natural ones to reduce the release rate in extended release formulations (Fernández-Pérez et al., 2000; Villafranca-Sánchez et al., 2000). The clay mineral may also be modified with organic and inorganic compounds, acting as "pillars", by permanently holding apart the silicate layers. Inorganic and organic "pillared clays", belong to the general class of pillared layered structures (PLS), including clay minerals, phosphates and layered double hydroxides (Van Damne et al., 1995). The great advantage of these materials is that by a suitable choice of pillar agent, it is possible to modulate the porosity as well as to change the surface character from hydrophilic to hydrophobic. When the hydrophobicity of the clay mineral surface is increased, the adsorption of hydrophobic molecules is expected to increase and attain extended release in aqueous solutions. Thus, organic modified smectites are widely used as adsorbents of non-polar bioactive substances (Meier et al., 2001). The success of this approach was shown with alachlor (El-Nahhal et al., 1998), norflurazon (Undabeytia et al., 2000) and hexazinone (Celis et al., 2002). Finally, surfactant modified montmorillonites also showed higher affinity for anionic species, such as Cr(VI) derivatives, compared to the unmodified clay minerals (Krishna et al., 2000; Aguzzi et al., 2006).

3.6 Aim of the Study

Over the last two decades, the field of controlled drug delivey has been faced with two major challenges. One has been achieving sustained zero order release of a therapeutic agent over a prolonged period of time. The second of these challenges is the controlled delivery of a therapeutic drug in a pulsatile or staggered fashion. The methodologies have been offered as possible solutions to these requirements. One is the fabrication of a delivery system that releases its payload at a predetermined time.

The second is to develop a system that can respond to changes in the local environment. This kind of systems can alter the rate of drug delivery in response to stimuli including pH, temperature … etc. The conventional delivery systems have some limitations about the minimal synchronization between the required time for therapeutically effective drug plasma concentrations and the actual drug-release profile exhibited by the dosage form. The focus of scientist has shifted towards idealized drug delivery wherein the required amount of active agent is made available at the desired time and site of action in the body. In this study we aimed to use hydrogel materials as solution for these requirements that has been faced in the field of controlled drug delivery. We hope to produce materials that are not only intelligent materials but also allow the controlled release of drug of Promethazine hydrochloride. We also want to investigate drug delivery capability of some clays in two pH solutions (pH=1.2 and 7.4 (PBS) that are similar to that of gastric and intestinal fluids.

Thirdly, aim is to lengthen the duration of Promethazine hydrochloride by using hydrogel as soft material and clays as hard materials.

CHAPTER FOUR

MATERIAL AND METHOD

4. 1 Materials

Chitosan (highly viscous) was purchased from Fluka (degree of deacetylation: 75-85%, average molecular weight: 500000-700000 g mol^{-1}) as a flaked material. Crosslinking agent, epichlorohydrin was supplied from Aldrich. KH_2PO_4, $Na_2HPO_4.12H_2O$, HCl, NAOH were obtained from Riedel de Haen. KCl and NaCl were bought from Merck.

KSF montmorillonite was supplied from Fluka. Citric acid monohydrate was purchased from Carlo Erba. The sample KSF is based on calcium-bentonite which is obtained in the region of Mainburg-Landshut in Germany. Iron rich smectite (IRS) was obtained from Çamlıca village/ Mustafakemalpaşa, Bursa/Turkey.

4.2 Chemical Composition of Clays and Their Preparation

KSF montmorillonite was purchased from Fluka (Fluka No: 69866). The KSF is based on calcium-bentonite. The chemical composition of KSF is presented in Table 4.1. The chemical composition of IRS was also given in Table 4.1. IRS was dried, and then washed with distilled water a lot of times to remove any dust and other water-soluble impurities. Before use in adsorption experiments, clays were oven-dried at 378 K for 2h and stored in a desiccator for further studies.

4.3 Synthesis of Crosslinked Chitosan Film

1 g amount of Chitosan flake was dissolved in 50 mL of 2% acetic acid solution in a beaker. It will take one night to dissolve completely. The solution was poured into a Petri dish which was placed in an oven at 50°C for 18h. Chitosan was rinsed with PBS to remove any residual acetic acid. Chitosan was put into NaOH solution

(pH=10) and was subjected to stirring for several hours. Then the solution was centrifuged to remove undissolved chitosan (4000 rpm)

Different amounts of crosslinking agent, epichlorohydrin,(400, 600 and 800 µL) was added and stirred at 60 ˚C for 3.5 h. The chitosan-epichlorohydrin hydrogel film (ChitEPI) was washed with deionized water to remove any unreacted epichlorohydrin. The samples were freeze dried for 12h.

Table 4.1 The chemical composition of the clays.

Component	Percentage by weight	
	IRS	KSF
SiO_2	48.21	55.0
Al_2O_3	13.10	18
Fe_2O_3	9.97	4.0
MgO	3.17	3.0
CaO	2.59	3.0
Na_2O	0.06	<0.5
K_2O	0.47	1.5
TiO_2	0.46	-
P_2O_5	0.01	-
MnO	0.02	-
Cr_2O_3	0.04	-
Sulphate	-	5.0
Ignition Loss	21.80	10.0

4.4 Characterization of Drug Carriers

4.4.1 pH Sensivity of hydrogel films

Freeze-dried hydrogels were immersed into the different buffer solution (changing in the range pH=2-8) for 3 h at 37 ˚C. The experiments were conducted in triplicates

and the results were given as averages. The swollen samples were taken out and dried with filter paper to remove surface water and weighted. The percent of swelling values for each pH were estimated. Besides, the reversible swelling behavior of ChitEPI hydrogels were also examined. The hydrogels that equilibrated at pH 1.2 alternated between solutions at pH 7.4 and pH 1.2.

4.4.2 SEM Analysis

The surface morphologies of clays and drug loaded clays were studied using a scanning electron microscope at an accelerating voltage of 20 kV. All samples were dried and coated with gold before scanning to increase conductivity. SEM photographs were taken at different magnifications (in the range of 1000X and 5000X). The elemental composition of clays and drug loaded clays was obtained by using X-Ray Florescence (XRF system Inc 500 Digital Processing) attached to a scanning electron microscope (Jeol JSM 60 SEM). The morphology of Chit-EPI films were also examined using SEM (Jeol JSM 60) equipped with energy dispersive X-Ray(EDX). Freeze dried hydrogels were coated with gold before scanning. The micrographs were taken at various magnifications (1000X and 10000X) at 10 kV

4.4.3 FTIR Measurements

In order to determine complementary evidence for the adsorption of PHCl onto clay samples, FTIR measurements were conducted. The FTIR spectra of clay samples and drug loaded clay samples were found using KBR pellets in the region of 400-4000 cm^{-1} with Perkin Elmer FTIR spectrophotometer (Spectrum BX-II). The samples were brought to constant weights in a drying oven at 35 ºC for 24 h. 100 mg of fine KBr powder was dried at 110 ºC for 2 h and mixed with 1 mg of sample. The background spectrum of each KBr pellet was found by subtracting it from the sample spectra. Freeze dried hydrogel film and drug loaded hydrogel film were characterized by FTIR in the range 400-4000 cm^{-1} with a resolution of 2 cm^{-1}.

4.4.4 Thermal Analysis

Differential scanning calorimetry (DSC) of ChitEPI hydrogel and drug loaded Chit-EPI in the temperature range of 5-500˚C were performed at a heating rate of 10˚C/min under Ar flow of 10 mL min^{-1} in SETARAM DSC Model 111 in Darmstadt Technical University, Ernst-Berl Institute, Department of Industrial Chemistry/Germany.

4.4.5 Equilibrium and Swelling Studies of hydrogel films

The swelling behavior of ChitEPI hydrogels were measured at two temperatures (4ºC and 37 ºC) in different pH solutions (pH=1.2 and 7.4) that are similar to that of gastric and intestinal fluids. In order to prepare 250 mL of PBS, 2 g of NaCl, 1.146 g of $Na_2HPO_4.12\ H_2O$, 0.06 g of KH_2PO_4 and 0.05 g KCl were mixed with distilled water. The pH values were adjusted to 7.4 by adding phosphoric acid. The pH values were precisely checked by a pH meter (WTW pH meter, with an accuracy of ±0.1). The swollen mass of the gels were measured at intervals after drying off excess water on the hydrogel surface using tissue paper, until the equilibrium swelling was attained. The swelling values were obtained by using the following equation.

Swelling % $=100\ [(m_t-m_o)/m_o]$

where m_o is the initial mass and m_t, the final mass of the hydrogel, after incubation at time t. Data points of swelling % are means of three determinations.

4.5 Loading Studies

4.5.1 Drug Loading onto Clay samples

Adsorption experiments were conducted in a batch equilibrium technique. Promethazine hydrochloride (PHCl) stock solution (10^{-3} M) was prepared by dissolving it in distilled water. Further working solutions were freshly prepared from stock solution for each experimental run. 0.1 g of clays were weighed and mixed with 25 mL aqueous solution of PHCl at about 10^{-5} M initial concentration in a series of reagent flasks at a constant speed 150 rpm in an isothermal mechanical shaker

(MEMMERT). Samples were subjected to shaking for 8 h to reach equilibrium. Samples were withdrawn after 8 h and centrifuged at 4000 rpm for 15 min. The supernatant was decanted and the equilibrium concentration of each solution was measured by spectrophotometer (Shimadzu UV-Vis 1601 model) at the λ_{max} value 250 nm. Similar experiments were carried out by varying temperature (17, 25 and 37 ºC), solution pH.

4.5.2 Drug loading onto hydrogel film

For the determination of the amount of loaded drug, 0.1 g of freeze-dried hydrogel films were immersed in borate buffer solutions (BBS: 0.9525 g $Na_2B_4O_710H_2O$ was dissolved in 100 mL distilled water. 50 mL of this solution was mixed with 5 mL of 0.1 M HCl and diluted with distilled water to 100 mL) at room temperature. After drug loading for 1 day, the amount of drug loaded was determined by measuring the absorbance values at 250 nm using UV-Vis spectrophotometer.

4.6 Release Studies

The release of loaded drug was determined in vitro by immersing the drug loaded samples (KSF, IRS and hydrogel films) in 10 mL of PBS (pH=7.4) and HCl (pH=1.2). The polyethylene bags were mixed end-over-end (50 rpm) in a shaker with water bath at 37±0.1ºC. At regular intervals, 2 mL of solution were withdrawn and the concentration of the release of drug was determined by using UV-Vis spectrophotometer at a wavelength of 250 nm. The solutions were replenished with 2 mL fresh medium to keep the volume of release media constant. The mass released at time (M_i) was calculated from the following equation (Leach et al., 2005);

$M_i=C_iV+\Sigma C_{i-1}V_s$

where C_i is the concentration of drug in the release solution at time t, V is the total volume of release solution(10 mL) and V_s is the sample volume (2 mL).

Data points of release are the means of three determinations. The releases were given in terms of percent of release as a function of time.

CHAPTER FIVE
RESULTS

5.1 Releasing of PHCl from Clay Carriers

5.1.1 Adsorption Isotherm

Equilibrium data of PHCl onto KSF and IRS at different temperatures were shown in Figure 5.1 and 5.2. As was shown in Figure 5.1, KSF has an adsorption capacity ranging from 0.20 to 0.25 mmol/g when the solution temperature is between 290 and 310 K. This can be considered as monolayer capacities that are increased with increasing solution temperature. It is probable that the mobility of drug, PHCl increases with increasing temperature for monolayer capacity.

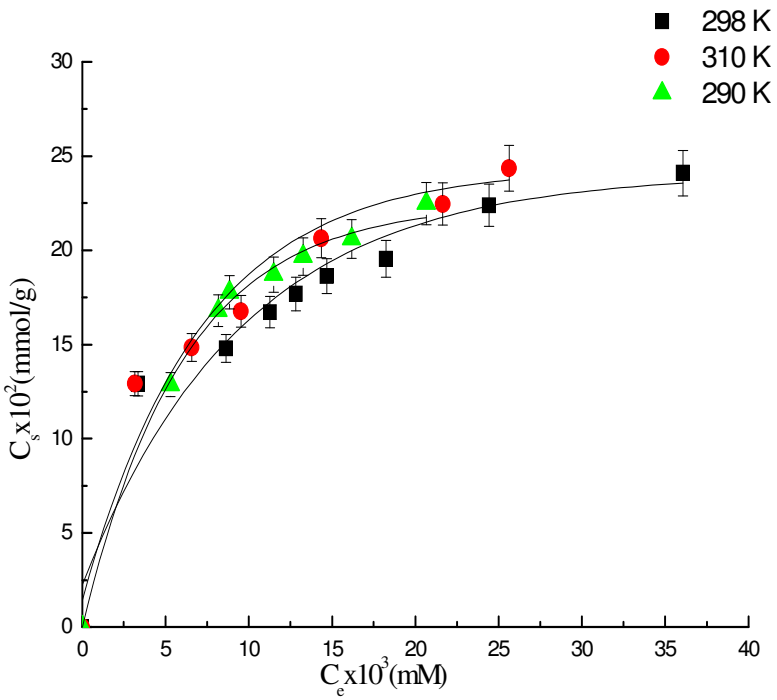

Figure 5.1 Adsorption of PHCl onto KSF at different temperatures

From Figure 5.2, the shapes of isotherms corresponding to 298 K and 310 K may be classified as L type isotherm according to Giles classification (Giles et al., 1960). However the shape of isotherm at 290 K can be suggested as C type. The L type isotherm suggests a relatively high affinity between the adsorbate and adsorbent.

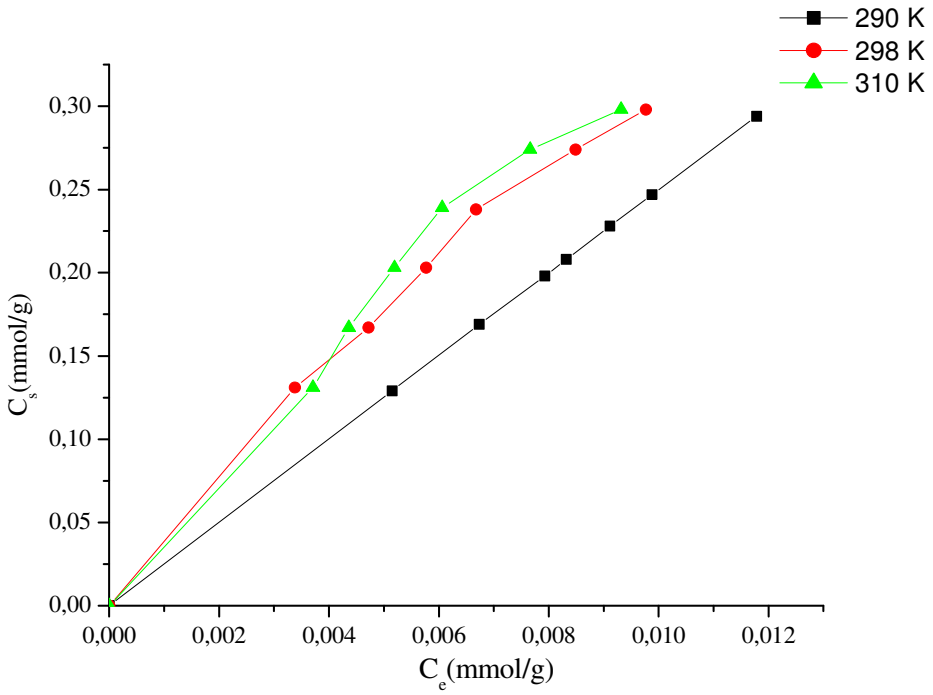

Figure 5.2 Adsorption of PHCl onto IRS at different temperatures.

The experimentally derived data were fitted to some adsorption models such as Freundlich, Langmuir and Dubinin Raduskevich (DR.). The Langmuir adsorption isotherm assumes that adsorption takes place at specific homogenous sites within the adsorbent and has found successful application in many adsorption processes of monolayer adsorption (Tunali et al., 2006). The linear form of Langmuir equation can be written by following:

$C_e/C_s = 1/C_mL + C_e/C_m$

where C_e is the equilibrium concentration (mmol L^{-1}), C_s the amount of sorbed drug (mmol g^{-1}). C_m is the monolayer adsorption capacity of the adsorbent (mmol g^{-1}). L is Langmuir constant related to adsorption energy. The values of C_m and L were obtained from the slope and intercept of the linear plot of C_e/C_s versus C_e. The results

were summarized in Tables 5.1 and 5.2. Compared to the Langmuir isotherm, the Freundlich model is generally found to be better suited for characterizing multi-layer adsorption process. Freundlich equation can be represented as follows:

$$\ln C_s = \ln K_f + n_f \ln C_e$$

K_f (relative adsorption capacity, mmol g^{-1}) and n_f (measurement of linearity) were computed from the intercepts and slopes of the straight lines of plot of $\ln C_s$ against $\ln C_e$. The results were given in Table 5.1 and 5.2 for KSF and IRS respectively.

Table 5.1 Isotherm constants for PHCl adsorption onto KSF at various temperature

	290 K	298 K	310 K
Linear form of Langmuir			
C_m (mmol g^{-1})	0.29	0.30	0.29
L	161.20	108.40	182.40
R	0.997	0.991	0.992
Linear form of Freundlich			
K_f (mmol g^{-1})	1.00	0.78	0.75
n_f	0.38	0.34	0.31
R	0.972	0.990	0.987
DR			
X_m(mol g^{-1})	1.62×10^{-3}	1.28×10^{-3}	1.07×10^{-3}
k (mol^2 J^{-2})	60.2	62.2	63.0
R	0.975	0.992	0.984
E (kJ mol^{-1})	-9.3	-14.0	-15.7

Table 5.2 Isotherm constants for PHCl adsorption onto IRS at various temperatures

	290 K	298 K	310 K
Linear form of Langmuir			
C_m(mmol/g)	1.73	1.00	1.47
L	1.45	44.02	29.63
R	0.069	0.954	0.641
Linear form of Freundlich			
K_f(mmol/g)	25.05	12.20	19.64
n_f	1.00	0.80	0.89
R	1	0.995	0.976
DR			
X_m(mol g^{-1})	0.014	0.025	0.044
k(mol^2J^{-2})	0.007	0.005	0.006
R	0.999	0.996	0.978
E(kJ mol^{-1})	-8.3	-9.6	-9.5

As can be seen in Table 5.1, both adsorption isotherms can well predict the adsorption of PHCl onto KSF with high correlation coefficients. Based on R values for PHCl adsorption onto KSF, linear form of Langmuir isotherms seems to produce a better fit in comparison with linear form of Freundlich isotherm at 290 and 298 K. The Langmuir equation is applicable to homogenous sorption, where the sorption of each molecule has equal sorption activation energy (Allen et al., 2004). It can be added that although the adsorption of PHCl onto KSF can be fitted by Langmuir or Freundlich isotherm, the assumptions of these isotherms may not be purely satisfied. According to Freundlich equation, K_f values are 0.75, 0.78 and 1.00 mmol/g for 310, 298 and 290 K respectively. The relative adsorption capacity values were increased with decreasing of temperature. It can be said that the values of n_f are smaller than 1, reflecting the favorable adsorption. For fixed values of K_f and C_e, the smaller value of n_f, the stronger is the affinity. If n_f value is smaller than 1, it indicates that increased adsorption modifies the sorbent in a way that increases the sorption capacity, as if forming new adsorption sites (Ghiachi et al., 2004).

For IRS, Freundlich equation appeared to be better conformity than Langmuir equation. As shown in Table 5.2, the greatest relative adsorption capacity value (K_f) was observed at the temperature of 290 K. The n_f values are related to the Giles classification, S, L, and C type isotherm. $n_f > 1$ correspond to S shape; $n_f = 1$ to C type and $n_f < 1$ to L type (Socias et al., 1998). This confirms that L type isotherm was observed at 298 and 310 K. However C type isotherm was observed at 290 K. This is consistent with the findings from adsorption isotherms. When n_f values are smaller than 1, this is indication of favorable adsorption. When the adsorption capacity values (C_m and K_f) obtained from Langmuir and Freundlich equation are compared, IRS has much greater capacity than that of KSF. The fit of Langmuir equation for KSF is better than Freundlich equation. However for IRS, the fit of Freundlich equation provides best fit. This may mean that adsorption of PHCl onto KSF is chemisorption, while adsorption of PHCl onto IRS is physisorption. This may be the reason why IRS has a greater adsorption capacity than KSF.

Dubinin-Radusckevich (DR) isotherm has been used to describe the sorption of PHCl onto KSF. The DR equation has the following form (Qadeer et al., 1995),

$\ln C_s = \ln X_m - k\varepsilon^2$

where X_m is DR monolayer capacity (mg g^{-1}), k is a constant related to adsorption energy; C_s is the amount of drug adsorbed per unit weight of adsorbent (mg g^{-1}) and ε is the Polanyi Potential, which can be expressed as

$\varepsilon = RT \ln (1+1/C_e)$

where C_e is the equilibrium concentration of drug in aqueous solution (mol L^{-1}), R is the gas constant and T is the temperature (K). When the plots of $\ln C_s$ against ε^2 at different temperatures were employed, the plot of the line yields k and the intercept gives the adsorption capacity, X_m.

The constant k is used to calculate the mean free energy E (kJ mol^{-1}) of sorption per molecule of the sorbate when it is transferred to the surface of the solid from infinity in the solution. The equation can be given as follow:

$E = -(2k)^{-0.5}$

The calculated values were presented in Tables 5.1 and 5.2. The importance of magnitude of E value is to give some information about the type of adsorption. If the magnitude of *E* is between 8 and 16 kJ mol^{-1}, the adsorption process follows by ion-exchange, while for the values of E<8kJmol^{-1}, the adsorption process is of a physical nature (Bekci et al., 2006). For KSF, X_m values increased from 1.07 x 10^{-3} to 1.62 x 10^{-3} mg g^{-1} with decrease in temperature from 310 to 290 K. As was seen from Table 5.1 that E values were found to be -9.3, -14.0 and 15.7 kJ mol^{-1} for 290, 298 and 310 K respectively. These values correspond to ion exchange. But, they are so close to the range of chemisorption in terms of the mean free energy values. With an increase of the temperature from 290 to 310 K, the mean free energy values also increases. According to DR equation, adsorption capacity values were equal to 1.62 x 10^{-3}, 1.28 x 10^{-3} and 1.07 x 10^{-3} mol/g for 290, 298 and 310 K respectively. It can be derived that the adsorption capacity values of DR isotherm raised as the solution temperature decreased. These findings are also consistent with K_f values obtained from Freundlich equation. In comparison with C_m monolayer capacity values obtained from Langmuir equation similar results were not observed.

For PHCl sorption onto IRS sample, the mean free energy values obtained in this study are -8.3, -9.6 and -9.5 kJ mol^{-1} at 290, 298 and 310 K respectively. This indicates a boundary of a physisorption and the predominance of van der Waals forces. This results in consistent with previous findings. X_m values are increasing with the increase in temperature.

5.1.2 Kinetics of Adsorption

The mass transfer of adsorption often involves many controlling mechanism of which the individual contribution may not be clearly recognized, at the same time during the course to approach adsorption equilibrium (Chang et al., 2004). In this respect, for simplicity, several kinetic models such as pseudo-first-order kinetic model, pseudo-first-order model and intraparticle diffusion model were used to describe the adsorption kinetic by means of lumped analysis of kinetics data.

5.1.2.1 Pseudo-first-order model

Pseudo-first-order equation can be expressed as below;

$1/q_t = (k_1/q_1)\ (1/t) + 1/q_1$

where k_1 is the pseudo-first-order rate constant (min^{-1}), q_t is the amount of drug adsorbed (mg g^{-1}) at different times t, q is the maximum adsorption capacity (mgg^{-1}) for pseudo-first-order adsorption (Özcan & Özcan, 2004). Plots of $1/q_t$ versus 1/t for the adsorption onto KSF were employed to generate the intercept values of $1/q_1$ and the slope of k_1/q_1. The values of k_1, q_1 and the correlation coefficients were given in Tables 5.3 and 5.4.

5.1.2.2 Pseudo-second-order-model

The pseudo-second-order kinetic equation is as follows;

$t/q_t = 1/\ (k_2 q_2^{\ 2}) + t/q_2$

where q_t is described earlier, k_2 is the pseudo-second-order rate constant; q_2 is the maximum adsorption capacity (mg g^{-1}) for the second order adsorption process (Ho

& Ofomaja, 2006). The plots for PHCl sorption onto KSF and IRS were presented in Figures 5.3 and 5.4 respectively. From the slope and intercept values, q_2 and k_2 values were calculated and the results were given in Tables 5.3 and 5.4.

5.1.2.3 Intraparticle diffusion model

For the intraparticle diffusion model, the following expression was used as

$q_t = K_p t^{1/2} + C$

where K_p is the intraparticle diffusion rate constant (mg g^{-1} $min^{-1/2}$), C is the intercept. When q_t is plotted against 1/T, a straight line with slope K_p and intercept. Intraparticle diffusion plots for adsorption PHCl onto KSF and IRS were shown in Figures 5.5, 5.6, 5.7, 5.8, 5.9 and 5.10. The calculated parameters were summarized in Tables 5.3 and 5.4. The values of the intercept give an idea about the boundary layer thickness (larger the intercept, the greater is the boundary layer effect) (Özcan & Özcan, 2004). It was also observed that intercept values increased as the solution temperature increased. Presumably, it may be said that at higher temperatures, the boundary layer effect is the greater. The same result is reported in Özcan & Özcan's report (Özcan & Özcan, 2004). Intraparticle diffusion plots do not pass through the origin. This may be indicative of some degree of boundary layer control. This also implies that the intraparticle diffusion does not only contribute to the rate determining step, but also other process may control the rate of adsorption simultaneously. For PHCl sorption onto KSF, the K_p values are calculated to be as 0.13, 0.06, 0.03 mg g^{-1} $h^{-1/2}$. This confirms that adsorption is also governed by the diffusion within pores of the adsorbent.

When the correlation coefficients of pseudo-first-order and pseudo-second-order model were compared, the latter is better than the previous one. It can be reached that adsorption system obeys the second order kinetic model. As given in Table 5.3, the maximum adsorption capacity values for pseudo-second-order kinetic model was not affected by temperature drastically. However an increase in temperature increases the rate constant of pseudo-second-order-adsorption from 4.3×10^{-3} to 12.9×10^{-3}(g mg^{-1} min^{-1}).

For IRS sample, the correlation coefficients at different temperatures for pseudo second order kinetic model were found to be 1. This indicates that the pseudo-second order kinetic model provides best fit to experimental data. Namely, the adsorption of PHCl on IRS follows pseudo-second-order kinetic model. When the adsorption capacity values calculated from pseudo-second-order kinetic model were examined, the greatest q_2 value was obtained at 290 K. This result is compatible with previous one computed from Freundlich equation.

The correlation coefficient values for intraparticle diffusion model are lower than that of pseudo-first-order and pseudo-second-order kinetic models. Since the plots of the amount of adsorbed versus the square root of time don't pass through the origins, the intraparticle diffusion model is not the only rate-limiting step, but also other kinetic models may control the rate of adsorption.

The rate constant values (k_2) increase from 0.018 to 0.027 g mg min^{-1} with the increasing of temperature from 290 K to 310 K. This result supports that adsorption follows a physisorption mechanism; increasing temperature increases the rate of approach to equilibrium (Ho and McKay, 1998;Tunali et al., 2006).

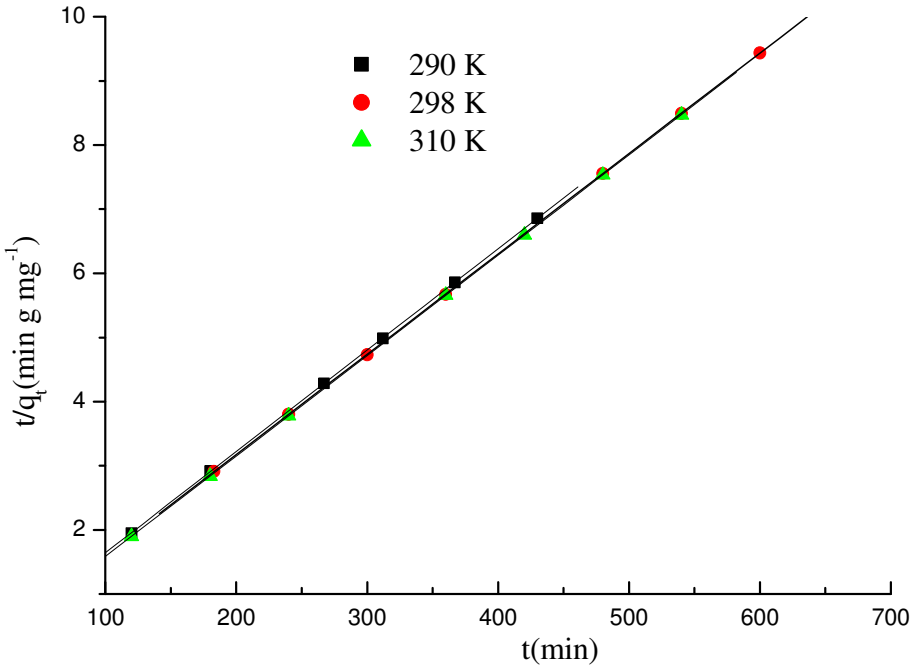

Figure 5.3 Second order plot for adsorption of PHCl onto KSF at 290, 298 K and 310 K

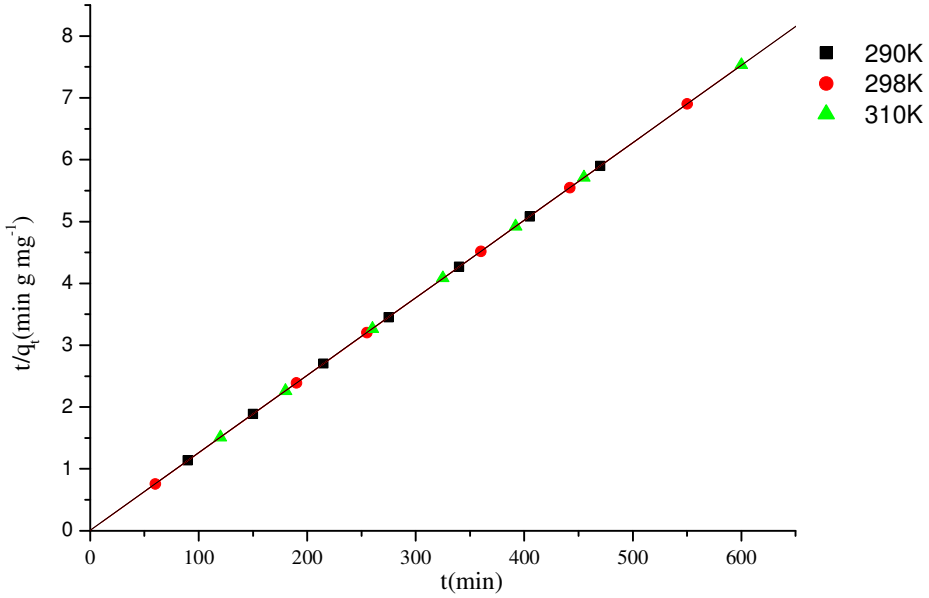

Figure 5.4 Second order plot for adsorption of PHCL onto IRS at 290, 298 K and 310 K

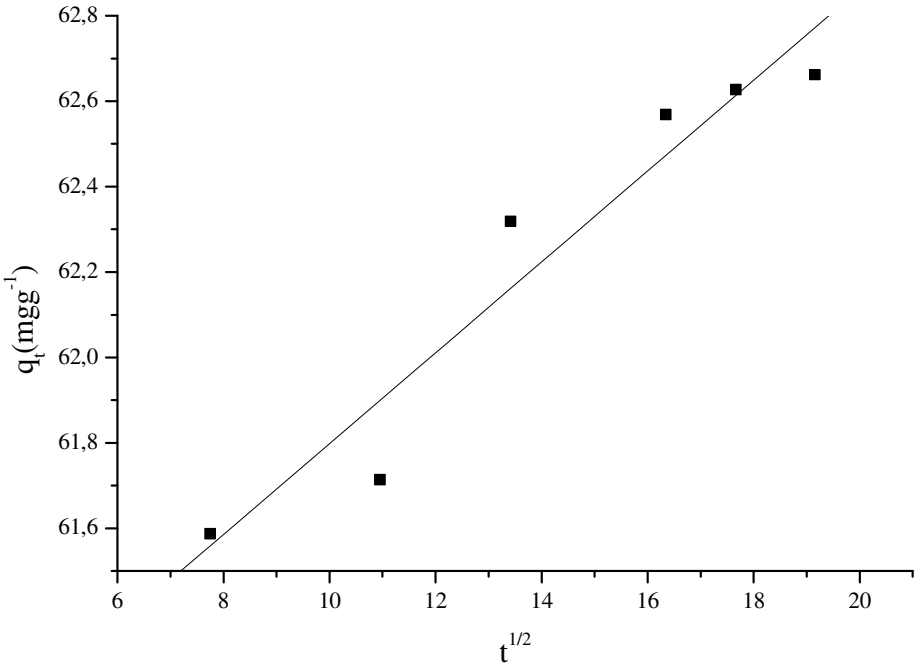

Figure 5.5 Intraparticle diffusion plot for adsorption PHCl onto KSF at 290K

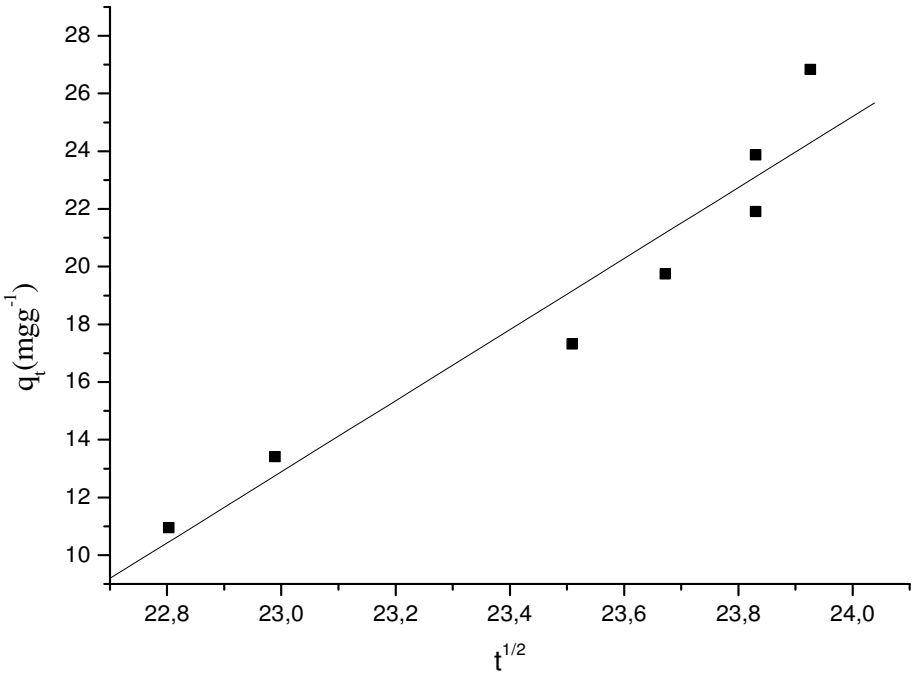

Figure 5.6 Intraparticle diffusion plot for adsorption PHCl onto KSF at 298K

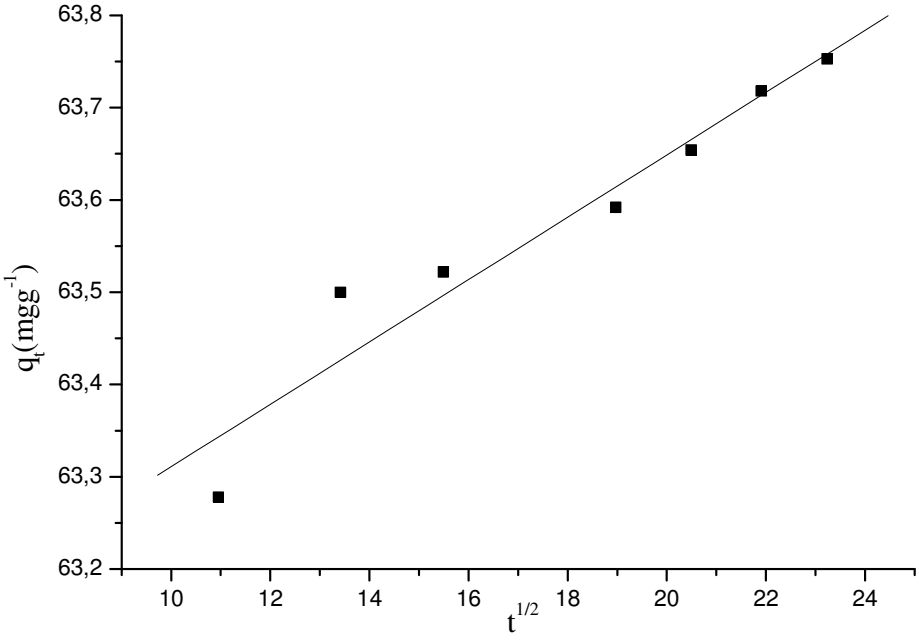

Figure 5.7 Intraparticle diffusion plot for adsorption PHCl onto KSF at 310K

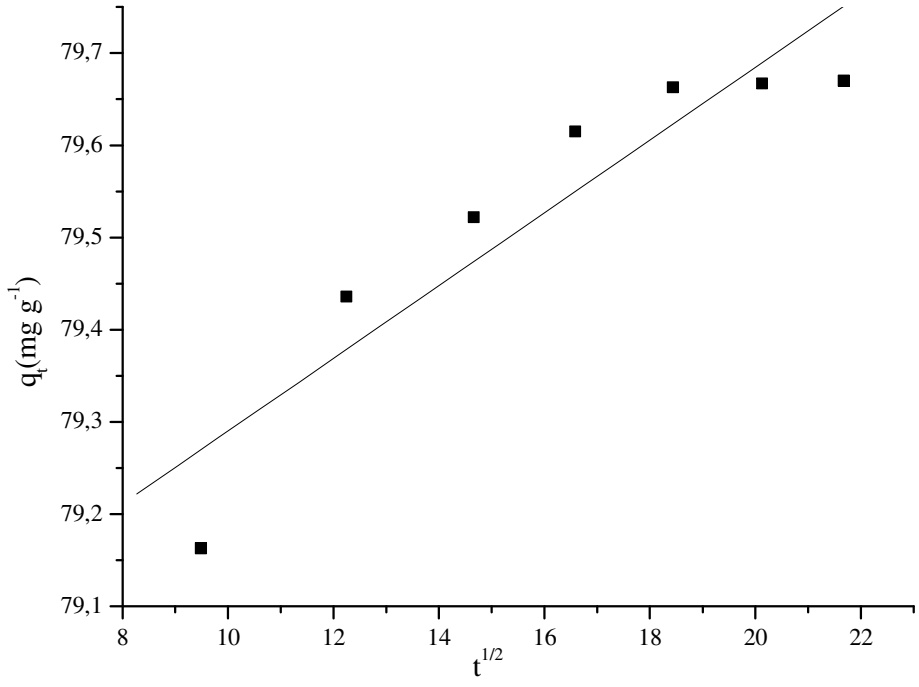

Figure 5.8 Intraparticle diffusion plot for adsorption of PHCl onto IRS at 290 K

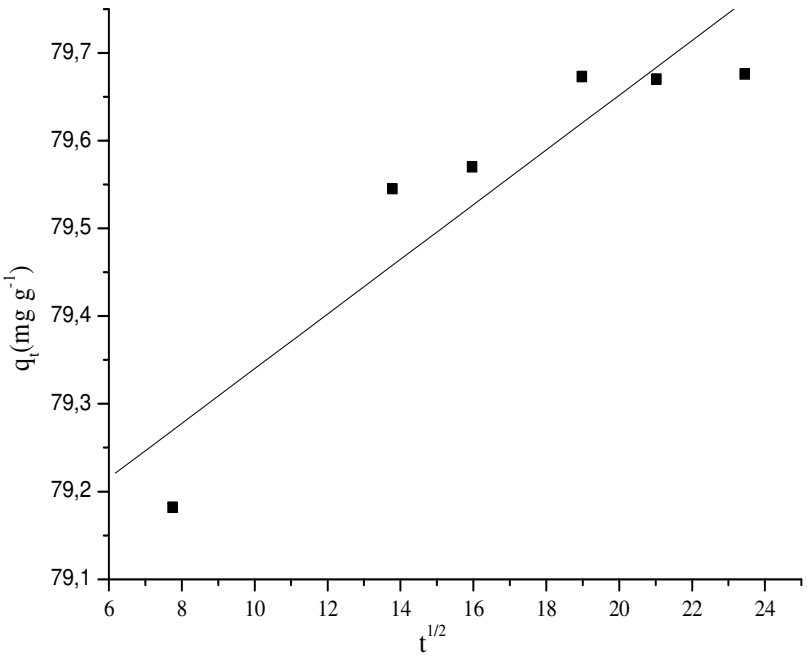

Figure 5.9 Intraparticle diffusion plot for adsorption of PHCl onto IRS at 298 K

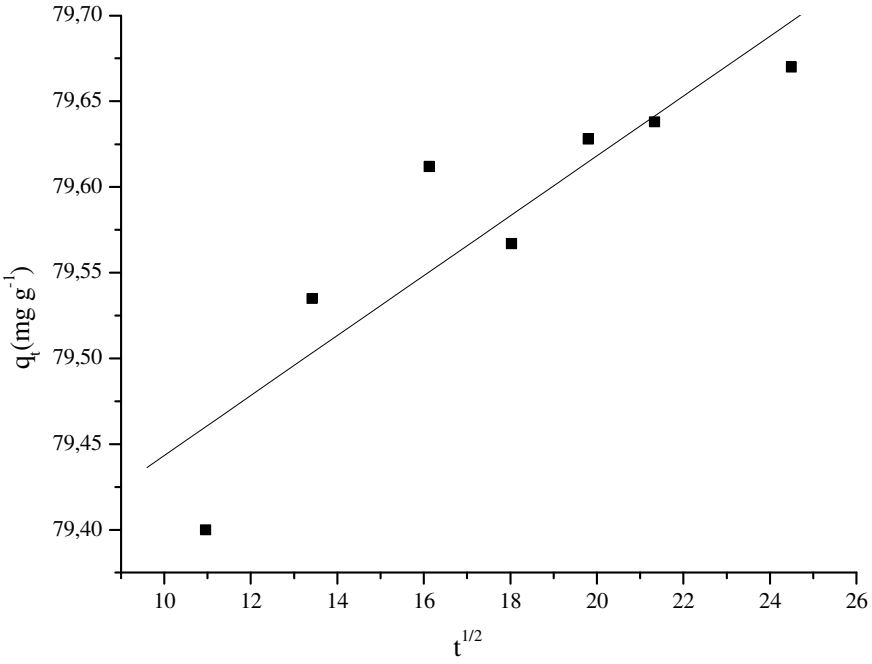

Figure 5.10 Intraparticle diffusion plot for adsorption of PHCl onto IRS at 310 K

Table 5.3 Kinetic parameters for the adsorption of PHCl onto KSF at various temperatures

	290 K	298 K	310 K
Pseudo First-Order			
k_1(min^{-1})	0.89	3.11	1.04
q_1(mg g^{-1})	17.12	63.90	63.83
R_1	0.947	0.959	0.973
Pseudo-Second-Order			
k_2 (g mg^{-1} min^{-1})	4.3 $x10^{-3}$	5.7 $x10^{-3}$	12.9 $x10^{-3}$
q_2 (mg g^{-1})	63.21	63.90	63.86
R_2	0.999	1	1
Intraparticle Diffusion			
K_p(mg $g^{-1}min^{-1/2}$)	0.13	0.06	0.03
C (mg g^{-1})	60.17	62.19	62.97
R_p	0.960	0.895	0.964

Table 5.4 Kinetic parameters for the adsorption of PHCl onto IRS at various temperatures

	290 K	298 K	310 K
Pseudo First-Order			
k_1(min^{-1})	0.74	0.42	0.47
q_1(mg g^{-1})	79.81	79.75	63.98
R_1	0.996	0.992	0.966
Pseudo Second Order			
k_2(g mg min^{-1})	0.018	0.026	0.027
q_2(mg g^{-1})	79.81	79.75	79.75
R_2	1	1	1
Intraparticle Diffusion			
K_p(mg g^{-1} $min^{-1/2}$)	0.04	0.03	0.02
C (mg g^{-1})	78.90	79.03	79.27
R_p	0.925	0.922	0.898

5.1.3 FTIR Analysis

FTIR was applied to identify the surface groups that are responsible for drug adsorption. Figure 5.11 illustrates the spectra of PHCl, KSF and PHCl loaded KSF. In the spectrum of KSF, the absorption bands at 3620 cm^{-1} is typical for smectites with high amount of Al in the octahedral (Madejova, 2003). The bands at 1633 and

481 cm^{-1} are assigned to the stretching vibrations of clay Si-O within the layer. As can be seen from Figure 5.11, the intensity of the band at 481 cm^{-1} increased after adsorption with PHCl. The stretching absorption band of Al-O-Si seemed at 531 cm^{-1} is diminished after adsorption with PHCl. A band at 3400 cm^{-1} in the spectra of KSF is due to stretching vibrations of the OH groups and shifted to 3428 cm^{-1} in the spectra of PHCl loaded KSF. The band at 1633 cm^{-1} also corresponds to the OH deformation of water.

As shown in Figure 5.11, N-H stretching vibrations in the quaternary ammonium group of the drug molecule appear at 2375 cm^{-1}. After PHCl treatment, this band can not be seen easily. Furthermore, the band located at 1456 cm^{-1} in the spectra of PHCl can be suggested as skeletal vibrations of the aromatic ring. The most important difference between two spectra (KSF and PHCl loaded KSF) is the band at 1468 cm^{-1}, which can be attributed to substituted aryl compound. This may also be acceptable evidence that PHCl is not only attached on the surface of KSF, but also may form chemical bonds with some groups such as Si-O within montmorillonite.

FTIR spectra of IRS, PHCl and IRS-PHCl were shown in Figure 5.12. From the spectrum of IRS, the absorption band at 3620 cm^{-1} can be attributed to lattice OH stretching vibration. Bound water stretching vibration was observed at 3422 cm^{-1}. After loading, lattice OH stretching vibration is located at 3625cm^{-1}. However bound water stretching vibration was shifted to 3434 cm^{-1}. It may be due to weak interaction between PHCl and OH group of water. Water bending vibration was detected at 1636 cm^{-1}. This band shifted to 1640 cm^{-1} when the drug is loaded. A strong band at 1033 cm^{-1} is typical for smectites and can be ascribed to Si-O stretching vibration. This broad band can be seen at 1046 cm^{-1} in the spectrum of IRS-PHCl. As can be seen from the spectrum of PHCl, there is an absorption band at 1456 cm^{-1} due to substituted aryl compound. After loading of PHCl, this band appears at 1462 cm^{-1}. From the spectrum of IRS-PHCl, it can be reached that loading of PHCl is confirmed by the appearance of absorption bands at 1462 cm^{-1}.

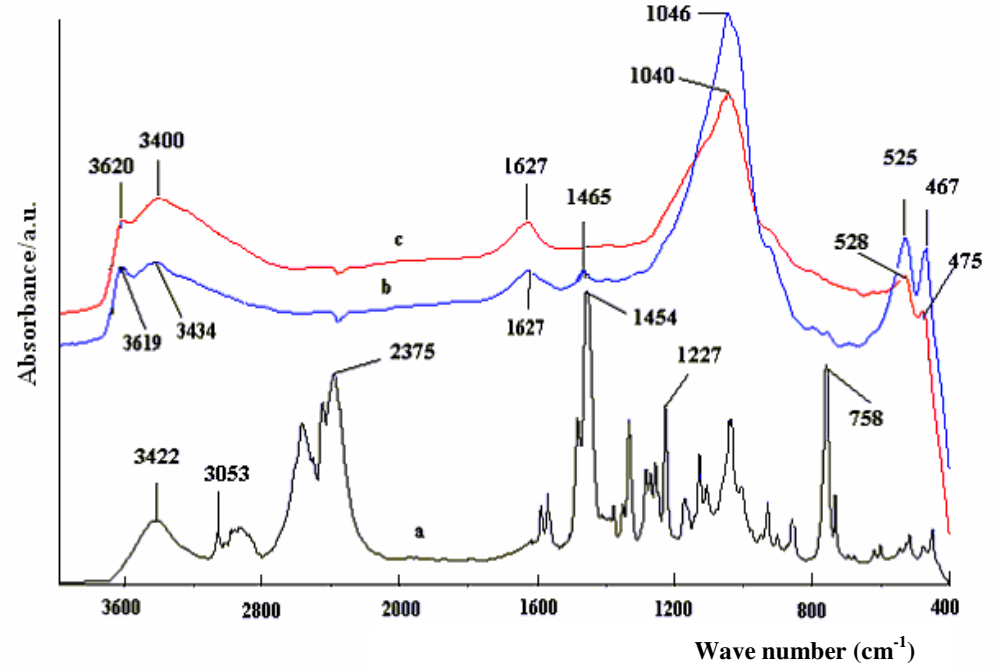

Figure 5.11 FTIR spectra of PHCl (a), adsorbed onto KSF (b), KSF (c)

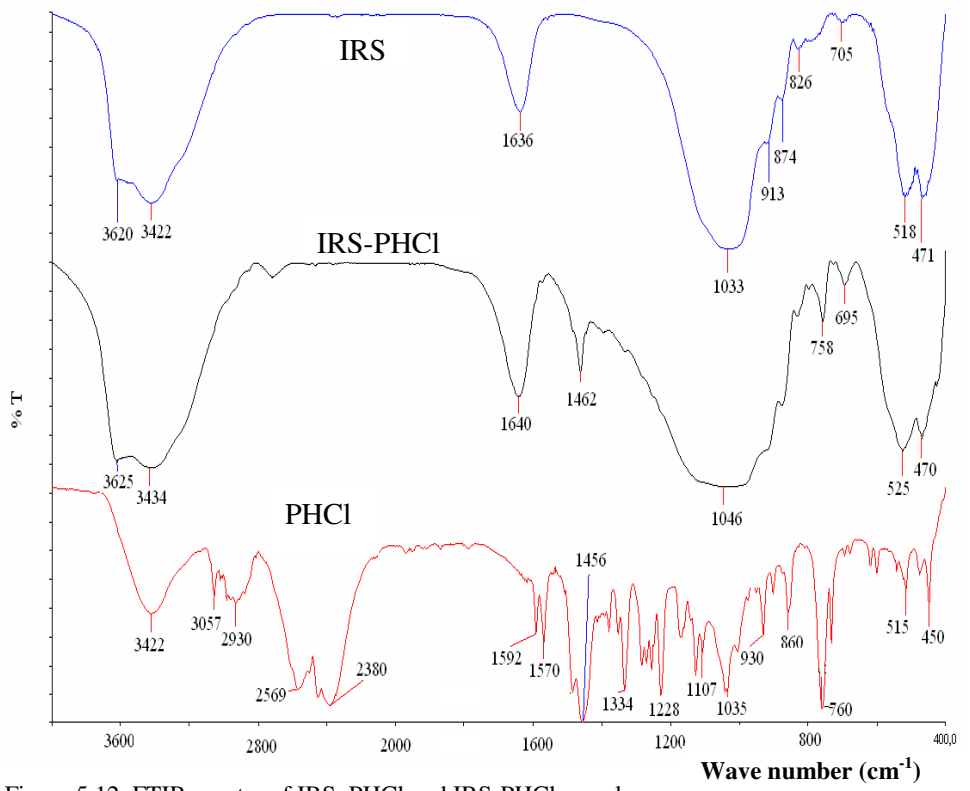

Figure 5.12. FTIR spectra of IRS, PHCl and IRS-PHCl samples.

5.1.4 SEM Analysis

The morphologies of KSF clay and PHCl loaded KSF was examined by scanning electron microscopy, SEM (Figure 5.13). The silicate particles disperse in various directions and appear to be flexible. As can be seen from Figure 5.13, the length and thickness of the layers have different dimensions and can not be considered as homogenous. The chemical content of the clay was determined using the semiquantitative EDS data (Figure 5.13 g, h, which showed that the natural clay is composed of MgO, Al_2O_3, SiO_2, K_2O, CaO, and Fe_2O_3. After adsorption of PHCl onto KSF, some white grains appear on the surface of the layer structure of KSF. White grains may contain a big amount of drug molecules. This idea can be supported by EDS analysis of point A (white grains) and point B (dark part) shown in the micrographs of e. The EDS analysis of point A (white grains) and point B (dark place) was presented in Figure 5.13. According to Figure 5.13b, the percentage of C atom in point A and point B was found to be 28.98 and 17.98 % respectively. This may indicate that the percentage of drug particles in white grains is quite high. The reason of high level of C atom in point B may be due to deposition of the powder samples on a carbon film for SEM analysis.

The morphologies of IRS and IRS-PHCl were revealed by Scanning Electron Microscopy. As shown in Figure 5.14, IRS is consisting of plates with different size. SEM image of IRS shows the layered crystalline microstructure of bentonite. The silicate particles whose distributions are heterogeneous disperse in various directions and seem to be flexible. The length and thickness of the layers seem to have different dimensions. After loading of PHCl, IRS has gained a more compact structure due to interaction between bentonite and aqueous solution of drug solution. As a result of treating of IRS with drug molecules, some agglomerates can also been seen.

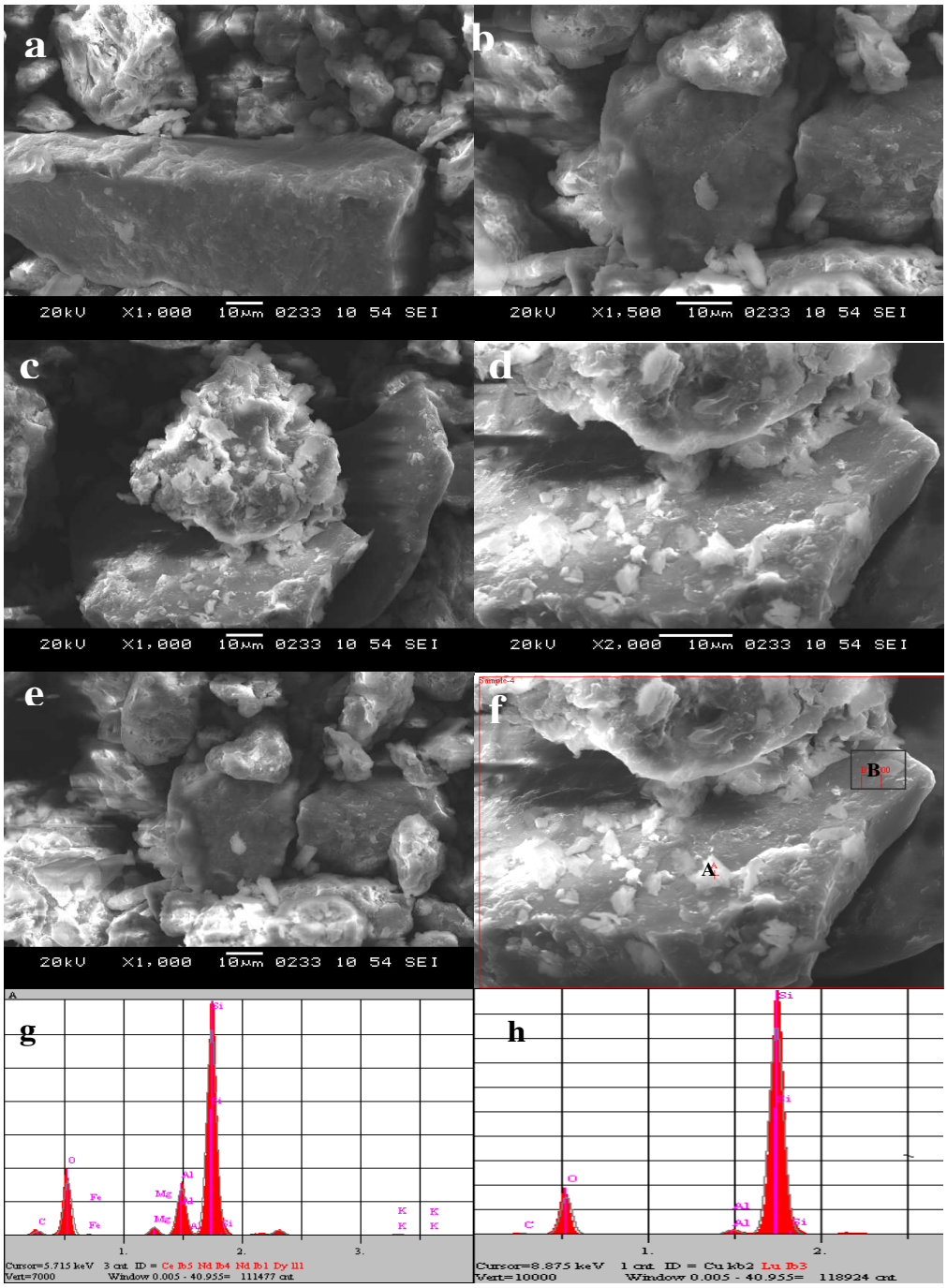

Figure 5.13 SEM Micrographs of a) KSF (x1000) b)KSF (x1500) c) PHCl loaded KSF (x1000) d) PHCl loaded KSF (x1500) e) PHCl loaded KSF (x1000) f) PHCl loaded KSF (x2000) g) EDS analysis of point A h) EDS analysis of point B

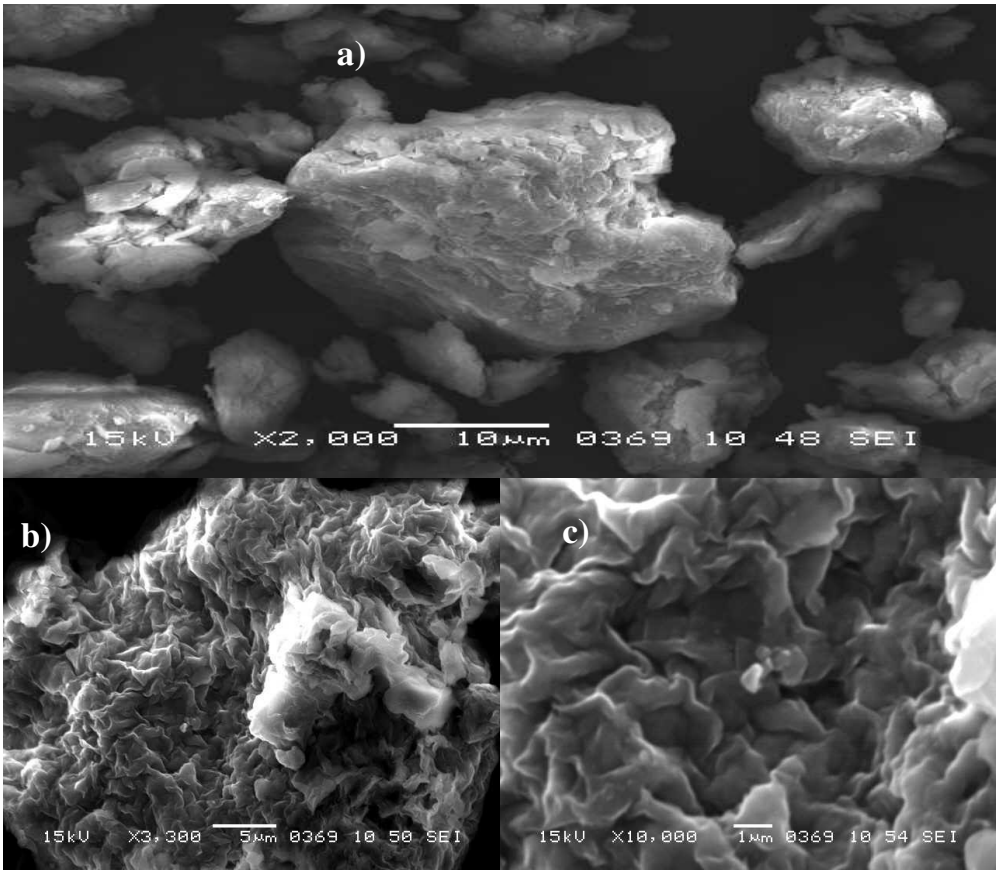

Figure 5.14. SEM images of a) IRS (x2000) b) IRS-PHCl (x3300) c) IRS-PHCl (x10000)

5.1.5 pH Effect

Some experiments were performed to find the optimum pH on the PHCl adsorption onto KSF and IRS using different initial pH values changing from 2 to 10. The amount of PHCl adsorbed was plotted against the equilibrium pH values. As was shown in Figure 5.15, the optimum pH value was found to be about 3.4. Since KSF is an acidic adsorbent, the equilibrium pH values are quite low. It can be realized that the amount of PHCl adsorbed increased until the pH value of 3.4. The pHs beyond that value, a decrease in adsorption was observed. It is clear that adsorption process is dependent on the pH of the solution. In the equilibrium pH range studied, PHCl becomes positively charged due to acidic media. Beyond the pH of 3.4, a decrease in

adsorption takes place owing to decrease of degree of ion-exchange between cationic drug and H^+ protons which exist on the KSF surface. Because at low pH values, silanol groups on the clay surface becomes more protonated. Moreover, according to the findings from DR isotherm and thermodynamic studies, the dominant adsorption type controlling adsorption was ion-exchange.

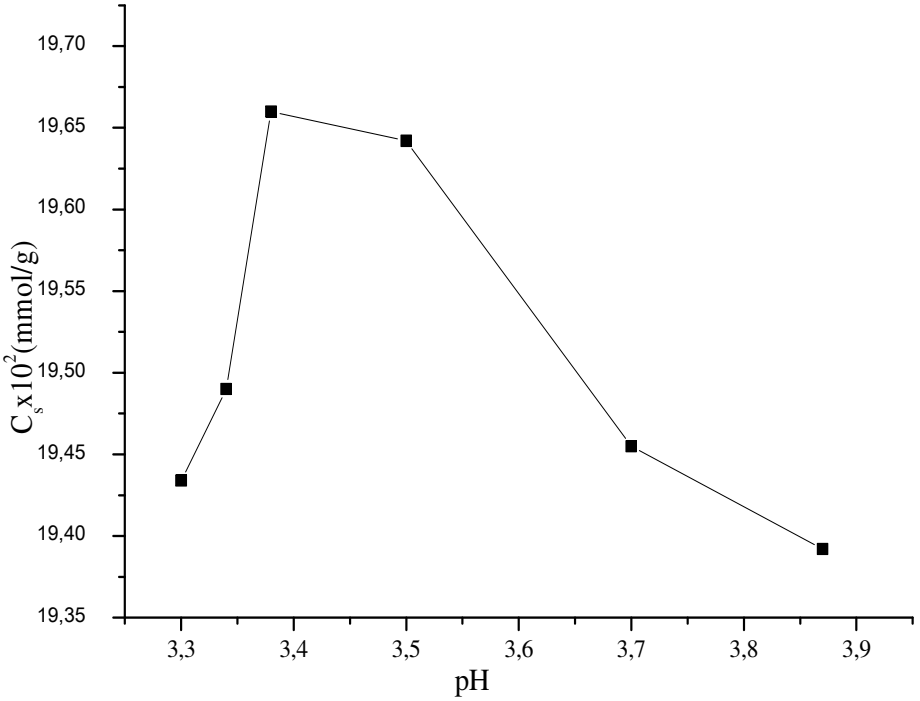

Figure 5.15 The effect of pH for the adsorption of PHCl onto KSF

The variation of PHCl adsorption onto IRS over a pH range of 1.5 and 6.5 was given in Figure 5.16. It shows the maximum adsorption of PHCl taking place at about pH 5. Between the pH values of 5 and 6.5, the amount of adsorbed was decreasing with the increasing of pH values. According to Figure 5.16, it can be claimed that adsorption is not highly dependent on pH of the solution.

In clay-aqueous systems the potential of the surface is determined by the activity of ions (e.g., H^+ or pH), which react with the mineral surface. For clay minerals the potential determining ions are H^+ and OH^- and complex ions formed by bonding with

H^+ and OH^-. The broken Si–O bonds and Al–OH bonds along the surfaces of the clay crystals result in hydrolysis (Tahir & Rauf, 2006). At low pH the reaction might be

$$SiOH + H^+ \rightarrow SiOH_2^+$$

At high pH values, the reaction may be

$$SiOH + OH^- \rightarrow SiO^- + H_2O$$

At lower pH values, clay had net positive charge and therefore it repels positively charged Promethazine which is the dominant species at low pH. Besides at high pH values the species of neutral Promethazine will also increase due to increase of degree of ionization. Consequently, at higher pH values, positive charge on the surface of the clay decreases. Therefore it doesn't favor the adsorption of drug within this range (5 and 6.5).

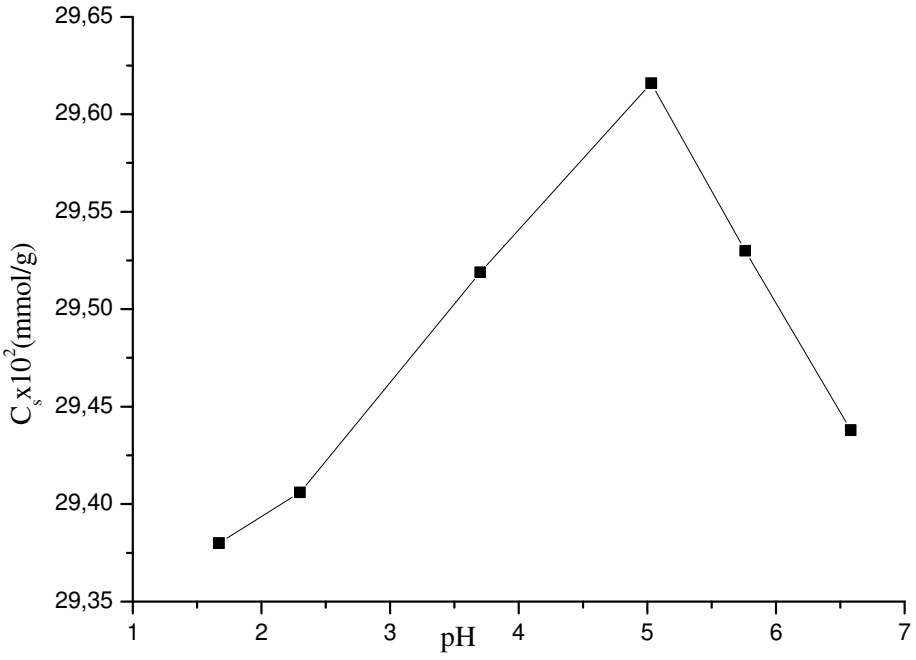

Figure 5.16 The effect of pH for the adsorption of PHCl onto IRS

5.1.6 Thermodynamic parameters

In order to find the activation energy values of adsorption process, the Arrhenius equation was used in the following:

$$\ln k = \ln A - E_a/RT$$

where E_a (the minimum energy that requires for the reaction to proceed) is the activation energy of sorption process, A is the Arrhenius constant, T is the solution temperature, k, is the rate constant for the second order kinetics. The activation energy (E_a) and Arrhenius constant (A) were estimated from the slope and intercept of the plot of ln k versus 1/T (Figure 5.17 for KSF and 5.18 for IRS). The magnitude of activation energy gives information about the type of adsorption. The physisorption process usually has energies in the range of 5-40 kJ mol^{-1}, while higher activation energies (40-800 kJ mol^{-1}) suggest chemisorptions (Nollet et al., 2003). The value of E_a was found to be 41.7 kJ mol^{-1} and 14.3 kJ mol^{-1} for PHCl sorption onto KSF and IRS respectively. For KSF, it can be said that, it is difficult to be sure of that the type of adsorption is considered as chemisorption, since the activation energy value obtained from experimental study is only slightly larger than 40 kJ mol^{-1}. Presumably, it indicates an ion-exchange process for PHCl adsorption onto KSF. This conclusion was also supported by DR isotherm. For IRS, adsorption can be suggested as physical adsorption, supporting previous findings.

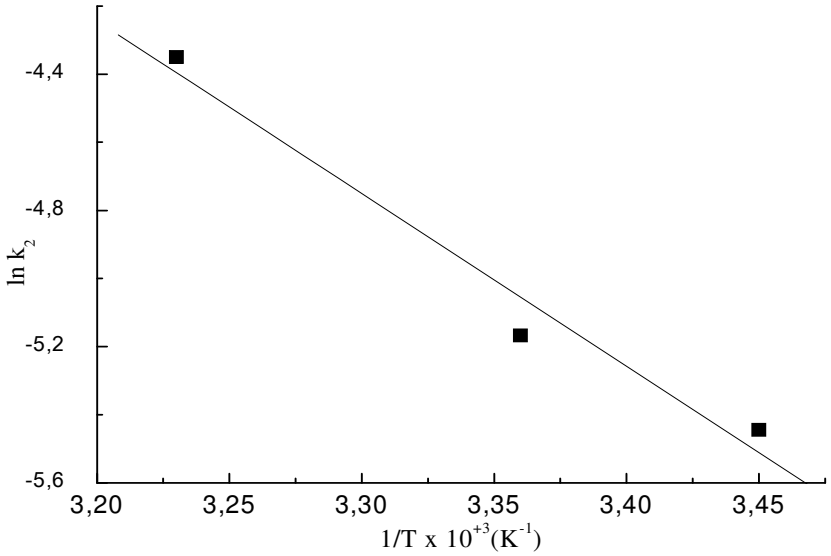

Figure 5.17 Arrhenius plot for PHCl adsorption onto KSF

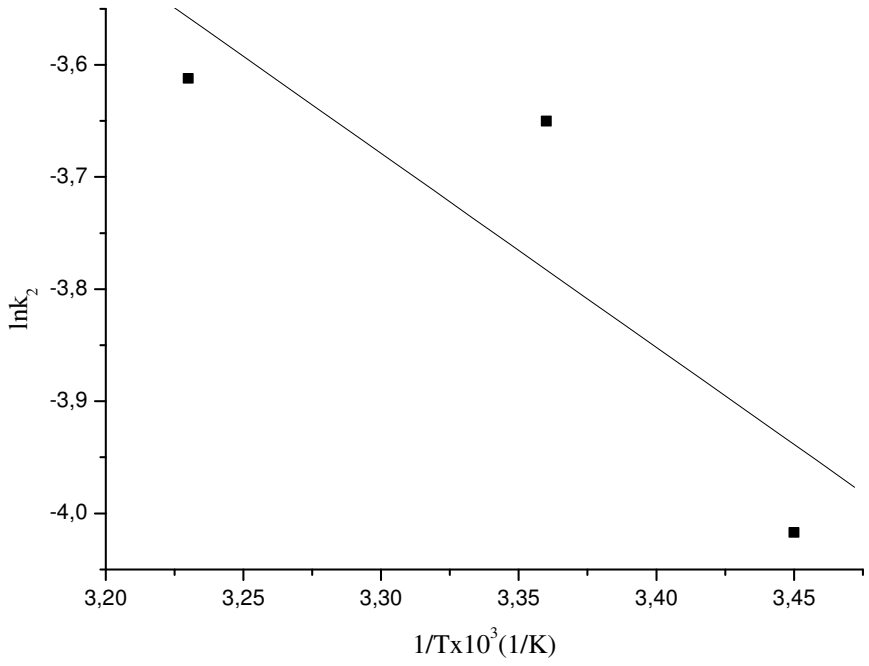

Figure 5.18 Arrhenius plot for PHCl adsorption onto IRS

In order to understand better the effect of temperature on the adsorption, it is important to study the thermodynamic parameters such as standard Gibbs free energy change, (ΔG°), standard enthalpy change ΔH^{o}, and standard entropy change, ΔS^{o}. The Gibbs free energy of adsorption was estimated from the following equation

$\Delta G^{o} = -RT\ln K_c$

Standard entropy change ΔS^{o} and standard enthalpy change, ΔH^{o}, of adsorption process can be found from van't Hoff equation as shown below

$\ln K_c = - \Delta H^{o}_{ads}/RT + \Delta S^{o}/R$

where R is the gas constant, K_c is adsorption equilibrium constant computed using the following equation

$K_c = C_s/C_e$

where C_s is the amount of adsorbed by adsorbent, and C_e is the equilibrium concentration of drug in the solution. The plot of $\ln K_c$ versus 1/T should be linear. ΔH^{o} and ΔS^{o} were computed from the slope and intercept of van't Hoff plots of $\ln K_c$ versus 1/T.

The results for PHCl sorption onto KSF and IRS were given in Tables 5.5 and 5.6 respectively. The van't Hoff plot for adsorption of PHCl onto KSF and IRS were presented in Figures 5.19 and 5.20.

Table 5.5 Thermodynamic parameters for PHCl adsorption on KSF

T/K	K_c	ΔG°/kJ mol^{-1}	ΔS°/kJ $mol^{-1}K^{-1}$	ΔH°/kJmol^{-1}
290	6.28	-4.43	0.19	49.74
298	11.59	-6.07		
310	23.86	-8.18		

Table 5.6 Thermodynamic parameters for PHCl adsorption on IRS

T(K)	K_c	ΔG^{o} (kJ mol^{-1})	ΔS° (kJ mol^{-1} K^{-1})	ΔH° (kJ mol^{-1})
290	39.17	-8.84		
298	36.62	-8.65	0.02	-3.20
310	35.86	-9.45		

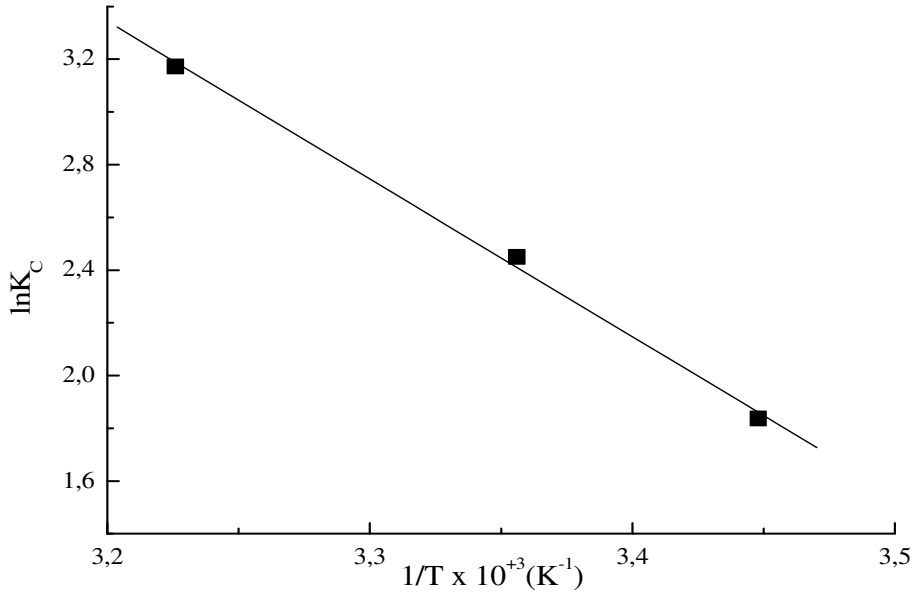

Figure 5.19 van't Hoff plot for the adsorption of PHCl onto KSF

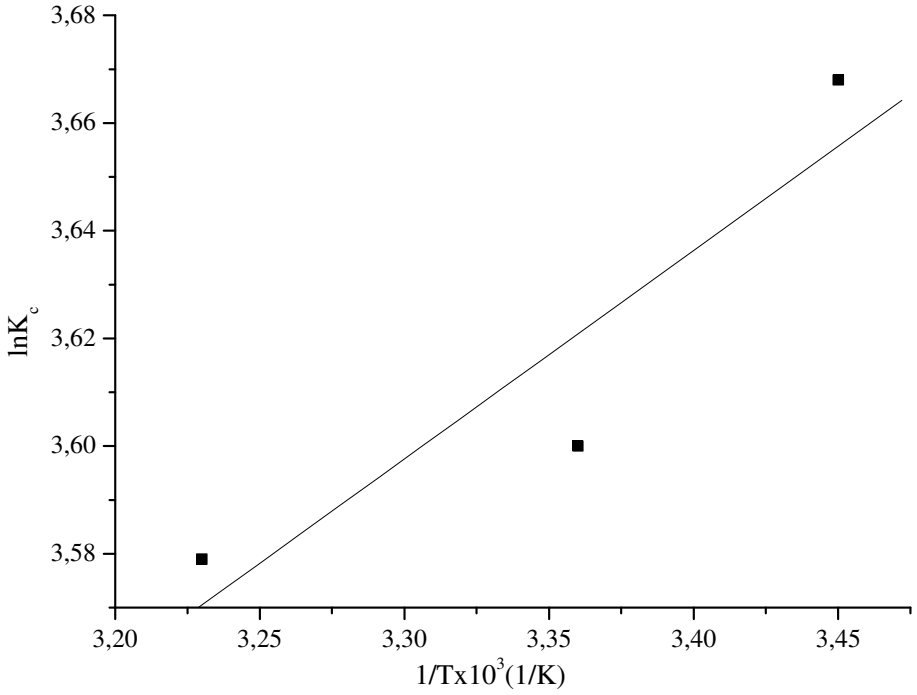

Figure 5.20 van't Hoff plot for the adsorption of PHCl onto IRS

For PHCl sorption onto KSF, the magnitude of the change in free energy can be used to determine the type of adsorption. In this study, ΔG^{o} values were found to be -4.43, -6.07 and -8.18 kJ mol^{-1}, indicating physisorption is between -20 and 0 kJ/mol; chemisorption has a range of -80 to -400 kJ mol^{-1} (Yu et al., 2001). It is seen that the temperature increased from 290 to 310 K, ΔG^{o} is increased from -4.43 to -8.18 kJ mol^{-1}. It can be concluded that physisorption contributes to the adsorption mechanism. For PHCl sorption onto IRS, the changes of free energy values in this study are in the range of -8.84 and 9.45 kJ mol^{-1}. Therefore the type of adsorption can be considered as physisorption for PHCl adsorption onto IRS. The negative values of ΔG^{o} at different temperatures for all samples indicate the spontaneous nature of the sorption process.

The positive values of the standard enthalpy change ΔH^{o}, 49.74 kJ mol^{-1}, imply that the interaction between drug molecules and KSF is endothermic in nature. If heat of an adsorption process is < 40 kJ mol^{-1}, it is physical process, and at the same time, the activation energy of a physical process is also generally low (Mc Bride, 1994). The positive values of the standard enthalpy change may be an indication of the occurrence of monolayer adsorption. This result is supported by its best Langmuir fit. ΔH^{o} values for PHCl adsorption onto KSF are greater than this value may show ion-exchange adsorption mechanism. It is probable that the activation energy of chemical process is high. This result is consistent with previous findings that define the adsorption as ion-exchange mechanism. For PHCl sorption onto IRS, the negative value of the standard enthalpy change (-3.20 kJ mol^{-1}) indicates exothermic nature of adsorption and physical adsorption due to lower than 40 kJ mol^{-1}.

ΔS^{o} values are 0.19 and 0.02 kJ $mol^{-1}K^{-1}$ for PHCl sorption onto KSF and IRS respectively. Positive value of ΔS^{o} corresponds to an increase in degree of freedom of the adsorbed drug molecules. Also, the positive value of ΔS^{o} above indicates that some structural changes may have taken place as a result of interactions of drug molecules with active groups in the clay surface (Yadava et al., 1991).

5.1.7 Release studies from clay carriers

As can be seen from the curve of PHCl release from KSF (Figure 5.21), relatively high releasing rate was observed in the initial 100 min. In the range of 100-200 min the release rate was reached constant. After 200 min, the release rate was increased again. The maximum amount of PHCl released is almost 56.8 % of the total in the range studied (0-540 min). Release of PHCl from KSF, in acidic solution is less than 1% (Figure 5.22). As shown in the graph of PHCl releasing from IRS in basic medium, (Figure 5.23) during 700 min, the amount of release of PHCl from IRS are increasing gradually. The maximum amount of PHCl released is 14.5 % of the total in the range studied (0-715 min). As can be seen in Figure 5.24, the release of PHCl from IRS in acidic conditions is increasing with time .Besides the amount of release of PHCl is lower than 5 % within 700 min.

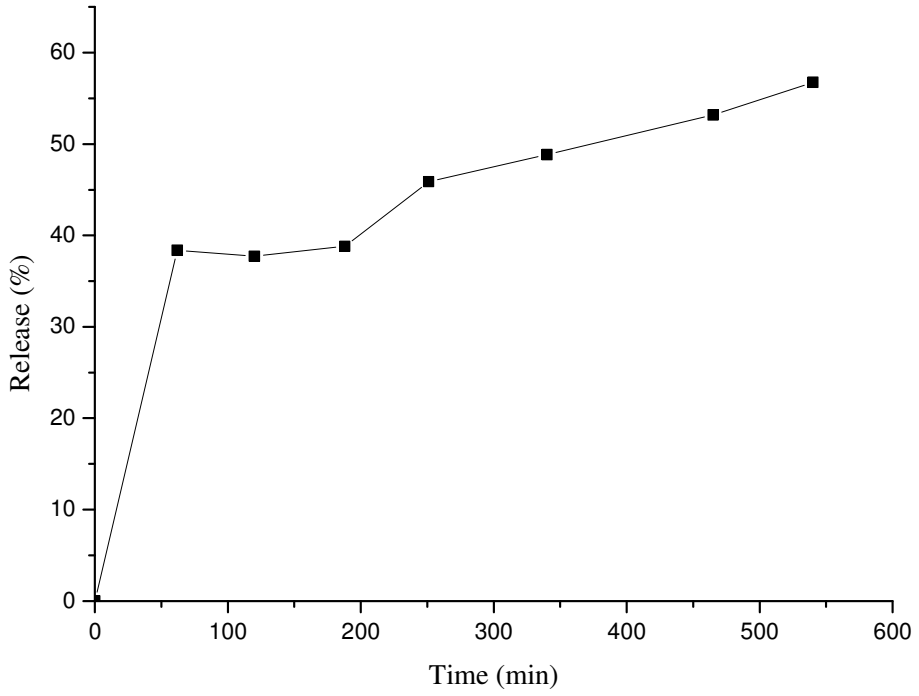

Figure 5.21 Releasing of PHCl from KSF in buffer solution (pH=7.4, T=37°C)

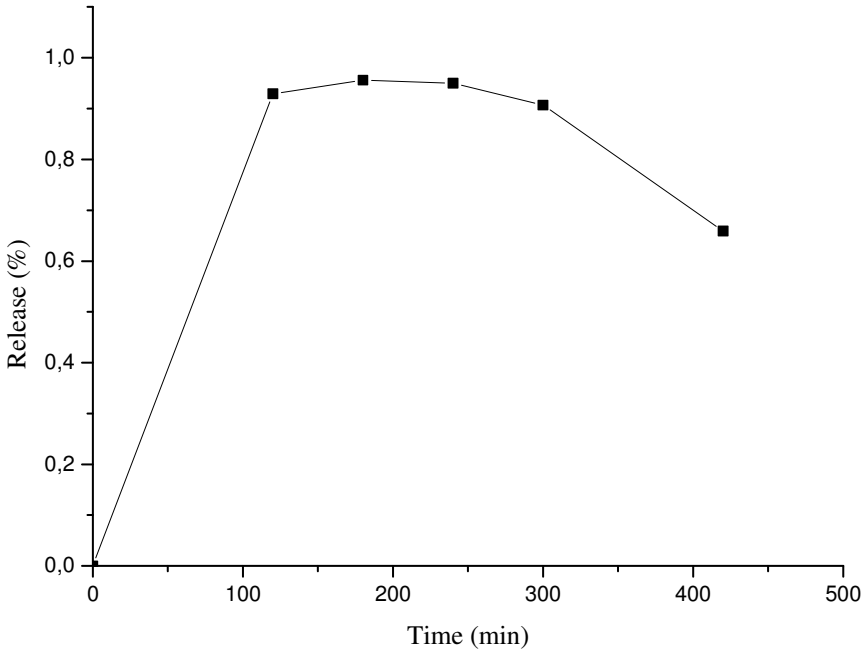

Figure 5.22 Releasing of PHCl from KSF in buffer solution (pH=1.2, T=37°C)

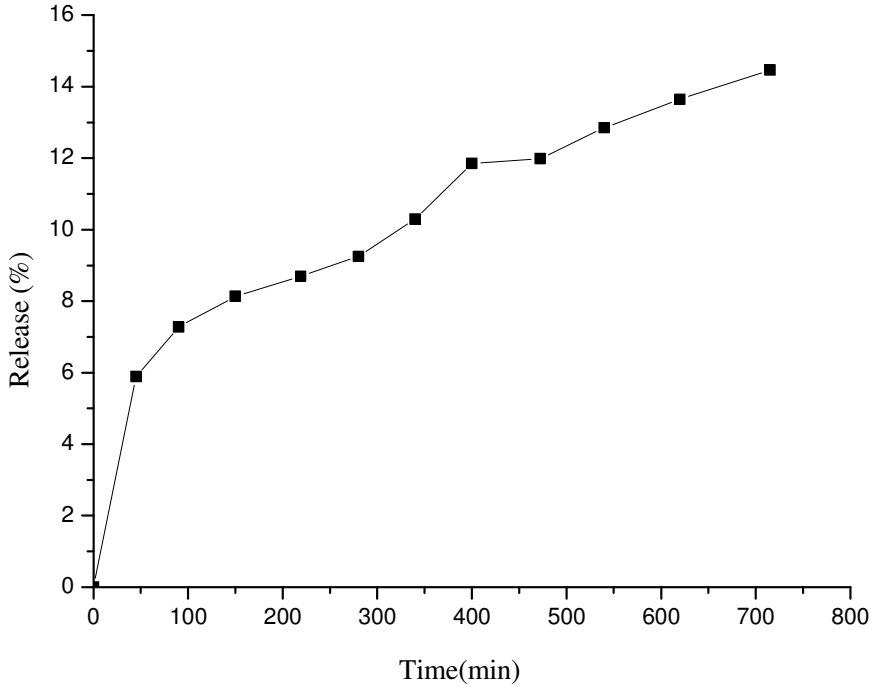

Figure 5.23 Releasing of PHCl from IRS in buffer solution (pH=7.4, T=37°C).

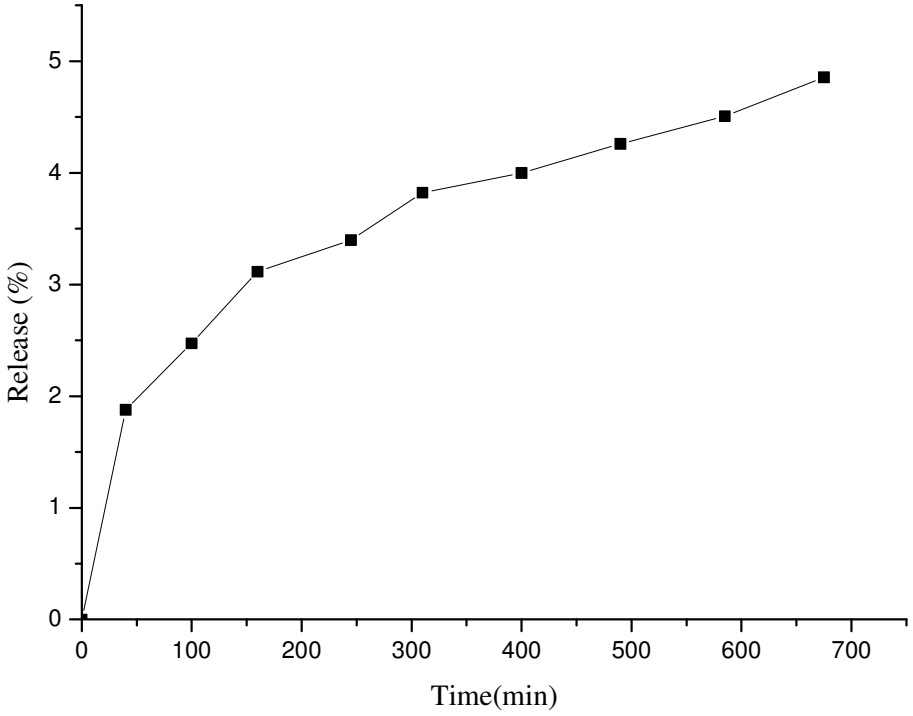

Figure 5.24 Releasing of PHCl from IRS in buffer solution (pH=1.2, T=37°C)

Fejer et al., (2001) obtained that 30% of the initial content of Promethazine hydrochloride was released in artificial intestinal juice within 350 min by using Wyoming montmorillonite. In this study during the same time interval, about 50 % of the initial content was released in artificial intestinal juice by using KSF. We lengthened the duration of Promethazine hydrochloride by using KSF

In order to reveal the kinetics of PHCl and TMP release from KSF, two kinetic models were applied to release data. These are zero order rate equation and first order rate equation. The zero order rates describe the systems where the drug release rate is independent of its concentration. The first order model describes the systems where drug release is concentration dependent (Sood & Panchagnula, 1998).

$Q_t=k_ot$

$\ln Q_t = \ln Q_o - k_1 t$

where, Q_t is the amount of drug released in time t, Q_o is the initial amount of the drug, k_o and k_1 are release rate constants for zero order and first order rate constant respectively. Since the release of PHCl from KSF and IRS are quite low in acidic medium, kinetic parameters for releasing of PHCl from KSF and IRS were given in basic conditions.

Table 5.7 Kinetic parameters for releasing of PHCl from KSF and IRS in pH=7.4

Type of clay	k_0(mg min^{-1})	R_0	k_1(mg min^{-1})	R_1
IRS	0.0016	0.864	$6.312\ 10^{-4}$	0.821
KSF	0.129	0.983	$9.924\ 10^{-4}$	0.974

As can be seen from the above Table 5.7, the fit of zero order and first order kinetic model for the releasing of PHCl from IRS is quite low. Zero order release model provides a better conformity than first order release model for the releasing of PHCl from KSF. When the rate constants obtained from zero order and first order kinetic model are compared, the rate constants k_0 and k_1 of PHCl release from KSF are greater than that of IRS. It can be derived that releasing of PHCl from IRS is slower than releasing of PHCl from KSF.

5.2 Releasing PHCl from ChitEPI hydrogels

5.2.1 Equilibrium swelling studies

The swelling behavior of ChitEPI hydrogels was studied as a function of pH, temperatures and ionic strength. The % equilibrium swelling values of ChitEPI hydrogels at 37 ˚C (pH=1.2 and 7.4) and 4°C (pH=7.4) were given in Figures 5.25, 5.26 and 5.27. The % equilibrium swelling of ChitEPI 400 was at about 100 % at pH 1.2. The swelling values at pH=7.4 was low in comparison with than that of pH=1.2. In the case of ChitEPI 600, hydrogel attained 300 % and 150 % swelling. ChitEPI800 hydrogels were swollen to 260 % and 175 % at equilibrium pH values of pH=1.2 and 7.4 respectively. These result indicate that difference observed in the swelling values at equilibrium due to variation of the volume of cross-linker, epichlorohydrin.

The percent equilibrium swelling values were found to be higher at pH 1.2 than at pH 7.4. It can be revealed that at acidic pH, NH_2 groups of Chitosan may be are protonated. This case causes repulsion between protonated NH_2 groups. At high pH values, the swelling values of ChitEPI hydrogels decrease due to increase of unprotonated amine groups. At higher pH values hydrogen bond may occur between amino groups of chitosan and OH^- groups. On this consideration, following reaction can be offered

$R\text{-}NH_2 + OH^- \longrightarrow R\text{-}NH_2\text{------}OH^-$

At high pH values, while the amount of protonated amine groups reduces, the amount of neutral $–NH_2$ group increases. Chitosan is a weak base with a pK_a value of the D-glucosamine residue of about 6.2-7.0. The lowest swelling value was observed at about 6.2.

As can be seen from Figures 5.26 and 5.27, Small differences were observed in the equilibrium swelling values of ChitEPI600 and ChitEPI800 at 4 °C and 37°C (pH=7.4). However equilibrium swelling values of ChitEPI400 hydrogels differ from each other.

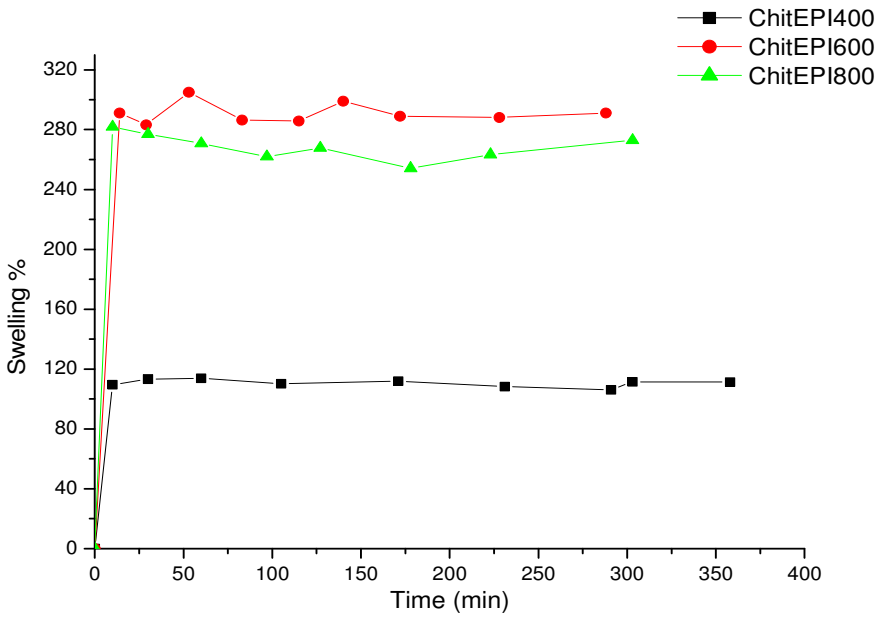

Figure 5.25 Swelling kinetics of ChitEPI hydrogels at pH=1.2 and 37 °C

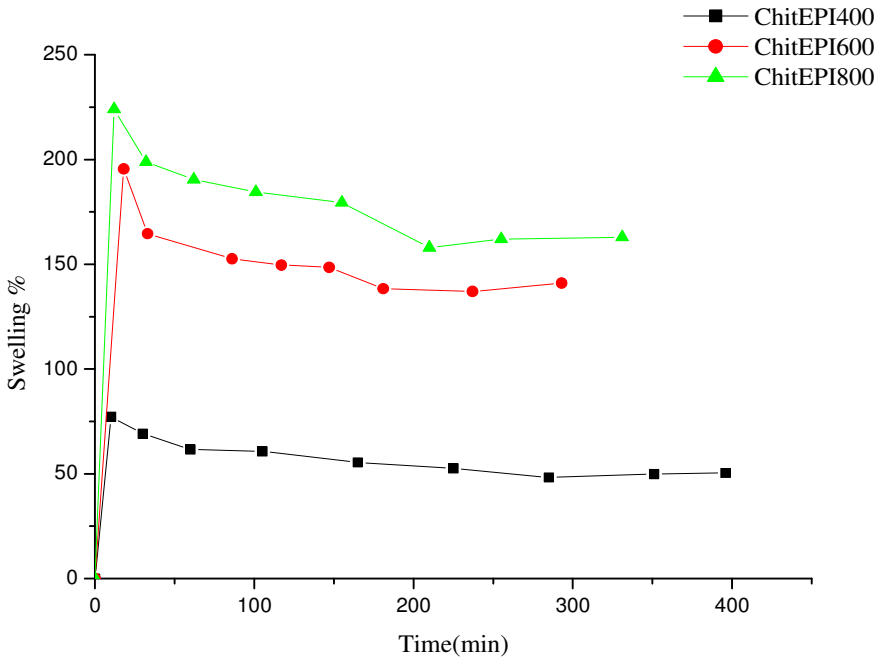

Figure 5.26 Swelling kinetics of ChitEPI hydrogels at pH=7.4 and 37 °C

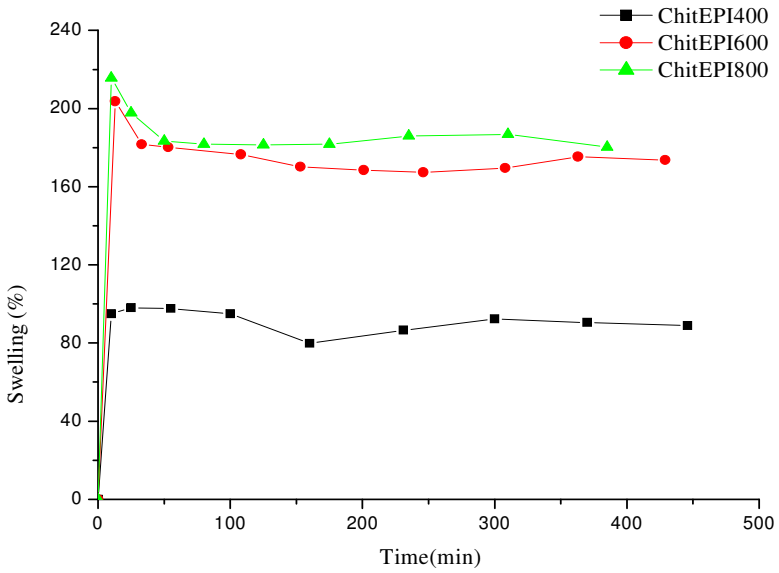

Figure 5.27 Swelling kinetics of ChitEPI hydrogels at pH=7.4 and 4 °C

5.2.2 Thermosensivity of hydrogels

In order to determine the thermosensitivity of hydrogels, experiments were carried out in PBS having a pH of 7.4 at 4°C and 37 °C. Temperature dependent reversible swelling behaviour of ChitEPI hydrogels were presented in Figures 5.28, 5.29 and 5.30 for ChitEPI400, ChitEPI600, and ChitEPI800 respectively. At first, the hydrogels were equilibrated at 37 °C, and then alternated between solutions at 4 °C and 37°C respectively. As can be seen from corresponding Figures, temperature increment (from 4 °C to 37°C) didn't exhibit a significant change in the equilibrium swelling values. It can be said that a reversible response was not observed in temperature dependent reversible swelling behavior of produced ChitEPI hydrogels. As a result, the swelling behavior of ChitEPI hydrogels does not appear to be temperature dependent, as shown in Figures 5.28, 5.29 and 5.30. It was clear that an increase in the temperature would not be useful on the equilibrium swelling of ChitEPI hydrogels.

It was observed that ChitEPI hydrogels was appeared to be insoluble in acidic and alkaline medium as well as distilled water. The proof of cross-linking of EPI to Chitosan is the capability of swelling of produced hydrogels in acidic conditions.

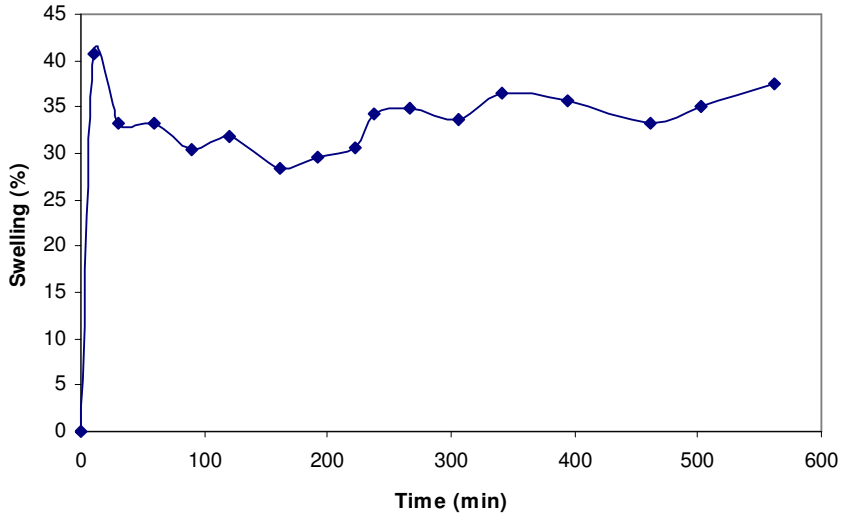

Figure 5.28 Temperature dependent reversible swelling behavior of ChitEPI400 (hydrogel samples equilibrated at T=37°C, then alternated between solutions at T=4°C and T=37°C)

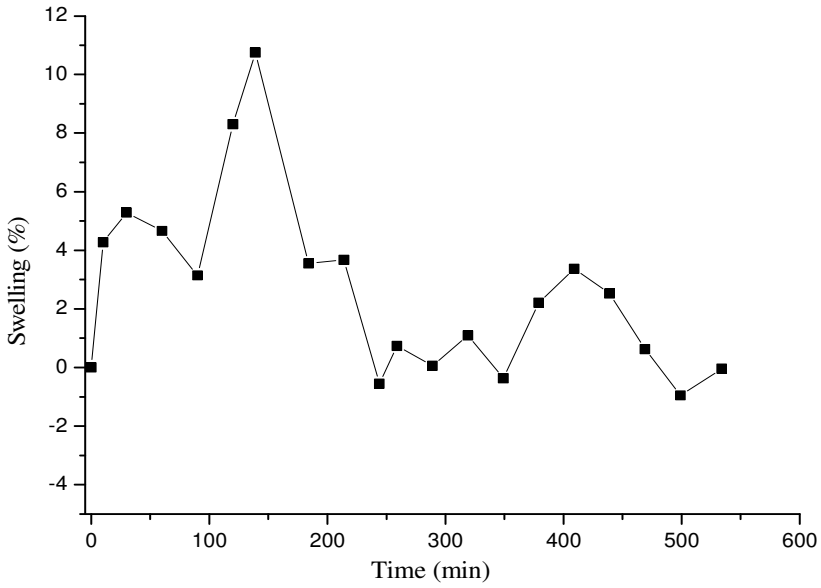

Figure 5.29 Temperature dependent reversible swelling behavior of ChitEPI600 (hydrogel equilibrated at T=37°C, then alternated between solutions at T=4°C and T=37°C.

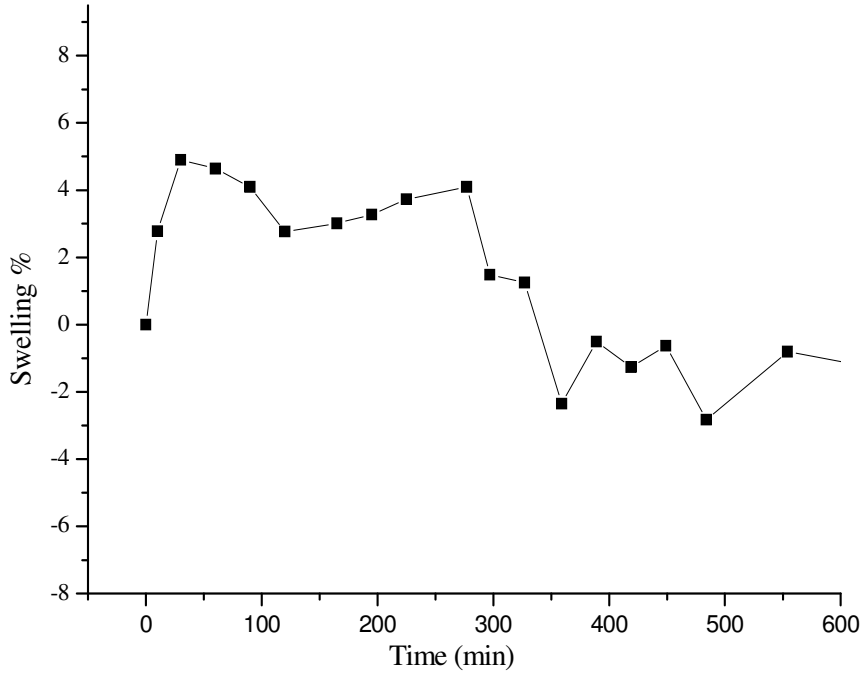

Figure 5.30 Temperature dependent reversible swelling behavior of ChitEPI800 (hydrogel equilibrated at T=37°C, then alternated between solutions at T=4°C and T=37°C.

5.2.3 pH-sensitivity of the hydrogels

The effect of pH on the equilibrium swelling ratio of ChitEPI hydrogels was given in Figures 5.31, 5.32 and 5.33 respectively. ChitEPI hydrogels appeared to swell well at low pH values. However they shrunk in the pH range of 6-7.

As shown in Figures 5.31, 5.32, and 5.33 swelling values were significantly decreased with the raise of pH in the range 2.5-6.5 in this study. In this pH range the greatest swelling value belongs to ChitEPI400 when compared the other produced hydrogels. Beyond the pH value of 6.3, the swelling values are increasing with the increase of pH. It is probable that the number of NH_3^+ was decreased with increasing of pH. The lowest swelling occurred almost at pH 6.3 for all hydrogels. When the pH was increased NH_2 group would be dominant group.

At low pH values (acidic conditions) amine groups in the ChitEPI hydrogels are protonated. This causes an electrostatic repulsion in the ChitEPI hydrogel and swelling occurs. In other words, along with decreasing pH, the amount of $-NH_3^+$ increases inside the hydrogels resulting in an osmotic pressure and makes the ChitEPI hydrogels swell.

According to Lin et al., (2007), if the Chitosan is not cross-linked with an agent, swelling values with pH variations will follow that way. In the acidic pH regions, the swelling of Chitosan decreased with a decrease of $–NH_3^+$ when raising the pH from 1.0 to 7.0. In alkaline environment, the amino groups were completely deprotonated. Namely, Chitosan swelled hardly when pH>7.0 could be due to the loss of solubility of the chain segments and also due the formation of new crosslinks by hydrogen bonding. When Chitosan was cross-linked by EPI, the pH value of 7.0 for Chitosan reduced to pH of 6.3. This can be due to the fact that NH_2 groups may interact with EPI. When some of the NH_2 groups are used in crosslinking, the amount of NH_2 groups gets lower. Moreover, swelling of the ChitEPI hydrogels in acidic medium are always greater than that in alkaline medium. As indicated above swelling increased with a decrease in the amount of cross-linkers at the same pH range. It was added that the higher degree of cross-linking causes the compactness of the hydrogel network will prevent the permeation of water and result in lower swelling. As conclusion, it can be claimed that the swelling behavior of ChitEPI hydrogel film seemed to be pH dependent.

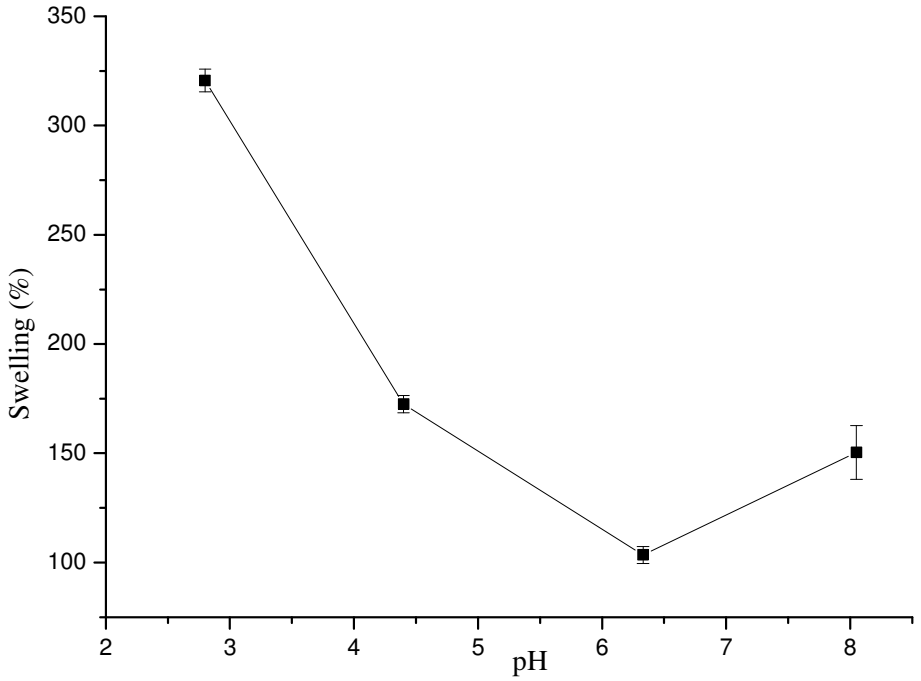

Figure 5.31 Effect of pH on the equilibrium swelling of ChitEPI400, T=37°C

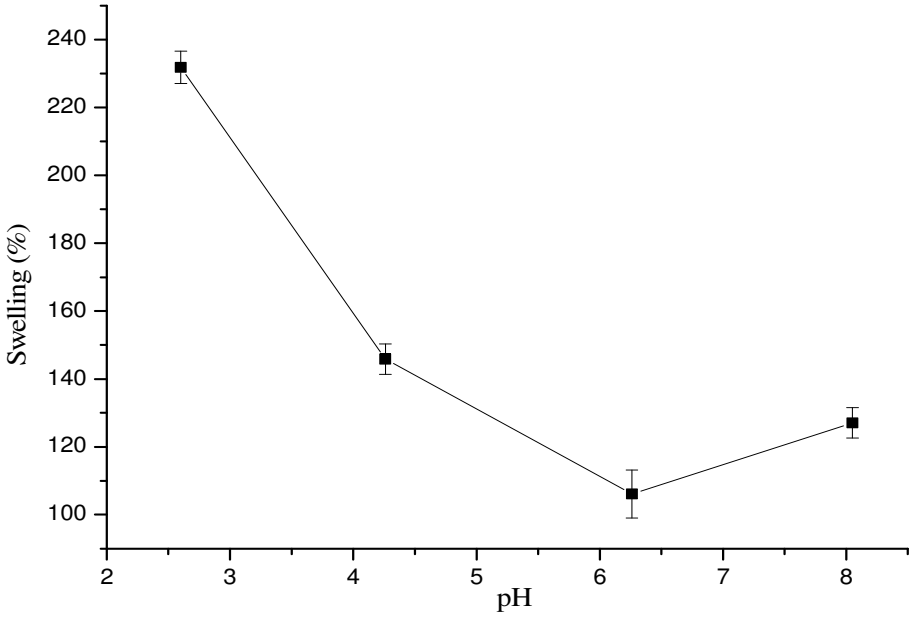

Figure 5.32 Effect of pH on the equilibrium swelling of ChitEPI600, T=37°C

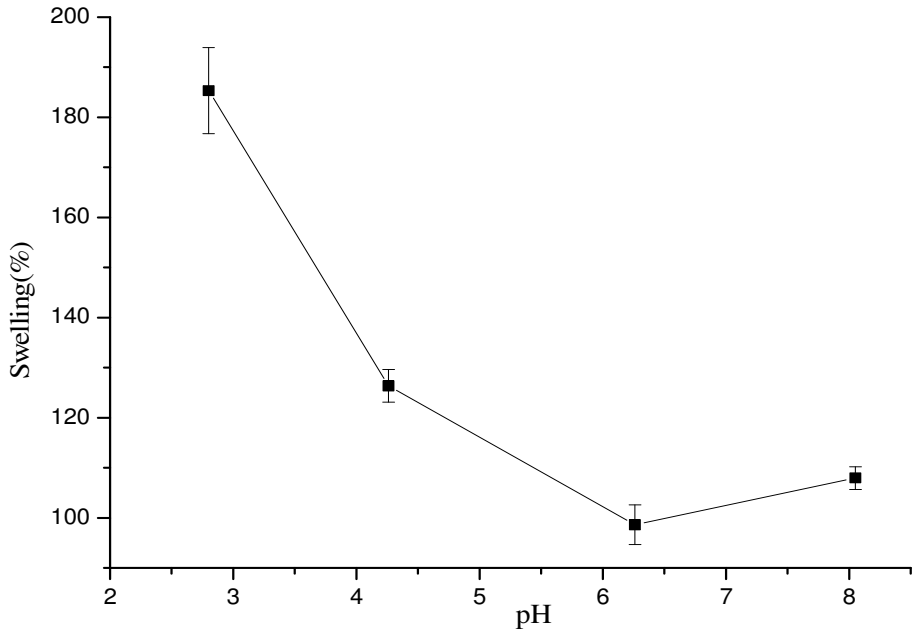

Figure 5.33 Effect of pH on the equilibrium swelling of ChitEPI 800, T=37°C

5.2.4 Swelling Reversibility of ChitEPI hydrogels

As observed in figures 5.34, 5.35, 5.36, the swelling reversibility of the ChitEPI hydrogels was alternately carried out at pH=1.2 and 7.4. After ChitEPI hydrogels equilibrated at pH=1.2, the samples were immersed in pH 7.4 for about 250-300 min. A shrinking was measured as about 30-35% for ChitEPI hydrogels at this pH. Then those were transferred into PBS, pH=7.4 for another 250-300 min and a swelling was observed to the equilibrium values of the hydrogels. When the pH values were varied repeatedly, ChitEPI hydrogel showed a reversible swelling behavior with a faster response than vinyl ether/acrylic acid terpolymer synthesized by Gumusderelioglu & Topal, (2005). It could be concluded that reversible swell-shrink properties of produced hydrogels would be beneficial characteristics for pH sensitive controlled release system with controllable swelling ability, when used as a drug carrier.

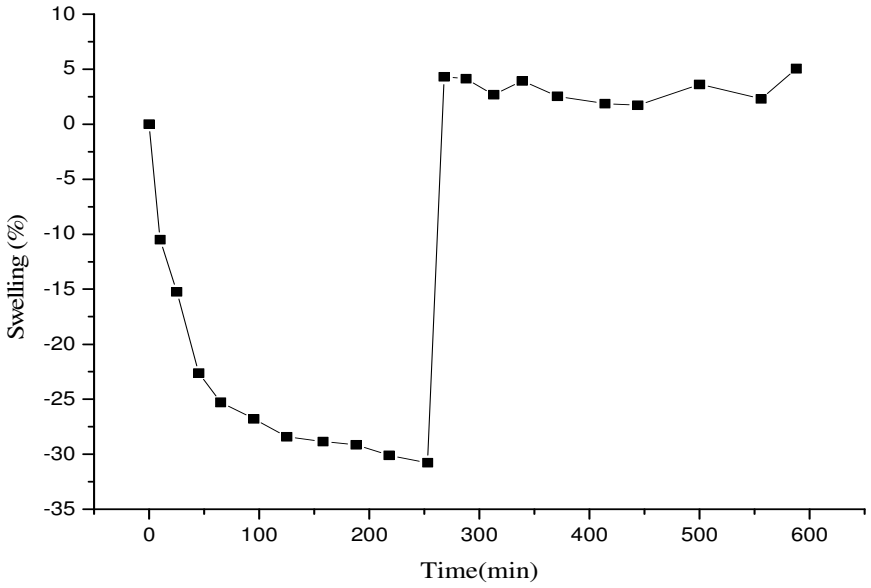

Figure 5.34 pH-dependent reversible swelling behavior of ChitEPI400 (hydrogel equilibrated at pH 1.2, then alternated between solutions at pH=7.4 and pH=1.2).

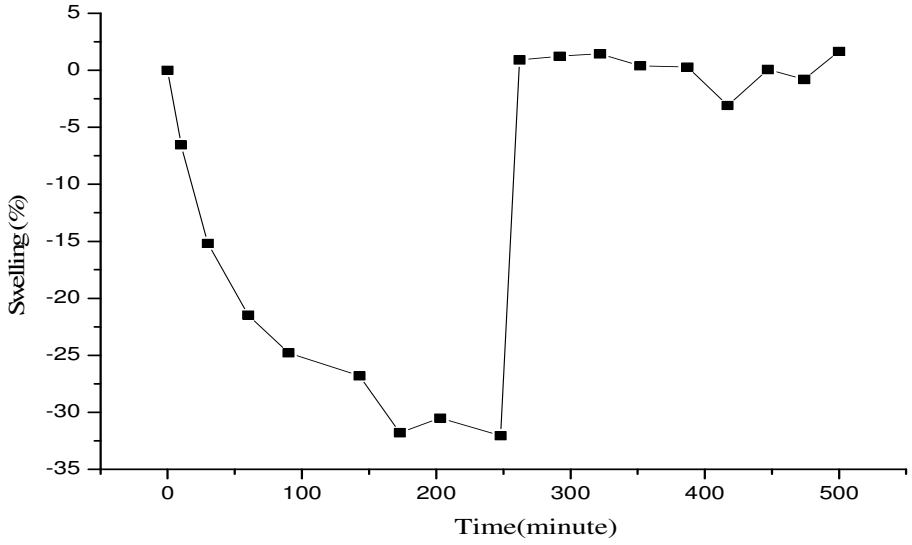

Figure 5.35 pH-dependent reversible swelling behavior of ChitEPI600 (hydrogel sample equilibrated at pH 1.2, then alternated between solutions at pH=7.4 and pH=1.2).

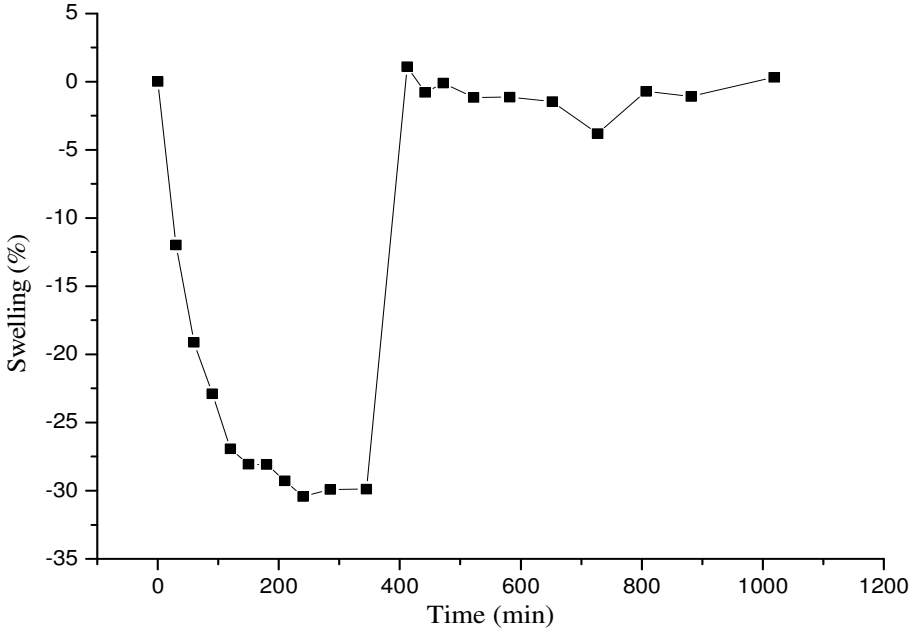

Figure 5.36 pH-dependent reversible swelling behavior of ChitEPI800 (hydrogel equilibrated at pH 1.2, then alternated between solutions at pH=7.4 and pH=1.2).

5.2.5 The Effect of Ionic Strength on swelling

The effect of NaCl concentration on the equilibrium swelling behavior in water at room temperature for ChitEPI hydrogels prepared at various EPI content was investigated. The hydrogels were equilibrated in water at room temperature and immersed in different NaCl concentrations (0.05, 0.1, 0.15 and 0.20 M). The swelling values for ChitEPI hydrogels at different ionic strength were given in Figure 5.37. It was noticed from Figure 5.37 that ChitEPI400 and ChitEPI600 hydrogel deswelled at various NaCl solutions. However ChitEPI800 hydrogel swells lower than 2%. The swelling values are increasing with the increase in concentration of NaCl from 0.05 to 0.2 M for ChitEPI400 and ChitEPI600. Moreover, The ChitEPI deswells more than ChitEPI600. It can also be added that highest swelling value for ChitEPI was 1.7% at 0.1 M concentration. Among the hydrogels, the highest deswelling value was observed at 0.2 M NaCl for ChitEPI400. This deswelling

phenomenon may be attributed to osmotic pressure difference between the inside of the gel and surroundings caused by redistribution of mobile ions. A very concentrated environment exist outside of the hydrogel Hence the amount of water which exist inside of the hydrogel will decrease and leads to a decrease in osmotic pressure and makes the hydrogel deswelled. It can also be added that the larger the concentration of mobile ions outside the hydrogel, decrease the gel –solvent (water) interactions.

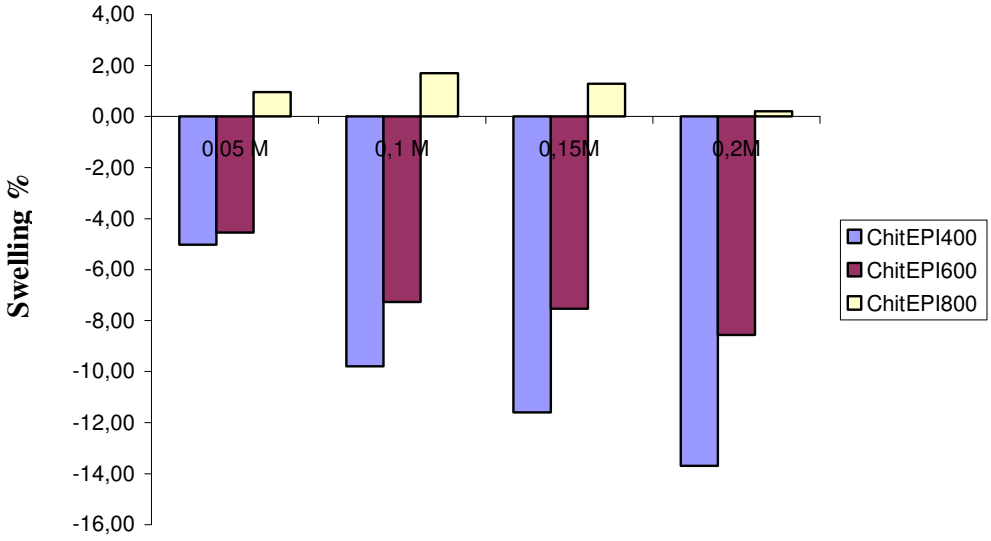

Figure 5.37 The Effect of NaCl on the swelling of Hydrogel

5.2.6. Release of PHCl from ChitEPI hydrogels.

The release of PHCl from ChitEPI hydrogels were performed by immersing PHCl loaded hydrogel in pH=1.2 and 7.4. It can be noticed that from Figures 5.38 and 5.39 shows cumulative release profiles from ChitEPI for pH=1.2 and 7.4 respectively. Considering the Figures 5.38 and 5.39, an initial burst was observed at pH 1.2 within 50 min. However the release of PHCl at pH=7.4 was quite low. Only about 10 % of the loaded drug was released during 600 min for all hydrogels. Besides considering PHCl release at pH=1.2 about 28 % for ChitEPI800, 36 % for ChitEPI400 and 49 % for ChitEPI600 was observed respectively. It can be added that approximately, 51% of the loaded drug was released during 720 min at pH=1.2 for ChitEPI600,

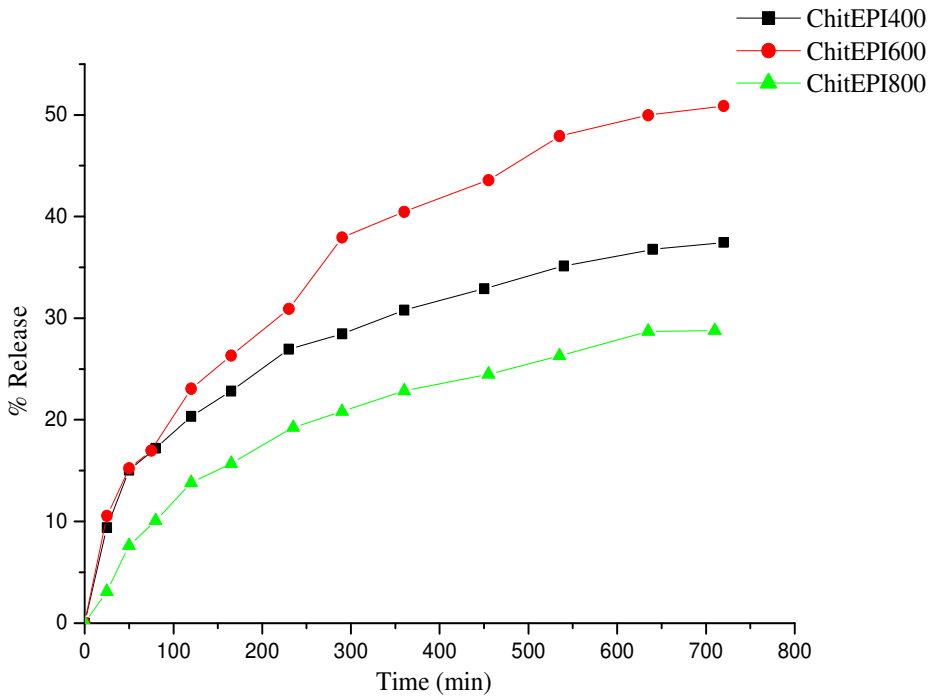

Figure 5.38 In vitro release measurement of PHCl from ChitEPI hydrogels at 37°C and pH=1.2

which can be considered as maximum value in this study in the time range of 720 min. The amount of drug released was much higher in acid medium than in PBS (pH, 7.4). This is an anticipated result. Because release of PHCl may depend on swelling of the hydrogel. If drug release follows diffusion controlled mechanism through swollen gels. The hydrogels behaves as a diffusion barrier for drug, PHCl. Comparing the release of PHCl from ChitEPI400, ChitEPI600 and ChitEPI800 at pH 1.2, it can be put forward to that the lowest release belongs to ChitEPI800.

The pH dependent release of PHCl from ChitEPI hydrogels expresses that ChitEPI hydrogels can be used for the delivery of drug in stomach and gastrointestinal tract whose pH rises from 1.5 to 3. However the loaded drug can be released in lesser amounts from hydrogel as it passes through the stomach. Upon reaching colon small amounts of drug can be release from ChitEPI. Drug release data were applied to different drug release models such as zero order rate equation and first order equation to identify release kinetics. The plots for zero order equation and

first order equation were given in Figures 5.40 and 5.41. The parameters obtained from these equations were summarized in Table 5.8 for all hydrogels. R values of first order equation for ChitEPI are 0.871, 0.902 and 0.817 for ChitEPI400, ChitEPI600 and ChitEPI800 respectively. As for zero order equation, R values are 0.906, 0.945 and 0.936 for ChitEPI400, ChitEPI600 and ChitEPI800 respectively. As indicated above, none of the hydrogel follows zero order drug release kinetics which is confirmed by poor correlation coefficients. However based on R values, zero order kinetic models provides better fit than first order kinetic model and also the fit of zero order kinetic model shows poor correlation.

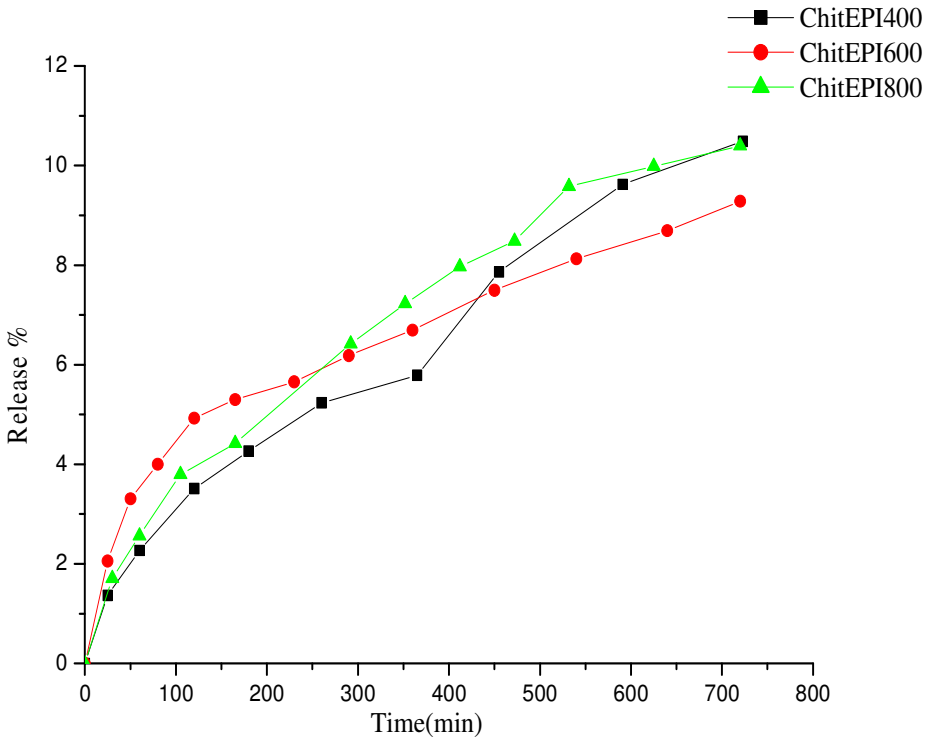

Figure 5.39 In vitro release measurement of PHCl from ChitEPI hydrogels at pH 7.4 and 37°C.

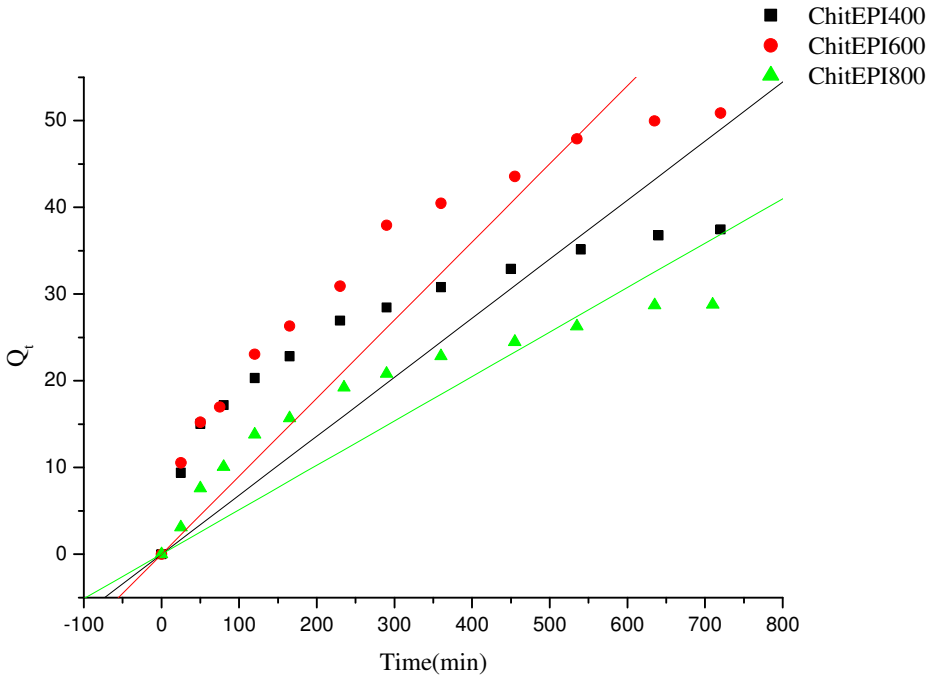

Figure 5.40 Zero order kinetic model for the release of PHCl from ChitEPI hydrogels at pH=7.4.

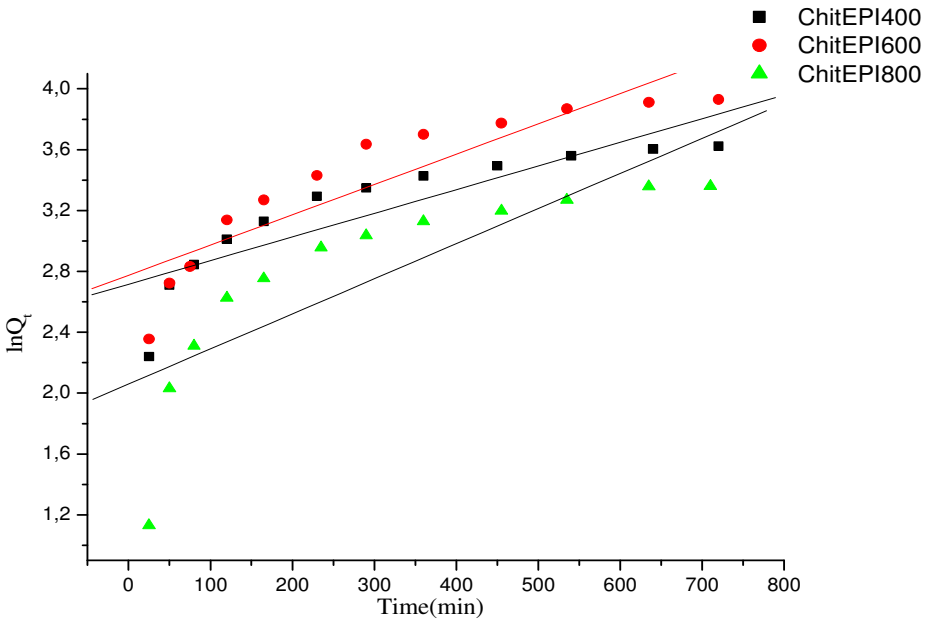

Figure 5.41 First order kinetic model for the release of PHCl from CHitEPI hydrogels at pH=7.4.

Table 5.8 Kinetic parameters for releasing of PHCl from ChitEPI hydrogels at pH=7.4

Type of Hydrogel	k_0(mg min^{-1})	R_0	k_1(mg min^{-1})	R_1
ChitEPI400	0.068	0.906	$1.55x10^{-3}$	0.871
ChitEPI600	0.090	0.945	$1.99 x10^{-3}$	0.902
ChitEPI800	0.051	0.936	$2.31 x10^{-3}$	0.817

5.2.7 The FTIR analysis

The FTIR spectra of Chitosan, ChitEPI400, ChitEPI600 and ChitEPI800 were given in Figure 5.42. At 1651 cm^{-1} in the spectrum of Chitosan can be assigned to amide I band, namely, C=O stretch of acetyl group. This is an indication of N-acetyl functional group of Chitosan. This is an expected result, because degree of deacetylation for Chitosan used in this study is changing from 60 to 90 %. After modification of Chitosan with EPI new bands at 1636cm^{-1} for ChitEPI400 and ChitEPI600; at 1637 cm^{-1} for ChitEPI800 can be attributed to an asymmetric NH_3^+ bending. C-N stretching vibration of Chitosan was detected at 1318cm^{-1}. This band was obtained at 1320cm^{-1} for ChitEPI400, 1322 cm^{-1} for ChitEPI600 and 1312 cm^{-1} for ChitEPI800. There is not so much difference at the band of C-N, after EPI was cross-linked. Therefore it can be claimed that EPI might not interact with Chitosan at the position of amide group. The band at 1538 cm^{-1} corresponds to the NH_2 bending. This band shifted to 1550 cm^{-1}, 1555cm^{-1} and 1551 cm^{-1} for ChitEPI400, ChitEPI600 and ChitEPI800 indicating that amino group of Chitosan may interact with EPI molecules. The strong band at 1089 cm^{-1} can be attributed to C-O stretching vibration. This band was lowered to 1084 cm^{-1} with the modification by EPI. The bands at 1030 cm^{-1} for synthesized hydrogels C-O stretch primary hydroxyl group (characteristic peak of $–CH_2–OH$ in primary alcohols, C–O stretch).

C-H stretching vibration can be seen at 2922 cm^{-1}in the spectrum of Chitosan. This band was appeared as a doublet (2935 cm^{-1} and 2890 cm^{-1} for ChitEPI400, 2935 and 2889 cm^{-1} for ChitEPI600 and 2932 and 2888 cm^{-1} for ChitEPI800) when chitosan was cross-linked by EPI. Besides, C-H bending vibration of Chitosan was observed at 1416 cm^{-1} and 1379 cm^{-1}. These bands were not so much after reaction

with EPI, suggesting very weak interaction. The absorption band of 3363 cm^{-1} can be considered as OH stretching vibration. However it may be added that this band may also contain N-H stretching vibrations. Because of the overlapping with OH stretching band, it can not be seen exactly. The OH stretching vibration at 3363 cm^{-1} for Chitosan shifted to 3338, 3350 and 3367 cm^{-1} for ChitEPI400, ChitEPI800 and ChitEPI600 respectively. As can be seen, ChitEPI600 when compared to the ChitEPI800 and ChitEPI400 increased slightly. Nevertheless, it can be claimed that the OH groups in Chitosan may function as the recognition sites for the binding of EPI. The FTIR spectrum of Chitosan exhibits the bands at 899 cm^{-1} and 1152 cm^{-1} which are owing to saccharide structure of Chitosan. These bands did not change when the Chitosan was cross-linked by EPI.

The FTIR spectra of ChitEPI+drug were rendered in Figure 5.43, 5.44 and 5.45. As can be seen following Figures, OH stretching vibrations can be seen as a broad band in the spectra of ChitEPI+drug. The bands at 1636 cm^{-1} and 1550 cm^{-1} for ChitEPI400 were overlapped after drug loading and became a broad band. The spectra of CHitEPI600 and ChitEPI800 at that region are almost similar to that of ChitEPI400. The C-O stretching band (at 1084cm^{-1}, for ChitEPI400, ChitEPI600 and ChitEPI800) also appears as a broad band after drug loading.

From FTIR analysis it was confirmed that drug loading occurs successfully. Moreover, NH_2 and OH groups in chitosan may function as the recognition sites for the binding of EPI.

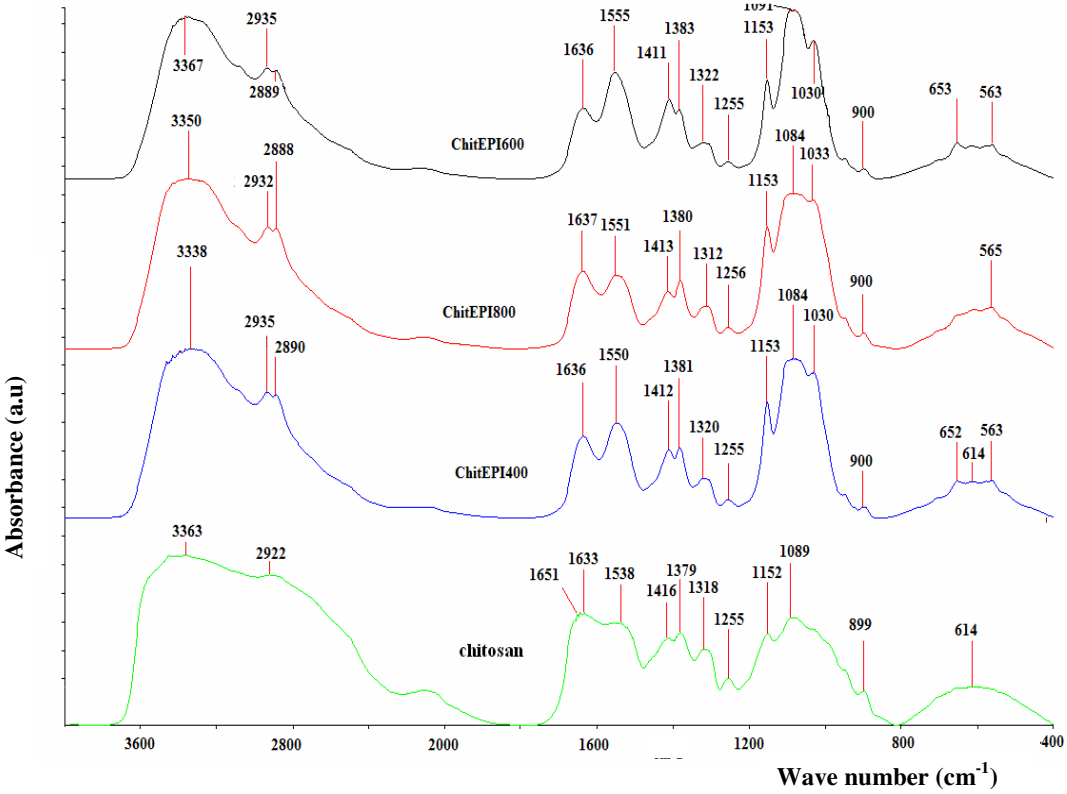

Figure 5.42. The FTIR spectra of Chitosan and synthesized hydrogels

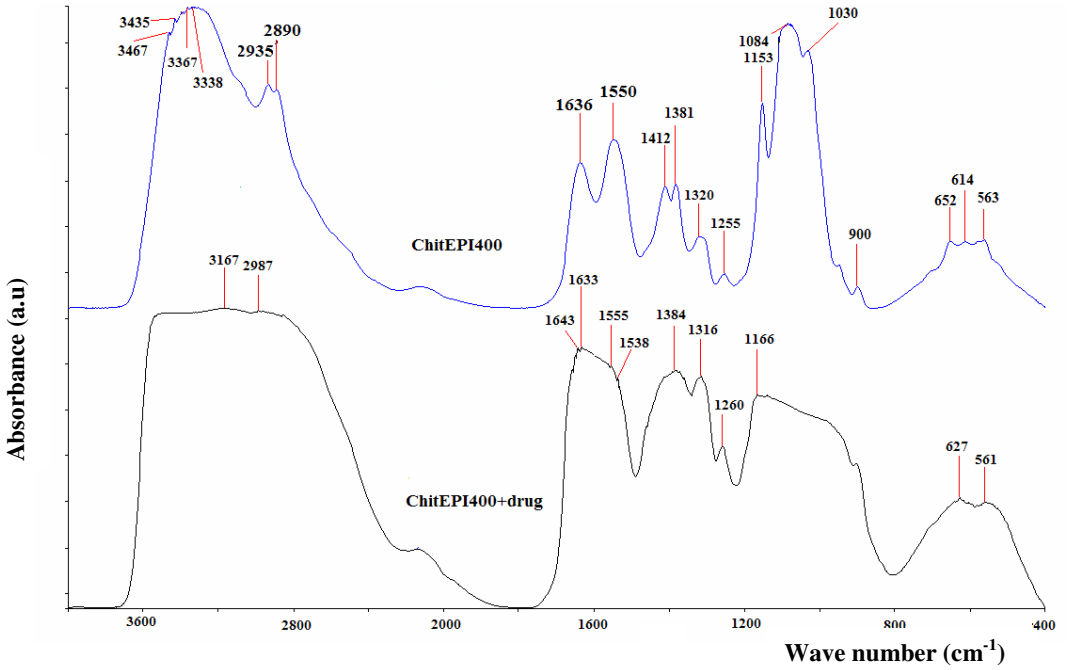

Figure 5.43. The FTIR spectra of ChitEPI400 and ChitEPI400+Drug

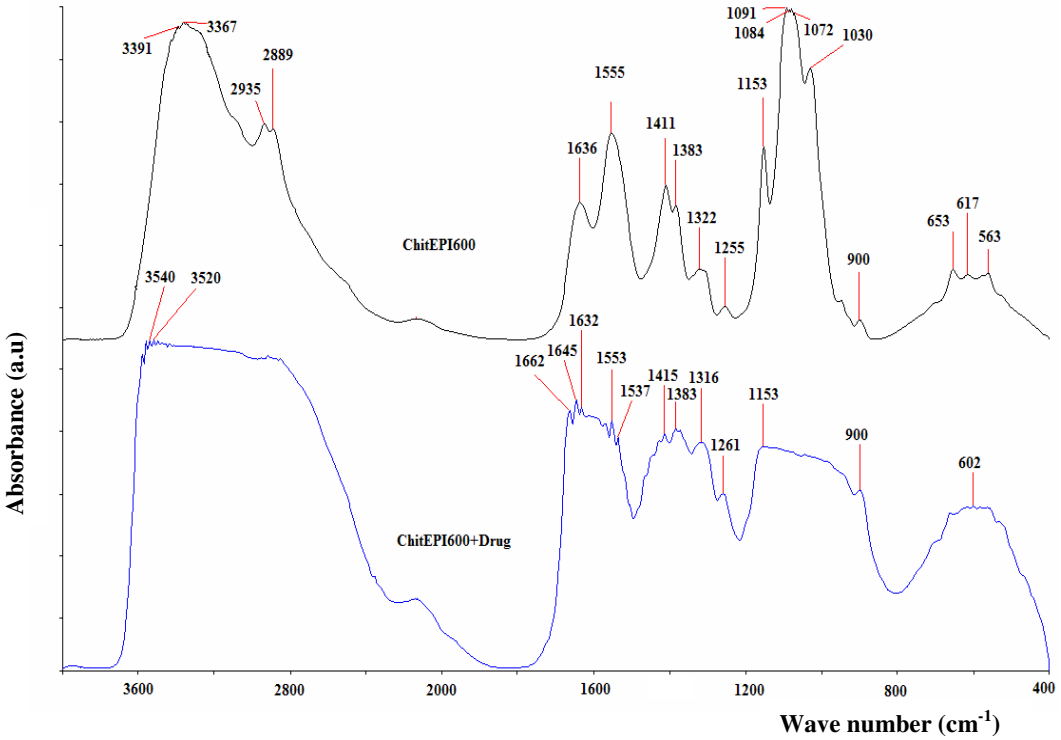

Figure 5.44. The FTIR spectra of ChitEPI600 and ChitEPI600+Drug

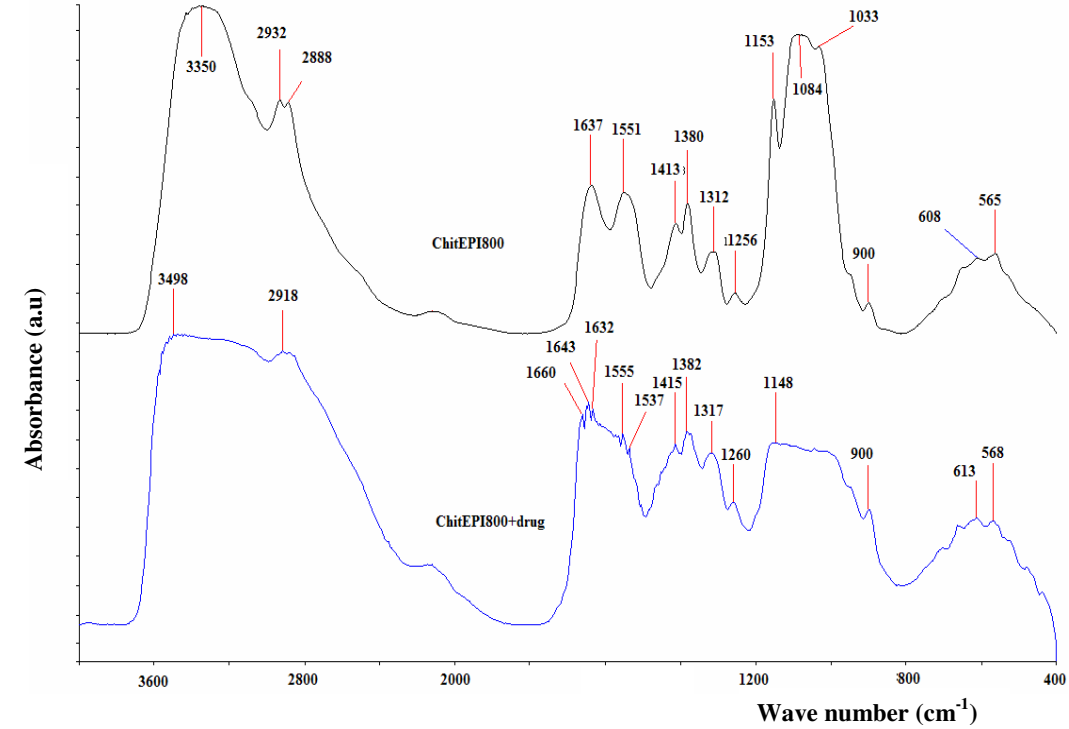

Figure 5.45. The FTIR spectra of ChitEPI800 and ChitEPI800+Drug

5.2.8. SEM Analysis of Hydrogels

SEM images of ChitEPI400, CHitEPI600 and ChitEPI800 were illustrated in Figures 5.46, 5.47 and 5.48 at different magnifications. The SEM micrographs of hydrogels loaded with PHCl were given in Figures 5.49, 5.50 and 5.51 respectively. As can be seen from cross-sections of ChitEPI400, there are macropores on the surface of film. Also they have long channels. As seen from 5.46a between two altitudes existing on the surface of ChitEPI400, long channels result in. The wideness of these channels is greater than 20 μm. The altitudes in Figure 5.46b seems brightness relatively. The deep surfaces namely pores have darkness view. These channels allow fast water retention by capillary forces. And this case reveals the reason of the fast swelling of hydrogels As illustrated in Figure 5.47a (for ChitEPI600) a superporous structure which have pore sizes in the range of hundreds of micrometers are observed. It is probable that large number of pores interconnected to each other and results in open channels. Due to capillary forces within superporous hydrogels the equilibrium swelling was reached in a short time. Because of the superporous structure, these hydrogels may have pharmaceutical, environmental and agricultural applications. In addition to these as seen from Figure 5.47 c and d, (SEM image of ChitEPI600) there are also large number of individual pores that are at about 5 μm and smaller than 5 μm. These pores are mostly circular and elliptical pores. Due to these pores, these hydrogels have also a macroporous structure. Namely, Figure 5.47 is the evidence for two different porous structure, macroporous and superporous in the same hydrogel. When the hydrogels are immersed in an aqueous solution, water molecules may diffuse easily into these gaps. As a consequence of this procedure enhancement of swelling values occurs. From Figure 5.48a (ChitEPI800) as the same with the other hydrogels, a highly porous structure can be seen for ChitEPI800 at 500X magnification. However as shown in Figure 5.48b a rough structure was observed at 2500X magnifications. And the pores within this micrograph are quite small and it is difficult to determine the size of the pores.

From SEM micrographs of ChitEPI +drugs it seems that some white grains were observed within the pores due to drug crystals. Especially ChitEPI600+drug displayed a highly porous structure and white grains with big masses can be realized in Figure 5.50d. As apparently shown by Figure 5.50a, b and c, ChitEPI600 exhibited interconnected pores with sizes in the order of a hundred μm.

SEM analysis demonstrated that the synthesized hydrogels have a porous structure. This is why the hydrogels swell in aqueous solutions.

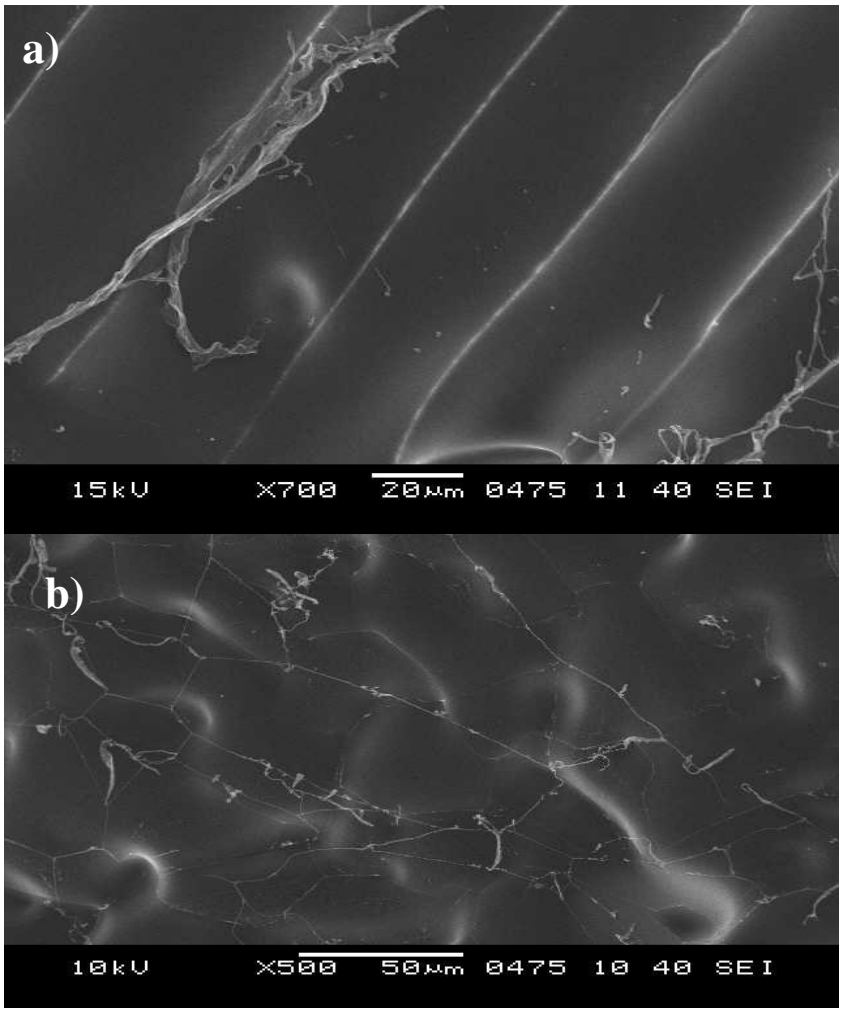

Figure 5.46 SEM analysis of ChitEPI400

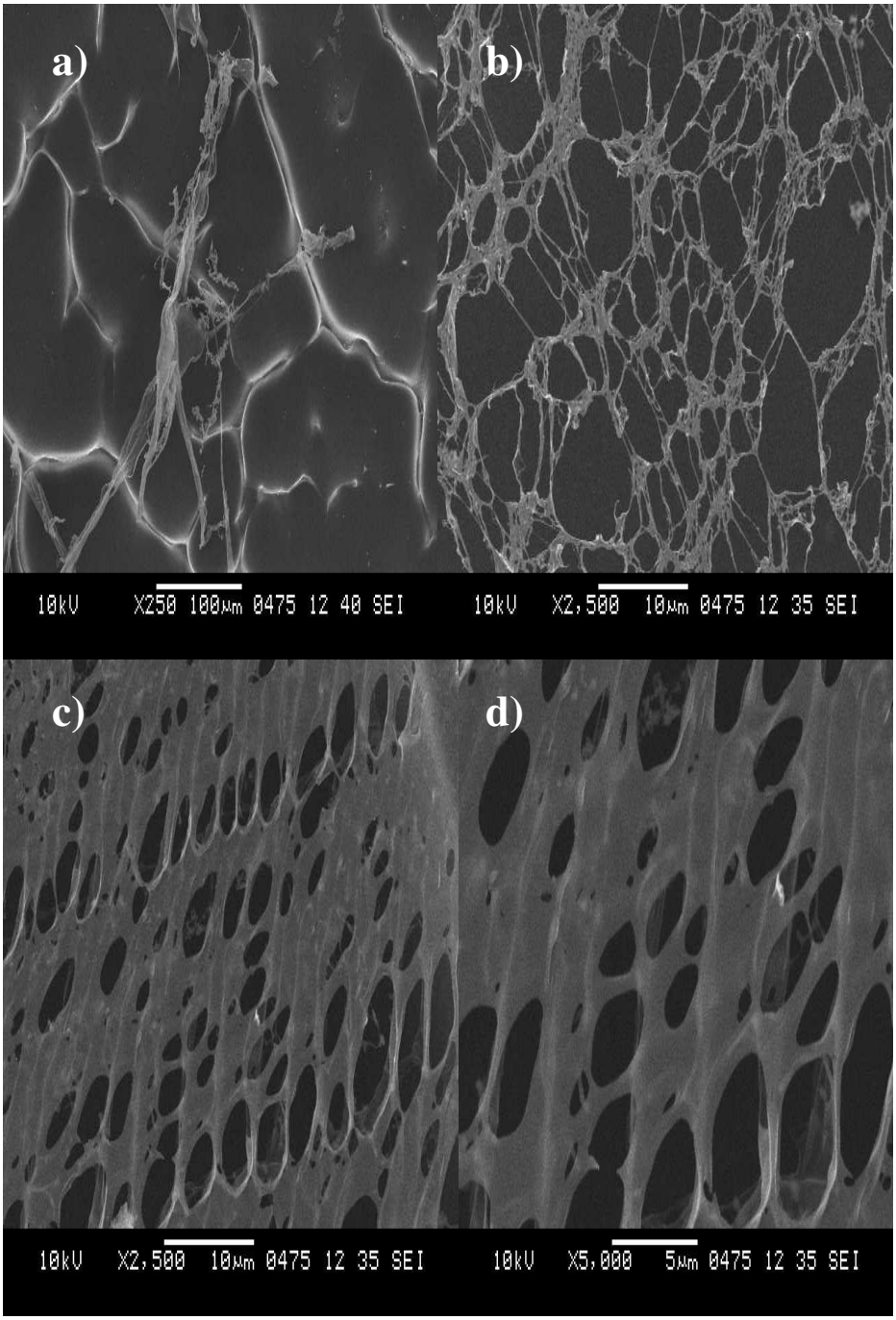

Figure 5.47 SEM analysis of ChitEPI600

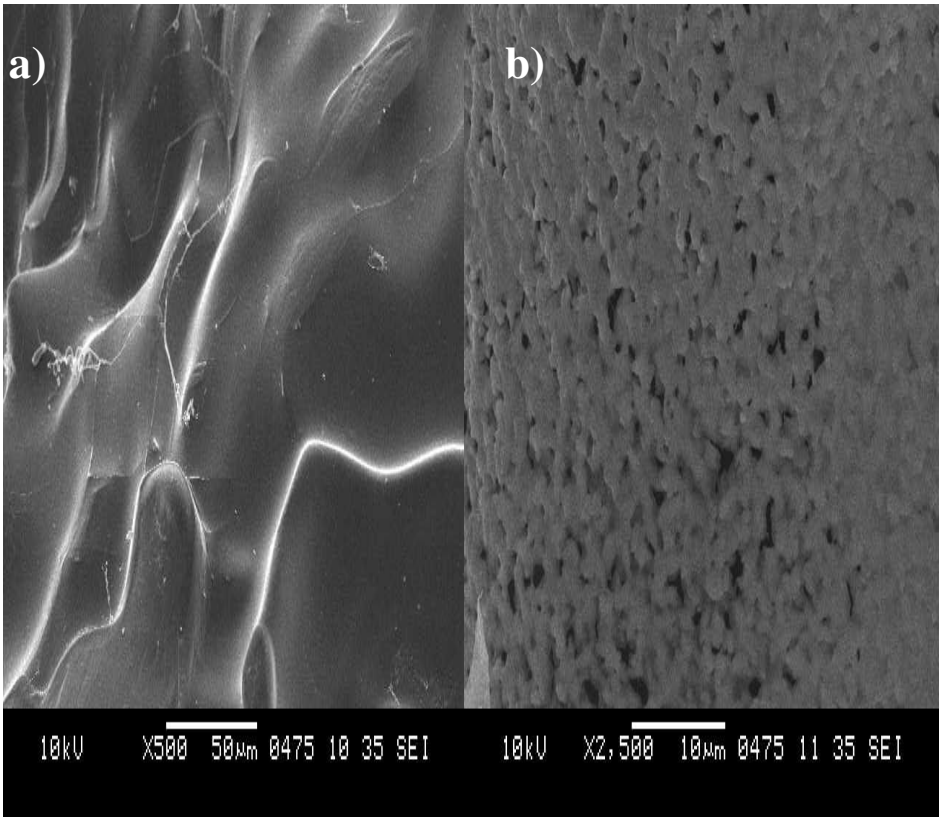

Figure 5.48 SEM analysis of ChitEPI800

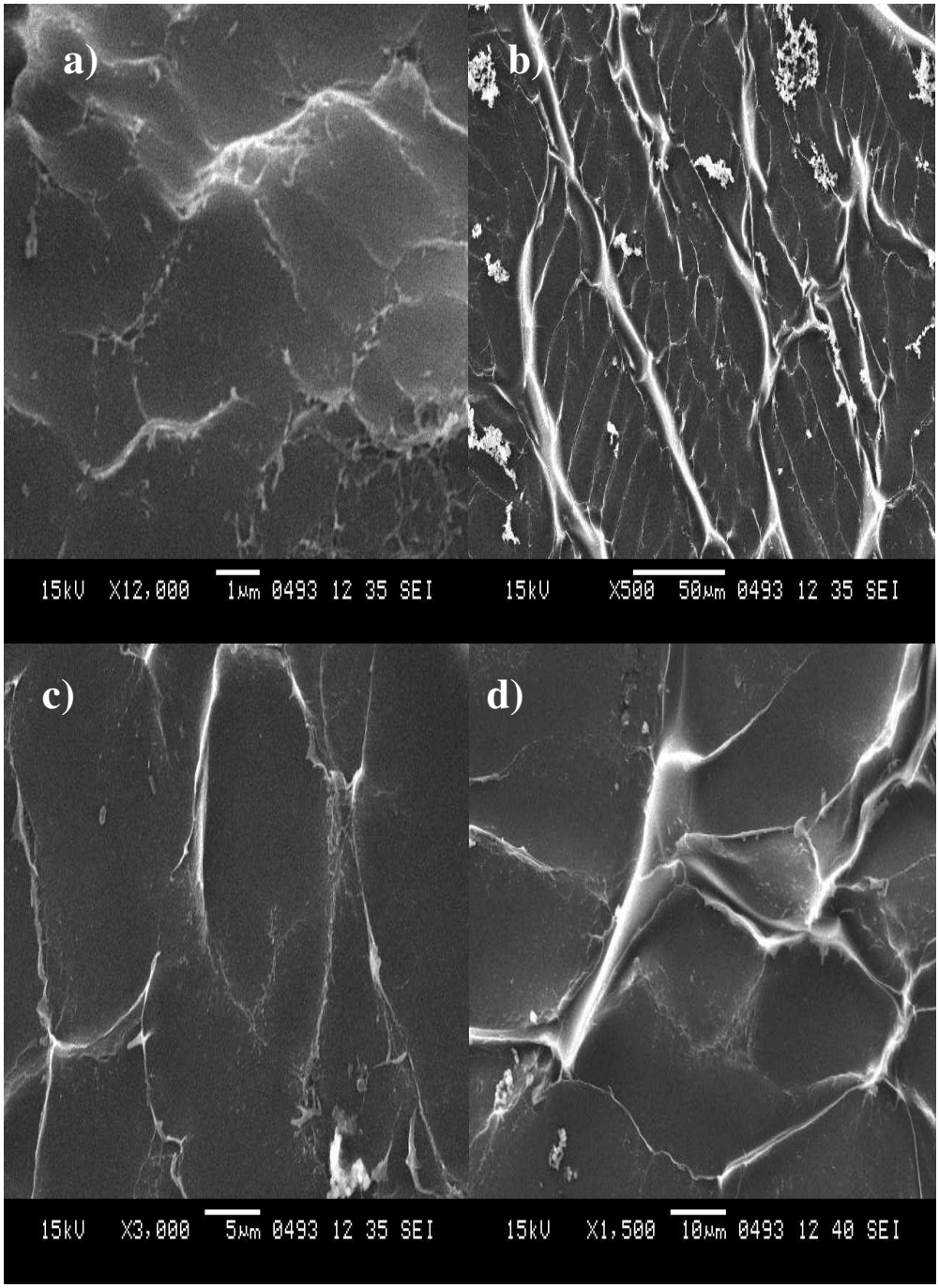

Figure 5.49 SEM Analysis of ChitEPI400+drug

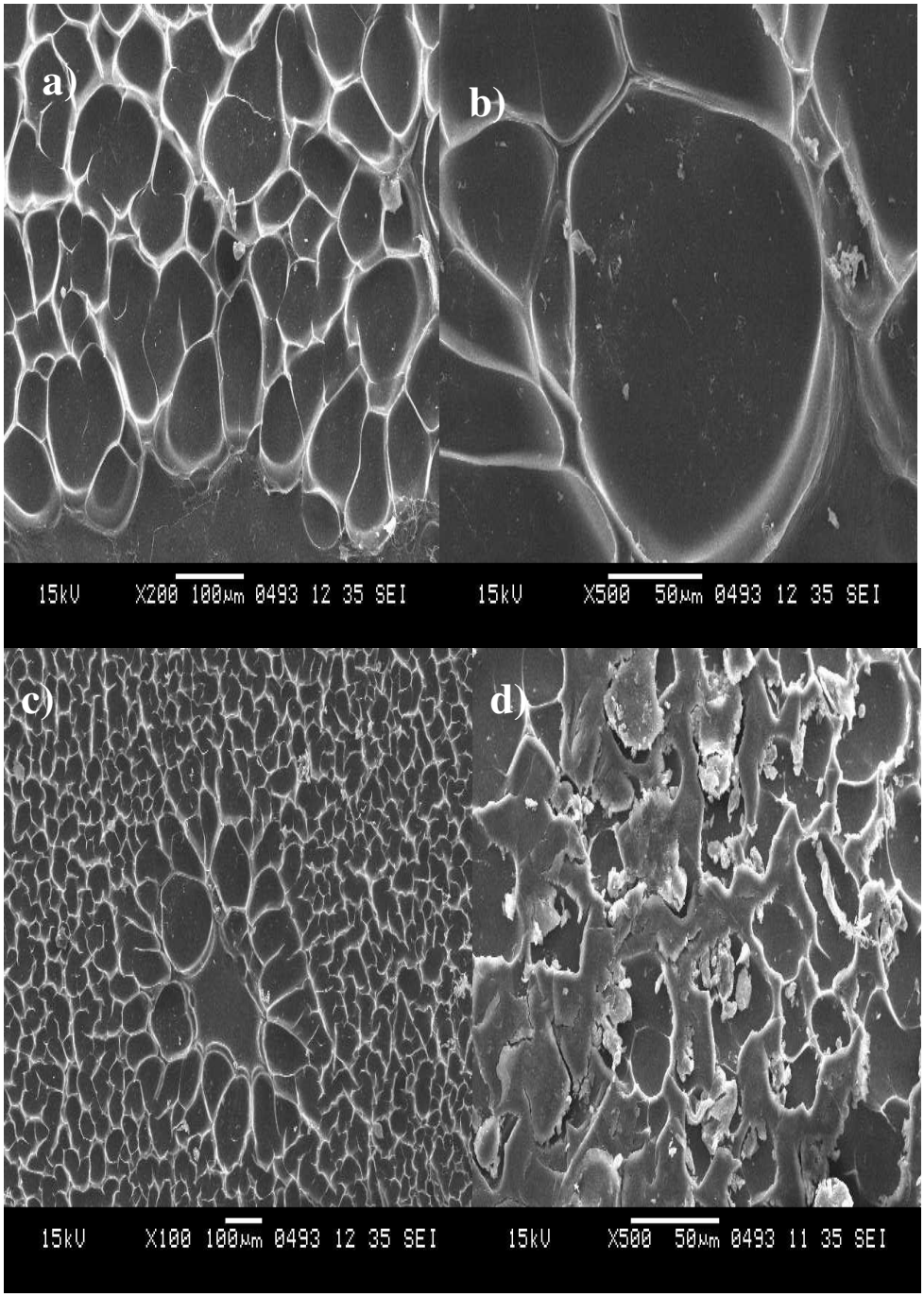

Figure 5.50 SEM Analysis of ChitEPI600+drug

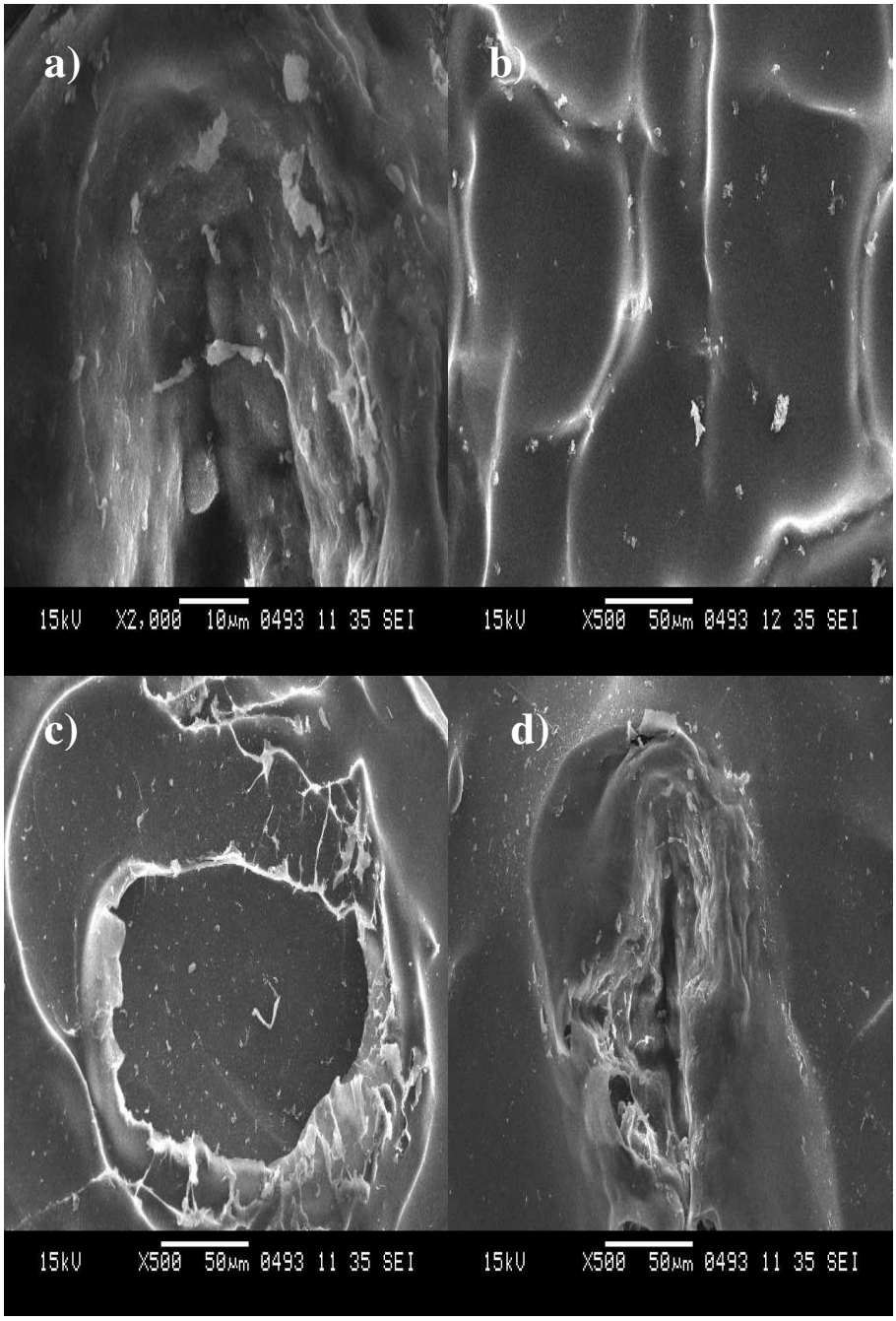

Figure 5.51 SEM Analysis of ChitEPI800+drug

5.2.9. Thermal Properties of Hydrogels

The thermal properties of ChitEPI hydrogel have been studied using DSC from 20 °C to 500°C. The DSC thermograms of Chitosan, ChitEPI400, ChitEPI600 and

ChitEPI800 were given in Figure 5.52. As shown by DSC analysis of Chitosan in Figure 5.52, an endothermic peak at 103°C represents melting endothermic peak of Chitosan. The melting endothermic peak of ChitEPI hydrogels was observed at 85°C, 92°C and 94 °C for ChitEPI400, ChitEPI600 and ChitEPI800 respectively. As can be seen from these results crosslinking of Chitosan with EPI melting temperatures were decreased. In addition to this, as the amount of crosslinker in Chitosan was increased, melting points of hydrogels also increased.

Heat flow values of hydrogels at melting temperatures were obtained to be -0.62, -1.45, -1.35 and -1.48 mW/g for Chitosan, ChitEPI400, ChitEPI600 and ChitEPI800 respectively.

The exothermic peaks in Figure 5.52 were observed due to thermal decomposition. For Chitosan sample the exothermic peaks was seen at 310°C. However exothermic peaks representing thermal decomposition of ChitEPI hydrogels was appeared to be 236, 235 and 240°C for ChitEPI400, ChitEPI600 and CHitEPI800. It is clear that the temperature of the exothermic peak of Chitosan was higher than those of ChitEPI hydrogels. Heat flow values at decomposition temperatures are 1.59, 1.00, 0.45 and 1.17 mW/g for Chitosan, ChitEPI400, ChitEPI600 and ChitEPI800.

The DSC thermograms of drug loaded hydrogels are shown in Figure 5.53 Thermograms of ChitEPI400+drug showed two endothermic peaks at 97°C and 197°C. ChitEPI600+drug have also two endothermic peaks at 94°C and 202 °C. Besides, there are two endothermic peaks for ChitEPI800+drug. One of them is at 93°C, but the other is a double peak at 187°C and 199°C. The DSC results indicate that ChitEPI hydrogels do not exhibit better thermal stability when compared to Chitosan.

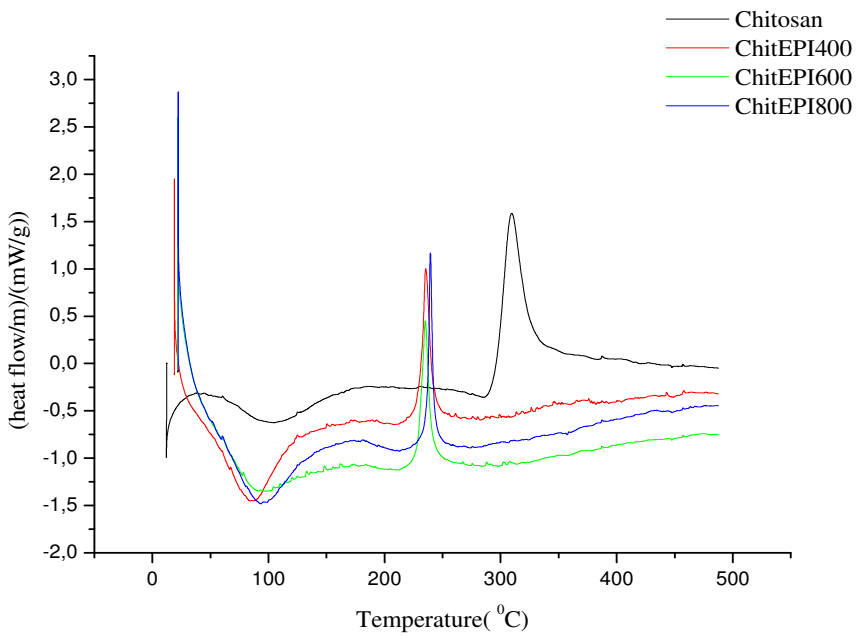

Figure 5.52 DSC thermograms for Chitosan and ChitEPI hydrogels

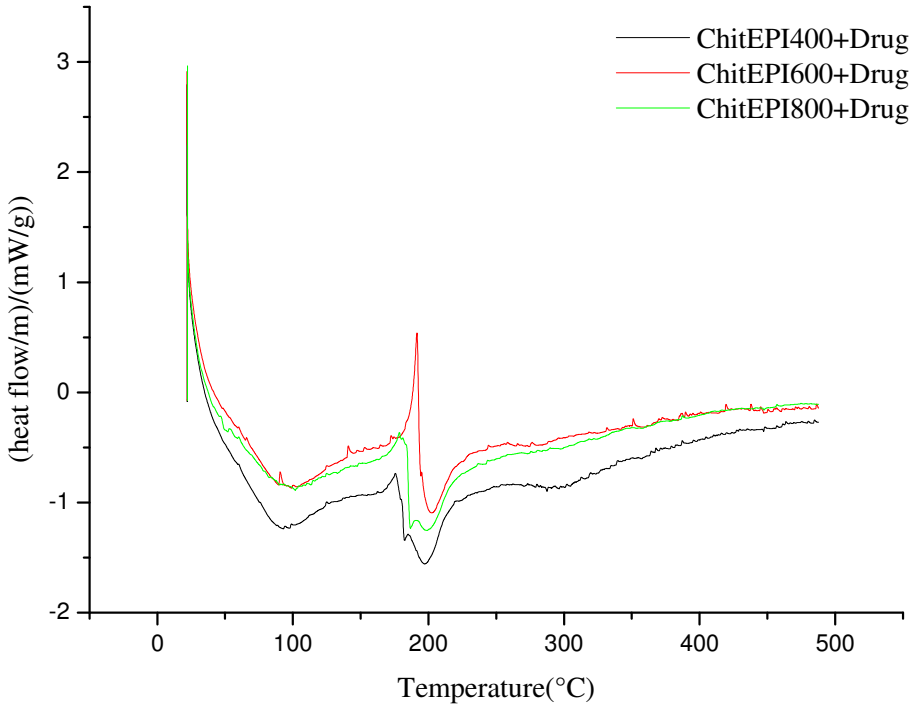

Figure 5.53 DSC thermograms for ChitEPI hydrogels+drug

CHAPTER SIX

CONCLUSION

6. Conclusion

Where the PHCl sorption on KSF sorption is concerned, with respect to the suitability of pseudo-second-order and pseudo-first-order kinetic models for adsorption of PHCl onto KSF, it has been determined that adsorption kinetics of model drug PHCl obeys pseudo-second-order kinetics. Nonetheless it is probable that sorption of PHCl can not be only described by kinetic model and it is a complex process. This was likely combined control of pseudo-second-order kinetic model and intraparticle diffusion. Langmuir, Freundlich and Dubinin Raduschkevich equations were used to describe adsorption of drug onto KSF. The equations were in good agreement with experimental results. However it can be said that Langmuir model provides the best correlation with the data according to correlation coefficients. From the thermodynamic studies, it is determined that physical adsorption may also be possible for adsorption mechanism. The mean energy of adsorption E determined in the D-R equation support the ion-exchange mechanism as a dominant adsorption type. It can be concluded that adsorption process was administrated combined control of ion exchange and physisorption. The adsorption process was spontaneous and a positive value of standard enthalpy change shows the endothermic nature of adsorption process.

From pH study for PHCl sorption onto KSF, the optimum pH value was determined to be about 3.4. KSF is an acidic adsorbent, therefore, the equilibrium pH values are quite low. The amount of PHCl adsorbed increased until the pH value of 3.4. Beyond the pH of 3.4, a decrease in adsorption generates due to decrease of degree of ion-exchange between cationic drug and H^+ protons which are on the KSF surface.

From the experiments conducted, it can be inferred that KSF may be used in the adsorption of PHCl.

For PHCl sorption onto IRS sample, the mean free energy values obtained in this study are 8.3, 9.6 and 9.5 kJ mol^{-1} at 290, 298 and 310 K respectively. This indicates a boundary of a physisorption and the predominance of van der Waals forces. When the adsorption capacity values (C_m and K_f) obtained from Langmuir and Freundlich equation are compared, IRS has much greater capacity than that of KSF. The fit of Langmuir equation for KSF is better than Freundlich equation. However for IRS, the fit of Freundlich equation provides best fit. This may mean that adsorption of PHCl onto KSF is chemisorption, while adsorption of PHCl onto IRS is physisorption. It may be the reason why IRS has a greater adsorption capacity than KSF. When the PHCl sorption onto IRS was concerned, the maximum adsorption of PHCl was observed at about pH 5. Between the pH values of 5.0 and 6.5, the amount of adsorbed was decreasing with the increasing of pH values

When the correlation coefficients of pseudo-first-order and pseudo-second-order model for PHCl sorption onto IRS were compared, the latter is better than the previous one. It can be reached that adsorption system obeys the second order kinetic model for PHCl sorption onto IRS. From SEM analysis of IRS samples, it was inferred that after loading of PHCl, IRS has gained a more compact structure due to interaction between smectite and aqueous solution of drug solution. As a result of treating of IRS with drug molecules, some agglomerates can also been seen in Figure 5.14.

The value of activation energy E_a was found to be 41.7 kJ mol^{-1} and 14.3 kJ mol^{-1} for PHCl sorption onto KSF and IRS respectively. For KSF, it is difficult to be sure of that the type of adsorption is considered as chemisorption, since the activation energy value obtained from experimental study is only slightly larger than 40 kJ mol^{-1}. Presumably, it indicates an ion-exchange process for PHCl adsorption onto KSF. This conclusion was also supported by DR isotherm. For IRS, adsorption can be suggested as physical adsorption,

For PHCl sorption onto IRS, the changes of free energy values in this study are in the range of -8.8 and -9.5 kJmol^{-1}. Therefore the type of adsorption can be considered

as physisorption for PHCl adsorption onto IRS. The negative values of ΔG^{o} at different temperatures for all samples indicate the spontaneous nature of the sorption process.

The maximum amount of PHCl released from KSF is almost 56.8 % of the total in the range studied (0-540 min). Release of PHCl from KSF, in acidic solution is less than 1%. As a result of conducted experiments with adsorption and releasing of PHCl from IRS, it has been reached that adsorption of PHCl onto IRS was achieved at very high level, but releasing of PHCl was at low level. Releasing of PHCl was 14.5 % at 715 min in phosphate buffer solution (pH=7.4). There was very little release (lower than 1.2 %) in acidic medium (pH=1.2).

When hydrogels are concerned, from the equilibrium swelling studies it has been determined that equilibrium of swelling reached in a very short time. It was obtained that an increase in the temperature would not be useful on the swelling equilibria of ChitEPI hydrogels. The swelling values were significantly decreased with the raise of pH in the range 2.5-6.5. In this pH range, the greatest swelling value belongs to ChitEPI400 when compared the other produced hydrogels. Beyond the pH value of 6.3, the swelling values are increasing with the increase of pH. It is probable that the number of NH_3^+ was decreased with increasing of pH. The lowest swelling occurred almost at pH 6.3 for all hydrogels. When the pH was increased NH_2 group would be dominant group. It is inferred that swelling behavior of Chitosan-EPI hydrogel film is pH dependent. When the pH values were changed repeatedly, ChitEPI hydrogel showed a reversible swelling behavior with a fast response. The reversible swell-shrink properties of produced hydrogels would be beneficial characteristics for pH sensitive controlled release system with controllable swelling ability, when used as a drug carrier. Moreover, the swelling values are increasing with the increase in concentration of NaCl from 0.05 to 0.2 M for ChitEPI400 and ChitEPI600. This deswelling phenomenon may be attributed to osmotic pressure difference between the inside of the gel and surroundings caused by redistribution of mobile ions. A very concentrated environment exist outside of the hydrogel Hence water which exist

inside of the hydrogel will decrease and leads to a decrease in osmotic pressure and makes the hydrogel deswelled.

SEM analysis demonstrated that the synthesized hydrogels have a porous structure. This is why the hydrogels swell in aqueous solutions. The DSC results indicate that ChitEPI hydrogels do not exhibit better thermal stability as compared with Chitosan. In addition to this, when the chitosan was cross-linked by EPI, the melting point of Chitosan EPI decreased. However, as the amount of cross-linker was increased, the melting point of hydrogel also increases. From FTIR analysis, it was confirmed that drug loading occurs successfully. Moreover, NH_2 and OH groups in chitosan may function as the recognition sites for the binding of EPI. For the synthesized hydrogels, drug release (PHCl) in pH=1.2, is greater than that in pH=7.4.

The release of PHC from synthesized hydrogels at pH=7.4 was quite low. Only about 10 % of the loaded drug was released during 600 min for all hydrogels. Besides considering PHCl release at pH=1.2 about 28 % release for ChitEPI800, 36 % for ChitEPI 400 and 49 % for ChitEPI600 was observed respectively. ChitEPI hydrogels can be used for the delivery of drug in stomach and gastrointestinal tract whose pH rises from 1.5 to 3. However the loaded drug can be released in lesser amounts from hydrogel as it passes through the stomach. Upon reaching colon small amounts of drug can be release from ChitEPI.

It could be concluded that reversible swell-shrink properties of produced hydrogels would be beneficial characteristics for pH sensitive controlled release system with controllable swelling ability, when used as a drug carrier.

REFERENCES

Abdel-Mohsen, M.G., Mohamed, H.A.& Abdel Wadood, H.M. (2001). Study of the effect of montmorillonite and florite on the dissociation constant, release and local anesthetic activity of lidocaine. *S.T.P. Pharm. Sci*. 11, 295–300.

Aguzzi, C., Viseras, C., Cerezo, P., Rossi, S., Ferrari, F.& Caramella, C. (2003). *Control of tetracyclines delivery by their interaction with veegum*. Proc. 30th Annual Meeting & Exposition of the Controlled Release Society, July 19–23. number 730.

Aguzzi C., Cerezo P., Viseras C.,& Caramella C. (2006). Use of clays as drug delivery systems: Possibilities and limitations, *Applied Clay Science,* In pres

Al-Gohary, O.M.N. (1991). An in vitro study of the interaction between mebeverine hydrochloride and magnesium trisilicate powder. *Int. J. Pharm*. 67, 89–95.

Al-Gohary, O. Lyall, J.& Murray, J.B, (1988). Adsorption of antihypertensives by suspensoids. Part 2. The adsorption of acebutolol, metoprolol, nadolol, oxprenolol and timolol by attapulgite, charcoal, kaolin and magnesium trisilicate. *Pharm. Acta Helv*. 63 (1), 13–18.

Allen, S.J, Mckay, G., & Porter, J.F. (2004). Adsorption isotherm models for basic dye adsorption by peat in single and binary component systems, *Journal of Colloid and Interface Science,* 280, 322-333.

Armstrong, N.A.& Clarke, C.D. (1971). The adsorption of crystal violet by kaolin. *J. Pharm. Pharmacol.* (Suppl. 23), 95–100.

Arayne, M.S.& Sultana, N. (1993). Erythromycin–antacid interaction. *Pharmazie* 48, 599–602.

Bae, Y. H., Vernon, B., Han, C. K., & Kim, S.W. (1998). Extracellular matrix for a rechargeable cell delivery system, *J. Control. Release* 53, 249–258

Bailey, S. W. (1980). Summary of recommendations of AIPEA nomenclature committee on clay minerals, *American Mineralogist* 65, 1-7.

Bekci, Z., Seki Y.& Yurdakoc K. (2006). Equilibrium studies for trimethoprim adsorption on montmorillonite KSF, *Journal of Hazardous Materials B*, 133, 233–242.

Bojemueller, E., Nennemann, A.& Lagaly, G. (2001). Enhanced pesticide adsorption by thermally modified bentonites. *Appl. Clay Sci*. 18, 277–284.

Browne, J.E., Feldkamp, J.R., White, J.L.& Hem, S.L. (1980).Characterisation and adsorptive properties of pharmaceutical grade clays. *J. Pharm. Sci.* 69 (7), 816–823.

Clay Minerals, Retrieved December 2006 from http://en.wikipedia.org /wiki/Clay_minerals

Bilia, A. (1992). In vitro evaluation of a pH-sensitive hydrogel for control of GI drug delivery from silicone-based matrices, *Int. J. Pharm.*, 130, 83-92

Bouwstra, J. A. & Junginger, H. E. (1993). *Hydrogels*. In Encyclopaedia of Pharmaceutical Technology (Swarbrick, J. and Boylan, J.C., eds), 441-465.

Brazel, C.S., & Peppas, N.A. (1996). Pulsatile local delivery of thrombolytic and antithrombotic agents using poly(Nisopropylacrylamide-co-methacrylic acid) hydrogels. *J. Control. Release* 39, 57–64.

Campoccia, D., Doherty, P., Radice, M., Brun, P., Abatangelo, G., & Williams, D. F. (1998). Semisynthetic resorbable materials from hyaluronan esterification, *Biomaterials* 19, 2101–2127.

Carstensen, J.T. & Kenneth, S. (1971). Nature of bonding in montmorillonite adsorbates. I: surface adsorption. *J. Pharm. Sci*. 60, 733–735.

Castela-Papin, N., Cai, S., Vatier, J., Keller, F., Souleau, C.H.& Farinotti, R. (1999). Drug interactions with diosmectite: a study using the artificial stomach-duodenum model. *Int. J. Pharm*. 182, 111–119.

Celis, R., Hermosin, M.C., Carrizosa, M.J.& Juan, C. (2002). Inorganic and organic clays as carriers for controlled release of the herbicide hexazinone. *J. Agric. Food Chem.* 50, 2324–2330.

Cerezo, P., Aguzzi, C., Viseras, C.& Cerezo, A. (2003). *Caracterización de complejos farmaco-arcilla (timolol-sepiolita). II. Termogravimetría (ATG).* Proc. VI Congreso de la sociedad española de farmacia industrial y galénica. Granada (E), February 9–11, 27–29.

Chae, S. Y., Kim, S. W., & Bae, Y. H. (2001). Bioactive polymers for biohybrid artificial pancreas, *J. Drug Target.* 9, 473–484.

Chae, S. Y., Kim, S. W., & Bae, Y. H. (2002). Effects of cross-linked hemoglobin on functionality and viability of microencapsulated pancreatic islets, *Tissue Eng*. 8, 379–394.

Chang, C.F, Chang, C.Y., Chen, K.H., Tsai, W.T., Shie, J.L., & Chen, Y.H. (2004). Adsorption of naphthalene on zeolite from aqueous solution, *Journal of Colloid and Interface Science,* 277, 29-34.

Clarke, C.D.& Armstrong, N.A. (1972). Influence of pH on the adsorption of benzoic acid by kaolin. *Pharm. J*. 209, 44–45.

Corma Canos, A., Munoz Pallares, J.& Primo Yufera, E. (2000). Controlled-release emitter of semiochemicals, supported on a modified sepiolite. *PCT Int. Appl*.,. 29

Dékány, I., Turi, L., Fonseca, A.& Nagy, J.B. (1999). The structure of acid treated sepiolites: small-angle X-ray scattering and multi MAS-NMR investigations. *Appl. Clay Sci*. 14, 141–160.

Delgado, R., Delgado, G., Ruiz, A., Gallardo, V.& Gamiz, E. (1994). The crystallinity and several Spanish kaolins; correlation with sodium amylobarbitone release. *Clay Miner*. 29, 785–797.

Deshpande, A. A. (1992). Intravaginal drug delivery. *Drug Dev. Ind. Pharm.* 18, 1225–1279.

Dung P., Milas, M., Rinaudo M. & Desbrieres J. (1994). *Water soluble derivatives obtained by controlled chemical modifications of chitosan*. CERMA V-CNRS, B.P. 53 X. 38041 Grenoble Cedex, France.

El-Gindy, G.A., Ali, A.S.& El-Shinnawi, O.M. (2000). Preparation and formulation of sustained-release terbutaline sulphate microcapsules. *Bull. Pharm. Sci*. 23, 55–63.

El-Nahhal, Y., Nir, S., Polubesova, T., Margulies, L.& Rubin, B. (1998). Leaching, phytotoxicity, and weed control of new formulations of alachlor. *J. Agric. Food Chem.* 46, 3305–3313.

El-Nakeeb, M.A. & Yousef, R.T. (1968). Influence of various materials on antibiotics in liquid pharmaceutical preparations. *Acta Pharm. Swed*. 5 (2), 1–8.

El-Sayed, A.M., Ismael, A.E.M. & Assi, A.E. (1993). Dissociation constant of chlordiazepoxide in montmorillonite suspension and its pharmaceutical application for a controlled-release dosage form. *Acta Pharm. Hung*. 63, 257–266.

Fejer, I., Kata, M., Erös I., Berkesi O.& Dekany, I. (2001). Release of cationic drugs from loaded clay minerals, *Colloid Polym Sci.*, 279, 1177-1182.

Feil, H., Bae, Y. H., Feijen, J.S., & Kim, W. (1993). Effect of comonomer hydrophilicity and ionization on the lower critical solution temperature of N-isopropylacrylamide copolymers, *Macromolecules* 26 2496–2500.

Fernández-Pérez, M., Villafranca-Sánchez, M., González-Pradas, E., Martinez-López, F.& Flores-Céspedes, F. (2000). Controlled release of carbofuran from an alginate–bentonite formulation: water release kinetics and soil mobility. *J. Agric. Food Chem.,* 48, 938–943.

Forni, F., Iannuccelli, V., Coppi, G., Vandelli, M.A. & Cameroni, R. (1987). Montmorillonite as a drug carrier: surface deposition of papaverine on the papaverine–veegum complex. *Boll. Chim. Farm*., 126, 342–346.

Forni, F., Iannuccelli, V., Coppi, G. & Bernabei, M.T. (1989). Effect of montmorillonite on drug release from polymeric matrices. *Arch. Pharm.* 322, 789–793.

Gappa, H., Baudys, M., Koh, J. J., Kim, S. W., & Bae, Y. H. (2001). The effect of zinc-crystallized glucagon-like peptide-1 on insulin secretion of macroencapsulated pancreatic islets, *Tissue Eng.*, 7, 35–44.

Ghiaci, M, Abbaspur, A., Kia, R. & Seyedeyn-Azad, F. (2004). Equilibrium isotherm studies for the sorption of benzene, toluene, and phenol onto organo-

zeolites and as synthesized MCM-41, *Separation and Purification Technology,* 40, 217-229.

Giles C.H., McEvan T.H., Nakhwa S.N.&Smith D. (1960). *J. Chem. Soc.* 4, 3973-3993.

Graham, N. B. (1998). Hydrogels: their future, Part II., *Med Device Technol*; 9, 22–25

Graham, N. B. (1998). Hydrogels: their future, Part I., *Med Device Technol*; 9, 18–22.

Grim, R.E. (1968). *Clay Mineralogy*, 2nd edition, Mc Graw-Hill Book Company, New York, 41.

Gumusderelioglu M.& Topla I.U. (2005). Vinyl ether/acrylic acid terpolymer hydrogels synthesized by γ-radiation: characterization, thermosensitivity and pH-sensitivity, *Radiation Physics and Chemistry* 73, 272-279

Gupta, P., Vermani, K.& Garg, S. (2002). Hydrogels: from controlled release to pH-responsive drug delivery, *DDT,* 7,10, 569-579.

Guyton, A. C.& Hall, J. E. (1998). *Secretory functions of the alimentary tract*. In Textbook of Medical Physiology (Guyton, A. C. and Hall, J. E., eds), 815–832,

Hansten PD & Horn JR (1989). *Drug interactions*, 6th ed., Philadelphia, Lea & Febiger, 448.

Heskins, M., & Guillet, J. E. (1968). Solution properties of poly (N-isopropylacrylamide), *J. Macromol. Sci. Chem. (A2)* 1441–1455.

Hirotsu, S., Hirokawa, Y., & Tanaka, T. (1987). Volume-phase transitions of ionized N-isopropylacrylamide gels, *J. Chem. Phys.* 87, 1392–1395

Ho, Y.S., & McKay, G. (1998). Sorption of dye from aqueous solution by peat, *Chem. Eng. J.* 76, 115–124.

Ho Y.S. & Ofomaja A.E. (2006). Kinetic studies of copper ion adsorption on palm kernel fibre, *Journal of Hazardous Materials,* 137, 3, 1796-1802.

Hoffman, A. S., Afrassiabi, A., & Dong, L. C. (1986). Thermally reversible hydrogels: II. Delivery and selective removal of substances from aqueous solutions, *J. Control. Release* 4, 213–222.

Houpt, M. I. (1985). Comparison of chloral hydrates with and without promethazine in the sedation of young children. *Pediatric Dentistry*, **7**: 41-46.

Ito, A. (1994). Investigation of compressed coating tablet swelling with water as a new dosage form for elderly patients. *Jpn. J. Hosp. Pharm.* 20, 41–49.

Iwuagwu, M.A.,& Aloko, K.S., (1992). Adsorption of paracetamol and chloroquine phosphate by some antacids. *J. Pharm. Pharmacol.* 44, 655–658.

Jain, G.K. & Kakkar, A.P. (1992). Interaction study of diazepam with excipients in liquid and solid state. *Indian Drugs* 29, 545–556.

Kahela, P.& Hurmerinta, T. (1979). Adsorbates of spironolactone and bentonite - biopharmaceutical study in dogs. *Acta Pharm. Fennica*, 88, 155–159.

Kenneth, S. & Carstensen, J.T. (1972). Nature of bonding in montmorillonite adsorbates II: bonding as an ion-dipole interaction. *J. Pharm. Sci*. 61, 420–424.

Kim, S. W., Bae, Y. H., & Okano, T. (1992). Hydrogels: swelling, Drug Loading and Release, *Pharmaceutical Research,* 9, 283-290.

Krishna, B.S., Murty, D.S.R.& Prakash, B.S.J. (2000). Thermodynamics of chromium(VI) anionic species sorption onto surfactantmodified montmorillonite clay. *Journal of Colloid Interface Science.* 229, 230–236.

Lagaly, G. (2001). Pesticide–clay interactions and formulations. *Appl.Clay Sci.* 18, 205–209.

Leach J.B. & Schmidt C.E. (2005). Characterization of protein release from photocrosslinkable hyaluronic acid-polyethylene glycol hydrogel tissue engineering scaffolds, *Biomaterials,* 26, 125–135.

Lee, Y. M., Kim, S. H. & Cho, C. S. (1996). Synthesis and Swelling Characteristics of pH and Thermo-responsive Interpenetrating Polymer Network Hydrogel, Composed of Poly(vinyl alcohol) and Poly(acrylic acid), *J. of Applied Polymer Science,* 62, 301-311.

Levis, S.R.& Deasy, P.B. (2003). Use of coated microtubular halloysite for the sustained release of diltiazem hydrochloride and propranolol hydrochloride. *Int. J. Pharm.* 253, 145–157.

Lin Y., Chen Q., & Luo H. (2007). Preparation and characterization of N-(2-carboxybenzyl) chitosan as a potential pH-sensitive hydrogel for drug delivery, *Carbohydrate Research,* 342, 1, 87-95.

Madejova, J. (2003). FTIR techniques in clay mineral studies, *Vibrational Spectroscopy*, 31, 1-10 (2003).

Maheshwari, R.K., Sharma, S.N. & Jain, N.K. (1988). Adsorption studies of phenformin hydrochloride on some clays and its application in formulating sustained release dosage forms. Indian *J. Pharm. Sci.* 50 (2), 101–105.

Martindale (1989). *The Extra Pharmacopoeia*. Reynolds J. E. F., Parfitt K., Parsons A. V., Sweetman S. C. (eds), London, The Pharmaceutical Press, 1896**.**

Meier, P., Nueesch, R.& Madsen, F.T. (2001). Organic pillared clays. *J. Colloid Interface Sci*. 238, 24–32.

Mc Bride, M. B. (1994). *Environmental Chemistry of Soils,* Oxford Univertsity Press, Inc., Oxford, 416.

McGinity, J.W. & Lach, J.L. (1976). In vitro adsorption of various pharmaceuticals to montmorillonite. *J. Pharm. Sci.* 65 (6), 896–902.

Newman, A. C. D. (1987*). Chemistry of Clays and Clay Minerals*, Mineralogical Society, Monogr., No. 6., John Wiley & Sons Inc., 49-53.

Nollet, H, Roels, M., Lutgen, P., van der Meeren, P., & Verstraete, W. (2003). Removal of PCBs from wastewater using fly ash, *Chemosphere*, 53, 655-665

Özcan, A.S, & Özcan, A. (2004). Adsorption of acid dyes from aqueous solutions onto acid-activated bentonite, *Journal of Colloid and Interface Science*, 276, 39-46.

Park, K., & Shalaby, S.W. (1993). Biodegreadable hydrogels for Drug Delivery. *Technomic Publishing*, 3, 5.

Park, K. H., & Bae, Y. H. (2002). Phenotype of hepatocyte spheroids in Arg-Gly-Asp (RGD) containing a thermo-reversible extracellular matrix, *Biosci. Biotechnol. Biochem.* 66, 1473–1478.

Peppas, N. A. (1987). *Hydrogels in medicine and pharmacy*. Florida: CRCPress.

Peppas, N. A. & Bures, P. (2000). Hydrogels in pharmaceutical formulations. *Eur. J. Pharm Biopharm,* 50:27–46.

Prestwich, G. D., Marecak, D. M., Marecak, J. F., Vercruysse K. P., & Ziebell, M. R. (1998). Controlled chemical modification of hyaluronic acid*, J. Controlled Release* 53, 93–103.

Promethazine. Retrieved December 12, 2006, from http://www.inchem.org /documents/pims/pharm/prometha.htm

Qadeer, R, Hanif, J., Khan, M., & Saleem, M. (1995). Uptake of Uranium Ions by Molecular-Sieve, *Radiochimica Acta,* 68, 197-201.

Rao, K. V. R., & Devi, K. P. (1988). Swelling controlled-release systems: recent developments and applications. *Int. J. Pharm.,* 48, 1–13.

Sayed, H.A.M., El-Sayed, A.M., Osman, A.H.& Fathy, M. (1991). Design of sustained-release formulations of salbutamol. II. Clay sorbate systems. *Bull. Pharm. Sci.* 14 (1–2), 61–73.

Seki, Y. (2003). *Adsorption of some herbicides onto organo-clays from aqueous solution,* M. Sc. Thesis, D.E.U. Fen-Bilimleri Enstitüsü, İzmir Turkey, 90.

Siegel, R. A., & Firestone, B. A. (1988). pH-dependent equilibrium swelling properties of hydrophobic polyelectrolyte copolymer gels, *Macromolecules*, 21, 3254-3259.

Socias-Viciana, M. M., Hermosin, & M. C., Cornejo, J. (1998). Removing prometrone from water by clays and organic clays, *Chemosphere* 37 (2) 289-300.

Song, S. Z., Kim, S. H., Cardinal, J. R., & Kim, S.W. (1981). Progestin permeation through polymer membranes, V. Progestrone release from monolthic hydrogel devices, *J. Pharm. Sci.* 70, 216-219.

Sood, A., & Panchagnula, R. (1998). Drug Release evaluation of diltiazem CR preparations, *International Journal of Pharmaceutics* 175, 95-107.

Sood, A.,& Panchagnula, R. (1998). Drug release evaluation of diltiazem CR preparations, *International Journal of Pharmaceutics* 175, 95-107.

Sorby, D.L., (1965). Effect of adsorbents on drug absorption. I. Modification of promazine absorption by actived attapulgite and actived charcoal. *J. Pharm. Sci*. 54 (5), 677–683.

Sorby, D.L.,& Liu, G. (1966). Effect of adsorbents on drug absorption. II. Effect of antidiarrhea mixture on promazine absorption. *J. Pharm. Sci.* 55 (5), 504–510.

Tahir S.S. & Rauf N. (2006) Removal of a cationic dye from aqueous solutions by adsorption onto bentonite clay, *Chemosphere,* 63 (11), 1842-1848.

Tarsy D. (1975). Metoclopramide and pimozide in Parkinson's disease and Levodopa induced dyskinesias. *J. Neurol. Neurosurg. Psychaitr.*, 83, 331.

Thoma, K., Ullmann, E.,&Wolferseder, E., (1966). Effect of adjuvants in the manufacture of pharmaceutical preparations. XII. Drug releasefrom suspensions of colloidal silicic acid, white clay, and talc. *Sci. Pharm*. 34 (3), 191–202.

Tolls, J. (2001). Sorption of veterinary pharmaceuticals in soils: a review. *Environ. Sci. Technol*. 35 (17), 3397–3406.

Tunali S, Ozcan A. S., Ozcan A., & Gedikbey T. (2006). Kinetics and equilibrium studies for the adsorption of Acid Red 57 from aqueous solutions onto calcined-alunite, *Journal of Hazardous Materials B,* 135, 141–148.

Undabeytia, T., Nir, S.& Rubin, B. (2000). Organo-clay formulations of the hydrophobic herbicide norflurazon yield reduced leaching. *J. Agric. Food Chem.* 48, 4767–4773.

USP 29 (2006a). *Activaded attapulgite and colloidal activated attapulgite*. United States Pharmacopoeia 29 and National Formulary 24. US Pharmacopoeial Convention, Rockville, MD (USA), 221–222.

USP 29 (2006b). *Magnesium trisilicate*. United States Pharmacopoeia 29 and National Formulary 24. US Pharmacopoeial Convention, Rockville, MD (USA), 1303–1304.

Van Damne, H., Tomlinson, A.A.G., Palvadeau, P., Purnell, H.J.& Gangas, N.H.J. (1995). *Coordinated European Activity on Pillared Layered Structures* (CEA-PLS). Proj. BE-4275.

Vasanth Kumar, K., Ramamurthi V. & Sivanesan S (2006). *Biosorption of malachite green,* a cationic *dye onto pithophora sp., a fresh water algae. Dyes Pigments* 69, 102-107.

Vatier, J., Harman, A., Castela, N., Droy-Lefaix, M.T. & Farinotti, R., (1994). Interactions of cimetidine and ranitidine with aluminumcontaining antacids and a clay-containing gastric-protective drug in an “artificial stomach-duodenum” model. *J. Pharm. Sci*. 83 (7), 962–966.

Vernon, B., Gutowska, A., Kim, S.W., & Bae, Y. H. (1996). Thermally reversible polymer gels for biohybrid artificial pancreas, *Macromol. Symp.,* 109, 155–167.

Vernon, B., Kim, S. W., & Bae, Y. H. (1999). Insulin release from islets of Langerhans entrapped in a poly(N-isopropylacrylamide-co-acrylic acid) polymer gel, *J. Biomater. Sci. Polym.* Ed. 10, 183–198.

Vicente-Rodríguez, M.A., Suarez, M., Bañares-Muñoz, M.A.& Lopez- Gonzalez, J. (1996). Comparative FT-IR study of the removal of octahedral cations and structural modifications during acid treatment of several silicates. *Spectrochim. Acta Part A* 52, 1685–1694.

Vikas, A., Raghupathi, K.,& Sanjay, G. (2001). Ion-exchange resins: carrying drug delivery forward. *DDT* 6 (17), 905–914.

Villafranca-Sánchez, M., González-Pradas, E., Fernández-Pérez, M., Martinez-López, F., Flores-Céspedes, F.& Ureña-Amate, M.D. (2000). Controlled release of isoproturon from an alginate-bentonite formulation: water release kinetics and soil mobility. *Pest Manag. Sci*. 56, 749–756.

Viseras, C., Cerezo, P., Aguzzi, C., Viseras, M.T., Caramella, C. & Cerezo, A. (2003). *Factorial design study on the interaction between timolol and sepiolite*. Proc. 1st EUFEPS Conference on Optimising drug delivery and formulation: new challenges in drug delivery. Versailles (F), September 29–October 1, pp. 138–139.

Viseras, M.T., Aguzzi, C., Cerezo, P., Viseras, C., López-Galindo, A., Valenzuela, C.& Caramella, C. (2005). *Study of adsorption kinetics of 5-aminosalicilyc acid in phyllosilicates for controlled drug delivery in the treatment of inflammatory bowel disease.* Proc. 1st PharmSciFair, Pharmaceutical Sciences Fair and Exhibition. Nice (F), June 12–17, PO-253.

Viseras C., Aguzzi C., Cerezo P.& Lopez Galindo, A. (2006). Uses of clay minerals in semisolid health care and therapeutic products, *Applied Clay Science*, in press

Wai, K.N. & Banker, G.S. (1966). Some physicochemical properties of the montmorillonites. *J. Pharm. Sci.* 55 (11), 1215–1220.

Weil, A. J. (1968). Exfoliative dermatitis after mediation with methylphenidate HCl. *Ann. Allergy*, 26, 402.

Yadava, KP, Tyagi, B.S., & Singh, V.N. (1991). Effect of Temperature on the Removal of Lead (II) by Adsorption on China Clay and Wollastonite, *J Chem Technol Biotechnol*, 51, 47-60

Yıldız, B. (2001). *Preparation of Temperature-Responsive Hydrogels & pH-Sensitive Hydrogels and Determination of Their Swelling Properties*, Hacettepe University M. Sc. Thesis, 95.

Yu Y, Zhuang, Y. Y, & Wang, Z.H. (2001). Adsorption of Water-Soluble Dye onto Functionalized Resin, *Journal of Colloid and Interface Science*, 242, 288-293.